UiT The Arctic University of Norway

Department of Computer Science and Computational Engineering

Enhancing Efficiency and Safety in Iron Ore Mining:

Innovative Solutions for Water Management in Conveyor Systems

Uzair Zulfiqar

Master’s Thesis in Engineering Design - Spring 2024

Abstract

This thesis report explores the critical challenge of water flooding in conveyor belt systems within the iron ore mining sector, with a focus on LKAB, a leading Swedish mining company. The study begins by outlining the significance of addressing water accumulation issues that compromise operational efficiency and safety in mining environments. Through an extensive literature review, the research delves into the history of mining, the pivotal role of iron ore in the global steel production industry, and the specifics of iron ore mining processes and their environmental implications. It further investigates bulk material handling in mining, highlighting the use of tanks, silos, and particularly belt conveyors, which are prone to water flooding, causing significant operational disruptions.

The report systematically reviews existing problems associated with current water removal solutions in conveyor systems, critically evaluating their effectiveness and identifying gaps. It presents an analysis of innovative approaches and patents in the field, notably examining JP2000318827Aand KR101500125B1, which propose advanced methods and devices for water removal and moisture separation in conveyor belts. These examinations provide insights into potential improvements and technological advancements that can mitigate water-related challenges in mining operations.

Future work suggested by the study includes the design of new products and detailed analysis, leveraging the findings to propose practical, efficient, and sustainable solutions to the issue of water flooding in conveyor belts. The thesis underscores the importance of continued research and development in this area to enhance the durability of mining infrastructure and ensure the safety and efficiency of operations.

Preface

This master's thesis investigates a critical challenge within the iron ore mining sector: water flooding in conveyor belt systems. The topic was proposed by maintenance engineers from LKAB, Daniel Valen Nilsen and Fred Yang, who provided invaluable practical insights and support. Their expertise helped shape this research to address the significant operational disruptions caused by water accumulation, particularly in the mining operations of LKAB, a leading Swedish mining company.

Throughout the research, several challenges were encountered. Gathering accurate and comprehensive data on water flooding required careful coordination with multiple departments and engineers within LKAB. Analyzing the environmental and operational factors that contribute to flooding in conveyor belt systems proved complex, requiring detailed simulations and structural assessments. Developing practical and innovative solutions involved rigorous testing and iterative design modifications to ensure the proposed approaches were effective and sustainable.

Despite these challenges, the report presents two innovative solutions for effectively draining water from conveyor belts using engineering design principles, fluid mechanics, and structural analysis. A comprehensive literature review explores existing solutions and relevant patents, such as JP2000318827Aand KR101500125B1, offering insights into advanced water removal techniques. The thesis recommends further research to refine these solutions and leverage practical analysis and design for sustainable management of water-related challenges.

I hope this report serves as a valuable contribution to ongoing research in mining and inspires the continued development of innovative strategies for enhancing mining infrastructure durability and safeguarding operational efficiency.

Acknowledgments

I would like to express my deepest gratitude to my advisor, Professor Per Johan Nicklasson, whose guidance and expertise were instrumental in developing the direction of this research. My Program Head, Guy Beeri, also provided unwavering support and resources that enriched this project. I would like to thank the maintenance engineers from LKAB, Daniel Valen Nilsen and Fred Yang, who offered this topic and provided essential insights.

Special thanks go to the faculty and staff at my institution for their assistance, and to my family and friends for their consistent encouragement throughout this process. Your support was invaluable in helping me complete this thesis.

Table of Contents

1 Introduction 10
1.1 Purpose of the Study 10
1.2 Background 10
1.3 Problem Statement 11
1.4 Significance of the Study 12
2 Literature Review 13
2.1 Bulk Material Handling in Mining 13
2.2 Review of Problems and Solutions 17
2.3 Innovative Approaches and Patents 21
3 Product Design 29
3.1 Clarifying Objectives 29
3.2 Establishing Functions 30
3.3 Setting Requirements 32
3.4 Determining Characteristics 33
3.5 Generating Alternatives 34
3.6 Evaluating Alternatives 35
3.7 Product Design Results: 38
4 Plate-Based Design 39
4.1 Design Philosophy 39
4.2 3D Model 39
4.3 Material selection: 41
4.4 Drag Coefficient and Pressure Analysis: 44
4.5 FEA Analysis: 51
4.6 Mass Flow Rate Analysis: 56
4.7 Deployment Mechanism of Plate: 59
5 Pump-Based Design 63

5.1 Design Philosophy 63
5.2 3D Model 64
5.3 CFD of pipe: 65
5.4 FEA 66
5.5 Deployment Mechanism of pipes: 68
6 Results 70
6.1 Plate-Based Design 70
6.2 Pump-Based Design 71
7 Conclusion 72
7.1 Discussion 72
7.2 Further Work 73
8 References 80
Appendix A - LKAB Drawing 82
Appendix B-Plate FEA Results 83
Appendix C-Plate Mass Flow CFD Results 87
Appendix D-Plate 2D Drawing 88
Appendix E-Pipe CFD Results 89
Appendix F-Pipe 2D Drawing 90
Appendix G-Plate-Based Design Rendered Images 91
Appendix H-Pump-Based Design Rendered Images 92

List of Figures

Figure 1-Infographic depicting the water accumulation in TR010 conveyor. (Source: LKAB) 11
Figure 2-Excavation and Construction of Underground Silos for Iron Ore Storage, (LKAB, Narvik)[3]. 15
Figure 3-Depiction of water accumulation in belt conveyor[13]. 22
Figure 4-Flat carrier roller [13]. 23
Figure 5-Edge-pressing roller inverting the belt [13]. 23
Figure 6-Belt when transporting material [13]. 24
Figure 7-General setup, side view[14]. 25
Figure 8-General Setup, cross-sectional view[14]. 26
Figure 9-Illustration of agitation mechanism [14]. 27
Figure 10-Chain linkage close-up[14]. 27
Figure 11-Cross-sectional View of the Conveyor Belt Demonstrating Water Drainage Through Perforations[14]. 27
Figure 12-Rational Method Chart [15] 29
Figure 13-Objectives Tree 30
Figure 14-Functions and Means Tree 31
Figure 15-House of Quality Chart 33
Figure 16-Weighted Objectives Tree 36
Figure 17-Plate Model (1st Iteration) 40
Figure 18-Plate Model (1st Iteration-Exploded View) 40
Figure 19-Plate Model (2nd Iteration) 40
Figure 20-Plate Model (3rd Iteration) 41
Figure 21-Ansys Granta Stages 43
Figure 22-Pass Materials 44
Figure 23-Meshing of Enclosure 46
Figure 24-Meshing of half plate inside the meshed enclosure (domain) 47
Figure 25-Meshing of Enclosure-transparent view 47
Figure 26-Drag Force Result 48
Figure 27-Drag Coefficient Result 48
Figure 28-Total Pressure Result 48
Figure 29-Residual Plot 49

Figure 30-Frontal Area 50
Figure 31-Plate Meshing.......... 51
Figure 32-Plate Boundary Conditions.......... 51
Figure 33-Deformation in 5mm CFRP Plate 52
Figure 34-Test Plate Boundary Conditions.......... 54
Figure 35-Test Plate Deformation Results.......... 54
Figure 36-Test Plate Max Stress Results 54
Figure 37-Plate FEA Results Graph 55
Figure 38-Deformation in 8mm CMA Plate.......... 56
Figure 39-Inlet and Outlets for Mass Flow Rate CFD 57
Figure 40-Mass Flow Rate CFD Transparent View 58
Figure 41-Mass Flow Rate CFD Velocity Contours 58
Figure 42-Plate in Disengaged Position. 60
Figure 43-Plate in Engaged Position 60
Figure 44-Actuator Schematic [17] 61
Figure 45-Pedrollo HF Centrifugal Pump [21].......... 63
Figure 46-3D Model of Pump-Based Design 64
Figure 47-Pipe domain (Without Elbow) 65
Figure 48-Pipe domain (With Elbow) 65
Figure 49-Pipe Support Frame FEA-Deformation.......... 67
Figure 50-Pipe Support Frame FEA-Total Stress 67
Figure 51-Pipe in Disengaged Position 69
Figure 52-Pipe in Engaged Position 69
Figure 53-Magnetic field sensor MB80-12GM50-E0-PUR [22] 76
Figure 54-Omron E2K-C Series [23].......... 77
Figure 55-Siemens SITRANS LUT400 Series [25] 78

List of Tables

Table 1-Performance Specification Table 32
Table 2-Generating Alternatives Table 34
Table 3-Evaluation Chart 37
Table 4-Stage Criteria Table 43
Table 5-Material Selected for Finite Element Analysis 44
Table 6-Plate FEA Results 52
Table 7-Mass Flow Rate CFD Results 58
Table 8-Datasheet for Actuator [18] 62
Table 9-Pipe CFD Results 66
Table 10-Pipe Support Frame-FEA Results 68
Table 11-Plare Design Results Summary 70
Table 12-Pump Design Results Summary 71

1 Introduction

1.1 Purpose of the Study

This maters’s thesis will be conducted on a subject provided by the maintenance department of LKAB Norge AS. This study allows the use of various engineering and design skills that have been taught in the Master of Engineering Design program to come up with a technical and an innovative solution for LKAB Norge AS.

1.2 Background

1.2.1 Brief Overview of LKAB

LKAB, or Luossavaara-Kiirunavaara AB, is a Swedish multinational mining and minerals company that specializes in iron ore production. Established in 1890, LKAB is one of the oldest and largest iron ore producers globally. The company primarily operates in northern Sweden, where it runs its main iron ore mines, such as Kiruna and Malmberget.

LKAB's primary focus is on producing high-quality iron ore pellets, which are essential for steel production. The company is committed to sustainability and innovation, continuously working on enhancing its production methods to minimize environmental impact and improve operational efficiency.

Apart from iron ore, LKAB also explores and produces other minerals like rare earth elements, phosphorus, and zinc. The company invests in new technologies and processes through its strong research and development department to optimize its operations and expand its product portfolio.

LKAB plays a crucial role in the Swedish economy, employing thousands of people directly and indirectly. The company is also actively involved in community development initiatives and collaborates with educational institutions to promote STEM education and research.

1.3 Problem Statement

A significant operational challenge has been identified in the form of water ingress within the silos. Preliminary observations suggest that the water could be penetrating through the hatches located above the underground silos. Additionally, there is a growing concern that over time, the internal walls of the silos may have developed cracks, thereby allowing water to seep into the system. Consequently, this infiltrating water accumulates along the TR010 conveyor positioned beneath the silos, often inundating the entire 600-meter stretch. The Figure 1 below illustrates the silo and the conveyor TR010.

The presence of this water not only presents a logistical challenge but also poses a risk of damaging critical infrastructure. Upon activation of the conveyor, the water is transferred to subsequent conveyors, culminating in the flooding of the screening station. Beyond causing operational disruptions, this situation poses a significant risk to the machinery, including the degradation of essential components such as idlers and pulleys, and creates adverse working conditions for the personnel involved.

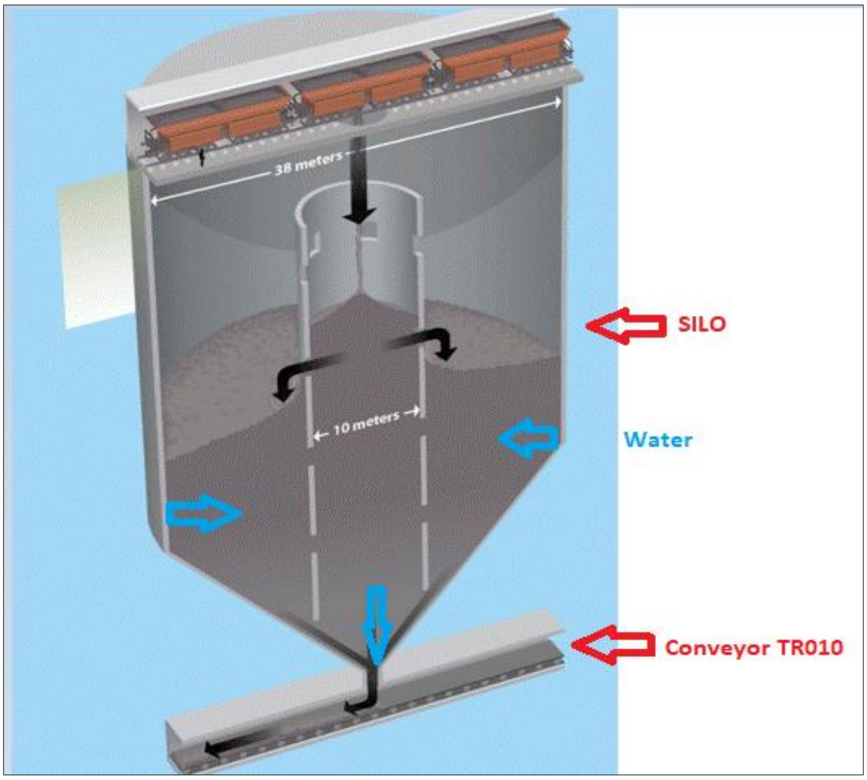

Figure 1-Infographic depicting the water accumulation in TR010 conveyor. (Source: LKAB)

Water flooding in conveyor belts of iron ore storage silos is a common issue faced in the iron ore industry. This problem occurs when water accumulates on the conveyor belt's surface within the silo, leading to reduced efficiency, increased maintenance costs, and potential safety hazards. This paper will discuss the causes of water flooding in conveyor belts of iron ore storage silos, its impacts, and provide potential solutions to mitigate this problem.

1.4 Significance of the Study

The development of a system to counter water flooding in conveyor belts holds significant importance, as it addresses numerous challenges faced by industries such as mining, agriculture, construction, and food processing facilities. The proposed solution offers an effective method for water removal without requiring any modifications to the conveyor or interrupting the production and transportation processes. These solutions aim to improve operational efficiency, reduce maintenance costs, enhance equipment reliability, promote worker safety, and optimize environmental management and material handling processes. By effectively managing water removal and preventing damage to conveyor belt components, the system ensures smooth transportation of materials, prolongs equipment lifespan, and maintains optimal production levels while minimizing potential hazards for workers and promoting sustainability.

2 Literature Review

This chapter presents a comprehensive review of existing literature relevant to water flooding in conveyor belt systems, with a particular focus on the iron ore mining sector. The chapter explores the context of mining practices and their evolution, highlighting the pivotal role of conveyor belts in bulk material handling. It examines various studies on the challenges posed by water accumulation in conveyor systems, the effectiveness of current water removal methods, and the impact of these issues on operational efficiency and safety. Additionally, a critical analysis of relevant patents and technological advancements in water removal solutions provides insights into innovative methods and devices that could improve water management in conveyor systems. This review forms the foundation for the proposed design solutions presented later in this report.

2.1 Bulk Material Handling in Mining

Bulk material handling systems are essential in the mining sector, playing a vital role in the movement, storage, and control of materials. These systems are designed to handle large volumes of materials, such as ores and minerals, in an efficient, safe, and environmentally friendly manner. Two integral components of these systems are silos for storage and conveyor belts for transportation. (See Appendix A - LKAB Drawing for LKAB silo and conveyor drawing)

2.1.1 Storage Solutions: Tanks and Silos

Storage solutions in various industries, including mining and agriculture, commonly involve the use of tanks and silos. Tanks are often employed for the storage of liquids and gases, providing a crucial function in the chemical, petroleum, and food processing sectors. Silos, on the other hand, are essential for storing bulk materials like grains, powders, and granules, as seen in agriculture, mining, and manufacturing industries. Both storage systems are integral in ensuring the efficient handling, preservation, and distribution of different materials, thus contributing significantly to the operational flow of supply chains and industrial processes. However, in the context of this discussion, silos hold a more pertinent role. Their design and functionality cater specifically to the needs of bulk solid storage, making them more relevant for detailed exploration. They offer unique advantages in terms of space utilization, material preservation, and automated handling, aspects that are crucial in the handling of solid materials.

2.1.1.1 Significance and Functioning

Storage silos are large, vertical, or inclined structures designed to store bulk materials. They offer several advantages, such as:

1. **Efficient storage:** Storage silos provide a controlled environment for storing materials, protecting them from external factors like weather, pests, and contamination.
2. **Easy handling:** These structures facilitate the handling and distribution of materials, enabling efficient transportation and processing.
3. **Space optimization:** Storage silos allow for the storage of large quantities of materials in a compact space, reducing the need for extensive storage areas.

2.1.1.2 Advantages and Disadvantages of concrete silos

The building of silos in concrete offers several advantages:

- Concrete silos are economical to construct and maintain (they require virtually no maintenance). Construction is relatively inexpensive because the basic materials for making concrete are usually locally available and suitable special building methods make rapid construction possible.
- Concrete silos are relatively insensitive to mechanical influences, whereas steel silos, for example, when used for storing environmentally polluting or dangerous substances must be surrounded by protective concrete walls to assure the required degree of safety.
- Concrete silos are eminently suitable for the storing of a very wide variety of substances; for example, if provided with a suitable liner, they may even be used for low temperature liquefied gases [1].

Unfortunately, concrete silos do have their disadvantages too. The most common problems with concrete silos are with leaks and cracks. Because concrete is incredibly strong, it’s also inflexible. This means that as it expands and contracts over time, the concrete itself will weaken and eventually begin to crack. Not only can cracked silos lead to the obvious problem of water seepage, but cracks in the concrete can also provide potential harmful bacteria with the opportunity to grow [2].

Figure 2-Excavation and Construction of Underground Silos for Iron Ore Storage, (LKAB, Narvik)[3].

In conclusion, underground storage silos for iron ore present a promising and sustainable solution for the efficient and safe storage of this vital raw material. By offering increased capacity, enhanced safety, and reduced environmental impact, these innovative structures play a crucial role in the modern iron ore handling industry. As technology and engineering techniques continue to advance, we can expect to see further development and adoption of underground storage silos, shaping the future of iron ore storage and transportation.

2.1.2 Belt Conveyors

Belt conveyors are among the most widely used forms of material transport in industries such as mining, agriculture, and manufacturing. Their ability to transport both bulk and unit loads over short and long distances makes them indispensable in many industrial processes. The diversity in conveyor types reflects the varied requirements of handling different materials under varying operational conditions.

2.1.2.1 Advantages and Applications

Conveyor belts offer several advantages, such as:

1. **Efficient transportation:** They facilitate the movement of materials and goods over long distances, reducing the need for manual handling and minimizing the risk of injury or damage.
2. **Automation:** Conveyor belts contribute to the automation of manufacturing processes, enhancing productivity, and reducing labor costs.
3. **Material handling:** They enable the handling of various materials, including heavy loads, fragile items, and bulk products, ensuring proper handling, and minimizing damage.

2.1.3 Water Flooding: Causes and Effects

Causes of Water Accumulation: Outdoor conveyor systems are directly exposed to rain, introducing significant amounts of water to the system. Snow and ice accumulating on conveyors can melt, contributing additional moisture, particularly in colder climates. In industries such as mining, washing stages can lead to water being carried onto and along the conveyor belt. High humidity or significant temperature differences can also cause condensation on the conveyor belt and its components. Operations that handle liquids may experience spills, leading to water accumulation on the conveyor system. Leaks or overflows from piping systems near or above conveyors can result in water exposure. Particularly in sectors like food processing or pharmaceuticals, conveyor belts undergo regular cleaning with water or cleaning solutions. Certain industrial processes use water sprays to cool products on the conveyor, adding moisture to the belt. In operations with significant dust generation, such as mining or bulk material handling, water sprays are used for dust suppression, introducing moisture to the conveyor area.

Effects of Water Accumulation: Water damage to belt conveyors affects various components of the system, impacting operational efficiency, equipment longevity, and workforce safety. This section explores specific components susceptible to water damage, the mechanisms of such damage, and the broader implications of water presence in the work environment.

Essential for supporting the conveyor belt and materials, idlers and rollers can corrode when exposed to water, particularly if it contains contaminants, compromising their structural integrity and functionality [4]. Bearings facilitate the smooth operation of rollers and pulleys. Water exposure can lead to lubrication washout, increasing friction, causing overheating, and eventual failure [5]. Gears and motors, which propel the conveyor belt, are also vulnerable to water-induced corrosion and electrical short circuits. Corrosion of the roller tube accelerates the destroying of the belt ultimately exposing the core of the belt [6].

The presence of excess water can significantly increase the risk of slip and fall accidents, posing serious injury risks to the workforce. Water intrusion into electrical systems not only compromises conveyor operations but also elevates the risk of electrical shocks to workers. Damp environments can foster health issues, including respiratory problems from mold and mildew growth, highlighting the need for effective moisture control.

2.2 Review of Problems and Solutions

2.2.1 Existing Problems with Current Solutions

To remove water from a flooded underground conveyor belt, several methods or techniques can be employed. These are discussed in detail below:

2.2.1.1 Pumping

Pumping is an essential method to remove water from flooded iron ore conveyor belts, as it helps in quickly and efficiently draining the accumulated water. The pumping method involves the use of various types of pumps, such as submersible pumps, high-capacity pumps, or even vacuum systems, depending on the specific situation [7].

2.2.1.2 Vacuuming

The vacuuming method relies on the principles of pressure difference and airflow. When a vacuum system is applied to a flooded area, it creates a pressure difference between the vacuum source and the water-filled space. This pressure difference drives airflow, which in turn removes water from the surface of the iron ore conveyor belt. Several vacuum systems and associated equipment can be used for removing water from flooded iron ore conveyor belts [8]. Various hoses, nozzles, and filters are essential components of vacuum systems, ensuring efficient water removal and preventing any clogging or damage to the equipment [9].

2.2.1.3 Gravity Drainage

The Gravity Drainage method relies on the principles of gravitational force and hydraulic gradient. When a slope is created, gravity pulls the water downhill, allowing it to flow away from the iron ore conveyor belt. This process is facilitated by the establishment of a hydraulic gradient, which is the rate at which the water level decreases along the slope [10].

2.2.1.4 Air Movement/Air Knives

Iron ore conveyor systems play a critical role in the mining and processing industry by facilitating the transportation of raw materials for further refinement. However, these systems are susceptible to flooding, particularly in scenarios where water ingress occurs due to natural elements or equipment failures. The accumulation of water on conveyor belts not only hampers operational efficiency but also poses risks of material degradation and equipment damage. In such situations, the use of air movement and air knives presents a viable solution for rapid and effective water removal.

Air knives are specialized devices that generate high-velocity air streams in a laminar flow pattern. These devices are typically positioned along conveyor belts to blow compressed air across the surface, effectively shearing off and carrying away excess water. Air knives come in various designs, including straight blades, curved blades, and adjustable nozzles, allowing for tailored air distribution based on the contours of the conveyor system. The operation of air knives is contingent upon factors such as air pressure, nozzle orientation, and nozzle-to-surface distance, all of which influence the efficiency of water removal [11].

2.2.1.5 Water Collection Trays

In the context of our ongoing exploration of solutions to counteract water accumulation on conveyor systems, an innovative approach involves the development of a contraption that harnesses the movement of the conveyor belt itself to facilitate water drainage. This device, strategically integrated into the conveyor system, is designed to optimize the removal of water, leveraging the kinetic energy generated by the moving belt to create a self-powered drainage solution. This section outlines the conceptual framework and potential benefits of such a device, considering its integration as part of a comprehensive strategy to enhance conveyor system efficiency and longevity.

The proposed contraption operates on the principle of utilizing the conveyor belt's motion to generate a flow that directs water away from the belt surface. By introducing a device onto the belt conveyor, this device guides the accumulated water towards designated drainage outlets. The design of the device can be optimized based on fluid dynamics principles to maximize water expulsion efficiency without hindering the conveyor belt's material transport capabilities.

Optimizing the design of the drainage device involves several key considerations:

Positioning and Angulation: Strategic placement of the device ensures that water is collected efficiently from the belt's surface. Angulation is optimized to use gravity to assist in water flow, enhancing the efficiency of water removal without requiring additional energy inputs.

Channel Design: The geometry of the channels or grooves is critical. Their design should minimize resistance to water flow, ensuring that water is swiftly guided away from the belt. Computational fluid dynamics (CFD) simulations can play a crucial role in determining the optimal shape and size of these channels to facilitate smooth water flow.

Material Selection: Materials used in the construction of the drainage device must be durable and resistant to corrosion and wear from continuous contact with water and the conveyed materials. Additionally, the choice of material should consider the environmental impact, opting for sustainable or recyclable options where possible.

2.2.1.6 Inclined & Perforated Conveyor Belts

Conveyor Belts: Leveraging Gravity for Efficiency

Inclined conveyor belts embody a straightforward yet effective mechanism for mitigating water accumulation. By introducing an angle of elevation, these belts capitalize on gravity to facilitate the swift drainage of water, thereby curtailing the contact between water and the belt surface. This not only aids in preserving the integrity of the conveyor belt but also enhances the overall operational efficiency by reducing the risks of slippage and corrosion. The selection of an optimal inclination angle is crucial, requiring a balance between efficient water drainage and the stable conveyance of materials.

Perforated Conveyor Belts: Engineering Precision for Drainage

Perforated conveyor belts offer a more direct approach to water management through their design, which incorporates strategic perforations across the belt surface. These openings allow water to pass through the belt rather than pooling on its surface, presenting an efficient solution to the challenges of water accumulation in both indoor and outdoor conveyor applications. The design considerations for perforated belts involve a careful assessment of the size and distribution of perforations to ensure that they facilitate effective drainage without compromising the conveyor's ability to transport materials securely.

Once the water has been removed from the conveyor belt through gravity drainage, it needs to be collected and removed from the system. Drainage systems, such as pipes, sumps, or gravity-fed channels, should be installed to transport the water away from the conveyor belt area [12].

2.2.2 Evaluation of Current Solutions

In addressing the issue of water accumulation on conveyor systems, a diverse array of solutions has been explored, each offering unique benefits and challenges. These methods range from traditional approaches such as pumping and vacuuming, which provide rapid water removal capabilities but may necessitate significant energy use and maintenance, to more passive techniques like gravity drainage, which utilizes gravitational forces for water expulsion with minimal energy requirements. Innovations in air movement, specifically through the use of air knives, offer a non-contact method for water removal, while the design modifications in conveyor belts, including inclined and perforated variants, present proactive approaches to mitigate water accumulation directly at the source.

It is important to note that some of these solutions require major modifications to existing conveyor systems, potentially involving extensive redesign and investment. As the report progresses, we will evaluate these solutions in greater detail in later chapters, aiming to develop an optimized approach by potentially combining multiple solutions based on their efficacy, energy efficiency, and ease of integration.

Before advancing to the solution development phase, the next topic will delve into relevant patents in the field of conveyor system design and water management. This exploration will provide valuable insights into existing technologies and innovations, laying the groundwork for identifying opportunities for improvement and innovation in our approach to addressing water accumulation on conveyor systems.

2.3 Innovative Approaches and Patents

In addressing the challenge of water removal in conveyor belt systems, a key area of focus has been the development of specialized methods to enhance efficiency and sustainability. Two notable advancements, set to be discussed in detail, have made significant strides in this regard:

- **JP2000318827A [13]**: "Belt Conveyor Draining Method and Device" Filed by Nippon Steel Corporation, this Japanese patent introduces an inventive method and apparatus for removing water from belt conveyors, particularly addressing the challenge of accumulated rainwater on outdoor conveyors. The innovation lies in altering the belt's cross-sectional shape to an inverted U-shape, facilitating efficient water drainage without interrupting conveyor operations. This method not only enhances safety and efficiency by preventing material slippage but also offers a cost-effective solution to water accumulation issues prevalent in industries like mining and steel production.
- **KR 101500125 B1 [14]**: "Belt Conveyor with Moisture Separation Device" Filed by POSCO, this South Korean patent describes a belt conveyor equipped with a moisture separation device, aiming to improve operational efficiency by seamlessly separating and removing moisture from materials during transport. The system comprises a drainage belt and a vibration-inducing component to enhance moisture separation, designed to operate without halting the conveyor. While offering a novel solution to moisture management challenges in bulk material handling, the implementation of this technology requires careful consideration of potential costs, risks, and irreversible changes to existing conveyor systems.

These technologies reflect the evolving landscape of material handling, specifically targeting the challenges associated with moisture in conveyor belt systems. The subsequent sections will explore the intricacies of these methods, shedding light on their operational mechanisms and contributions to modern material handling solutions.

2.3.1 Examination of JP2000318827A [13]: Belt Conveyor Draining Method and Device

Introduction

In addressing the operational challenges faced by industrial sectors, particularly within environments exposed to the elements, the innovative solutions provided by patents like JP2000318827A play a pivotal role. Filed by Nippon Steel Corporation on April 21, 2000, and officially published on October 27, 2004 [13], this patent introduces a revolutionary method and apparatus for the efficient removal of accumulated water from large, outdoor conveyor belts—a recurrent complication in industries such as mining and steel production. The inventive approach delineated in JP2000318827A not only optimizes operational efficiency but also significantly elevates safety standards, offering a cost-effective solution to a widespread issue.

The urgency of mitigating water accumulation on conveyor systems (as depicted in Figure 3) cannot be overstated. Conveyor belts, especially those extending over 200 meters in length and with widths ranging between 1200 to 1600 mm, are integral to the transportation of vast quantities of materials. However, their outdoor deployment renders them susceptible to rainwater accumulation, engendering operational inefficiencies and safety hazards. Through the lens of JP2000318827A, a novel method and apparatus are proposed, heralding a new era in conveyor belt maintenance and functionality by leveraging mechanical alterations to expel water effectively.

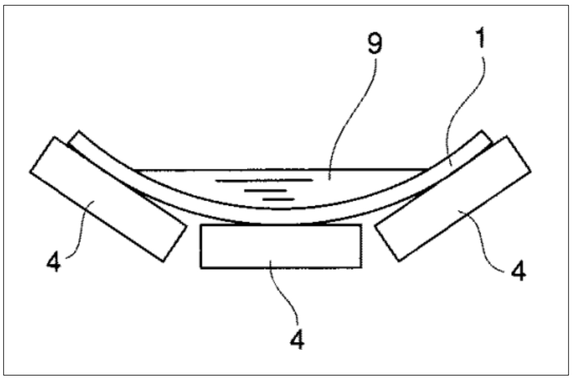

Figure 3-Depiction of water accumulation in belt conveyor[13].

Overview of the Invention

The core innovation of the patent lies in its unique approach to altering the conveyor belt's cross-sectional shape for enhanced water removal [13]. By pressing down on both edges of the belt, the invention transforms its shape into an inverted U, facilitating the efficient expulsion of water. This method contrasts sharply with traditional practices, which either inadequately address the problem or necessitate costly modifications to the conveyor system.

The water removal technique advocated by the patent involves a strategic alteration of the belt's shape at specific segments of the conveyor line, particularly where the belt transitions from horizontal to incline [13]. This is achieved by installing edge-pressing rollers that apply downward pressure on both sides of the belt, molding its cross-section into an inverted U-shape. This shape change is crucial for the method's effectiveness, allowing for the swift and complete removal of accumulated water.

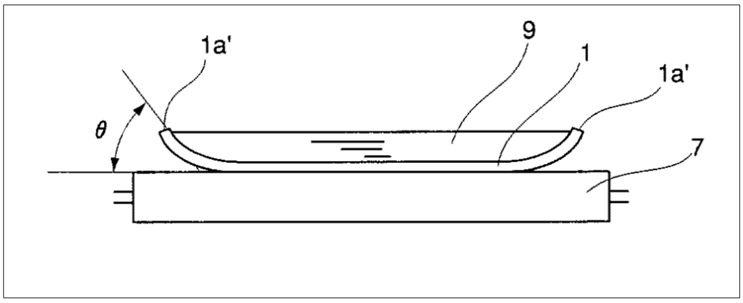

Figure 4-Flat carrier roller [13].

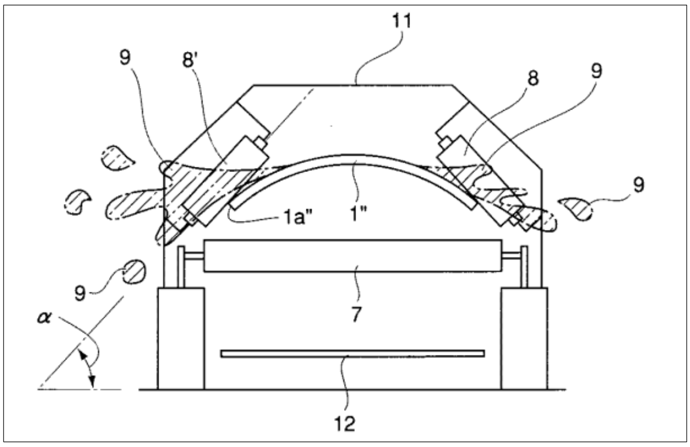

Figure 5-Edge-pressing roller inverting the belt [13].

The patented device comprises two main components: edge-pressing rollers and flat carrier rollers [20]. The two figures, Figure 4 and Figure 5, show these rollers. The edge-pressing rollers are instrumental in achieving the belt's inverted U-shape, while the flat carrier rollers support the belt's modified configuration. The device's strategic placement and configuration are pivotal to its success, ensuring that water removal does not interfere with the conveyor's normal operation or the safety of the transported materials.

Operational Advantages

Implementing this water removal system presents numerous benefits, including significantly reduced downtime due to water-related issues, minimized risk of material slippage or loss, and the avoidance of costly conveyor modifications [13]. Furthermore, the method's efficiency in removing water ensures that the conveyor belt can quickly return to optimal operating conditions, even after heavy rainfall. The interplay between the edge-pressing rollers and flat carrier rollers is meticulously designed to ensure the belt's modified configuration does not impede the transportation of materials or compromise the system's structural integrity (Figure 5 and Figure 6).

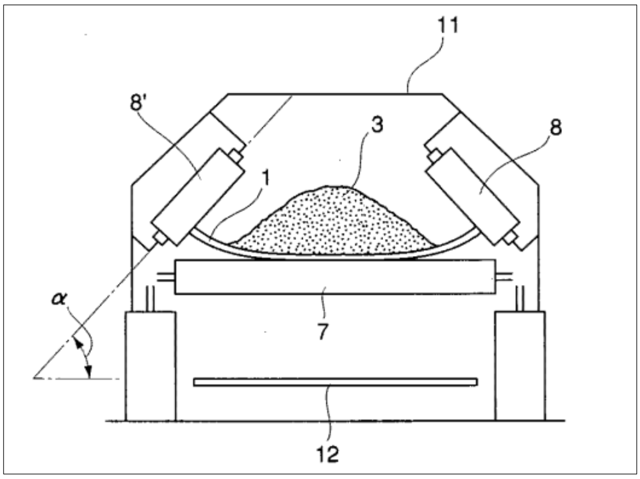

Figure 6-Belt when transporting material [13].

Conclusion

The innovation introduced in JP2000318827A marks a substantial advancement in the maintenance and operation of conveyor belts, addressing the critical issue of rainwater accumulation with a novel mechanical alteration. By transforming the belt's cross-sectional shape to facilitate effective water removal, this patent offers a pragmatic solution poised to significantly enhance industrial safety and operational efficiency. However, it's important to acknowledge that the implementation of this system may require substantial reconfiguration of existing conveyor setups. This level of modification introduces inherent risks, including potential disruptions to established workflows and the possibility of unforeseen complications arising from the integration of new components. Despite these challenges, the potential benefits of improved water management and reduced downtime present a compelling case for consideration. As industries continue to seek more reliable and efficient conveyor solutions, the insights provided by JP2000318827A will undoubtedly contribute to the ongoing evolution of conveyor technology, albeit with a cautious approach to its adoption and integration.

2.3.2 Examination of KR101500125B1 [14]: Belt Conveyor with Moisture Separation Device

Introduction

In a significant advancement filed by POSCO on August 14, 2013, and officially registered on March 2, 2015, the patent KR101500125B1 [14] reveals a sophisticated moisture separation device seamlessly integrated into a belt conveyor system. This invention, credited to inventors Na Jo-hyun and Kang Ju-wan, addresses critical operational inefficiencies and challenges encountered in industries such as steel manufacturing, where moisture in bulk materials can severely impact processing and transportation efficiency. By introducing a dual-component system that facilitates moisture separation from materials like raw coal during conveyance, all without halting conveyor operations, this innovation marks a pivotal shift towards enhancing operational continuity and productivity.

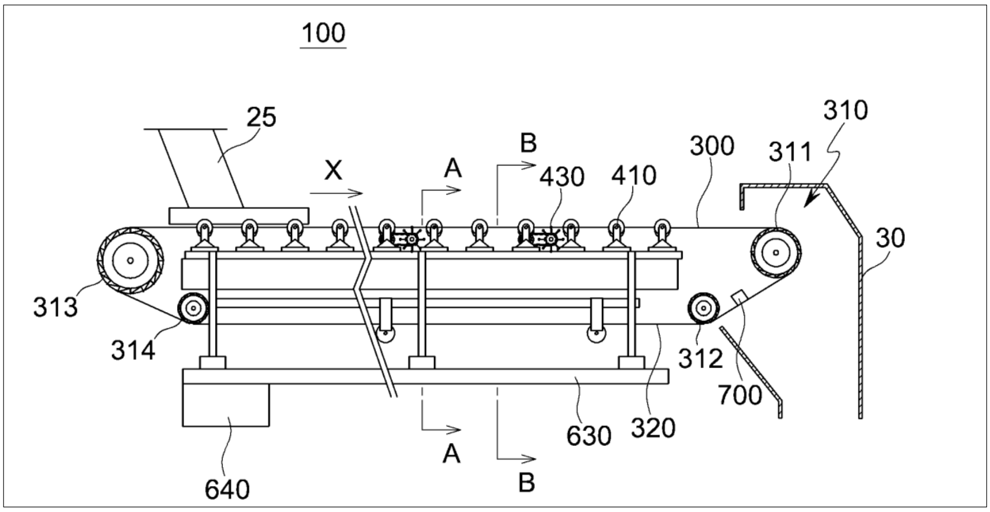

Figure 7-General setup, side view[14].

Conceptual Framework and Mechanism

Central to this patent is a two-component system designed to enhance the conveyor belt's functionality by efficiently separating contained moisture from the transported materials. The first component is a drainage belt made of a permeable material that facilitates the separation of moisture. The second, a vibration-inducing moisture separation part, is connected to the drainage belt, enhancing moisture separation by agitating the transported materials (Figure 7 shows the side view and Figure 8 illustrates the cross-sectional view).

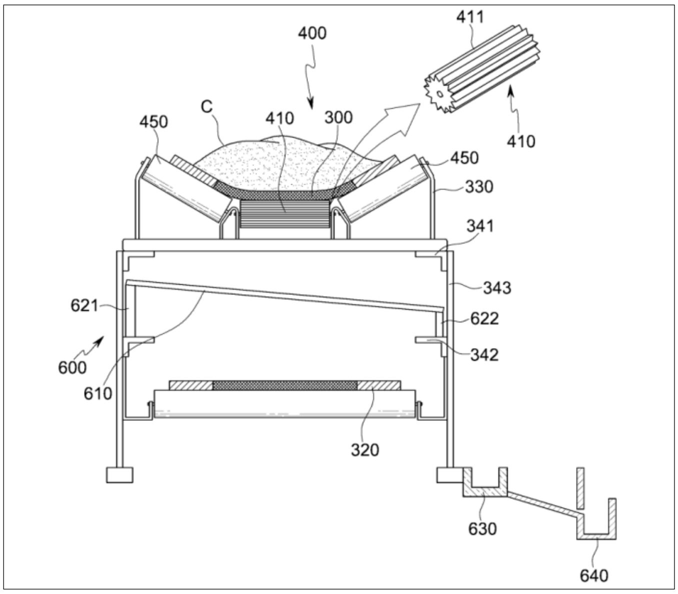

Figure 8-General Setup, cross-sectional view[14].

The device operates on a principle where upon detection of moisture by the control unit, the drainage belt is selectively activated to separate and remove moisture from the materials being transported. Notably, this process does not interrupt the conveyor's operation, significantly boosting productivity and operational efficiency.

Detailed Operational Insights

The moisture separation device includes multiple belt support frames underneath the drainage belt. A notable feature is the first vibration roller, which is in contact with the underside of the drainage belt, equipped with multiple vibration protrusions to facilitate moisture separation through agitation (Figure 9 and Figure 10 detail this interaction).

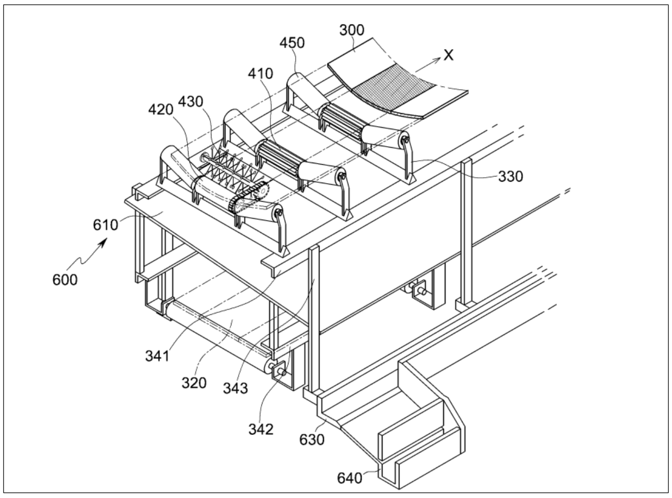

Figure 9-Illustration of agitation mechanism [14].

An innovative aspect of the design is the second vibration roller, positioned to strike the underside of the drainage belt enhancing the separation process with additional mechanical agitation. This roller's design includes a chain linkage to a rotary roller, expanding the vibratory effect across the belt's surface (Figure 10).

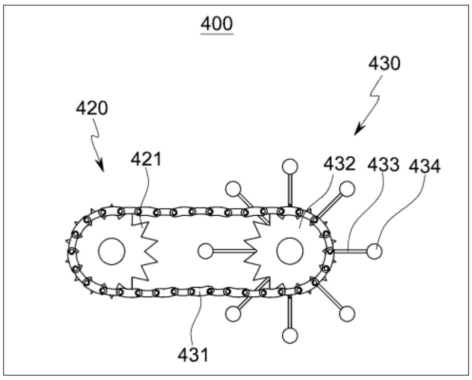

Figure 10-Chain linkage close-up[14].

For effective moisture drainage, the drainage belt incorporates a mesh made from steel wire, coupled with a filter fabric that allows moisture to pass while retaining the transported materials. This component is crucial for ensuring that separated moisture is efficiently drained away from the conveyor (Figure 11).

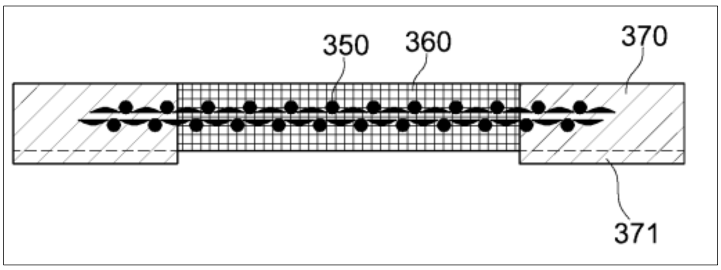

Figure 11-Cross-sectional View of the Conveyor Belt Demonstrating Water Drainage Through Perforations[14].

Implications and Utility

KR101500125B1's introduction of a moisture separation device within a belt conveyor system marks a significant leap in addressing the longstanding challenge of moisture management in bulk material transportation. The device's ability to operate without interrupting the conveyor's workflow presents a revolutionary approach to maintaining operational efficiency, particularly in environments where moisture content can significantly impact material handling processes.

The patent exemplifies a sophisticated blend of mechanical engineering and practical innovation, providing a solution that not only enhances the functionality of belt conveyors but also contributes to the sustainability and efficiency of industrial operations.

Conclusion

While POSCO's invention detailed in KR101500125B1 [14] represents a significant technological leap forward, offering a novel solution to the pervasive challenge of managing moisture in conveyor systems, it's imperative to approach its integration with careful consideration. The installation of this moisture separation device onto existing conveyor systems may necessitate substantial modifications or even complete overhauls of the current infrastructure. Such processes not only entail considerable financial investment but also introduce a level of risk associated with the potential for operational disruptions during the integration phase. Furthermore, once implemented, reversing these modifications could prove to be either highly challenging or outright impossible, locking the system into a specific operational mode. This permanence demands a thorough evaluation of the potential long-term impacts on the conveyor system's functionality and the broader operational ecosystem. Therefore, while the innovative approach to moisture separation presented by this patent promises to elevate operational efficiency and safety, the implications of its adoption extend beyond immediate benefits, warranting a comprehensive assessment of its feasibility, costs, and potential risks involved.

3 Product Design

In the development of the water removal system, the rational model of design as articulated by Nigel Cross [15] has been employed to systematically devise and refine our solution. In our case during the design process, it is assumed that the water flooded conveyors have little amount of raw material on it. And when the raw material is present the system should not attempt water removal.

This methodology underscores a logical, structured approach to design, emphasizing the analysis of the problem, generation of solutions, and iterative testing. The specific process steps utilized in our project, which align with Cross's principles, are detailed in the Figure 12. This visual representation illustrates how each phase of the design was approached and executed, ensuring a methodical progression from conceptualization to final design. It shall be noted that most of the parameters in the following tables and charts are based on assumptions and intuitions instead of experimentation.

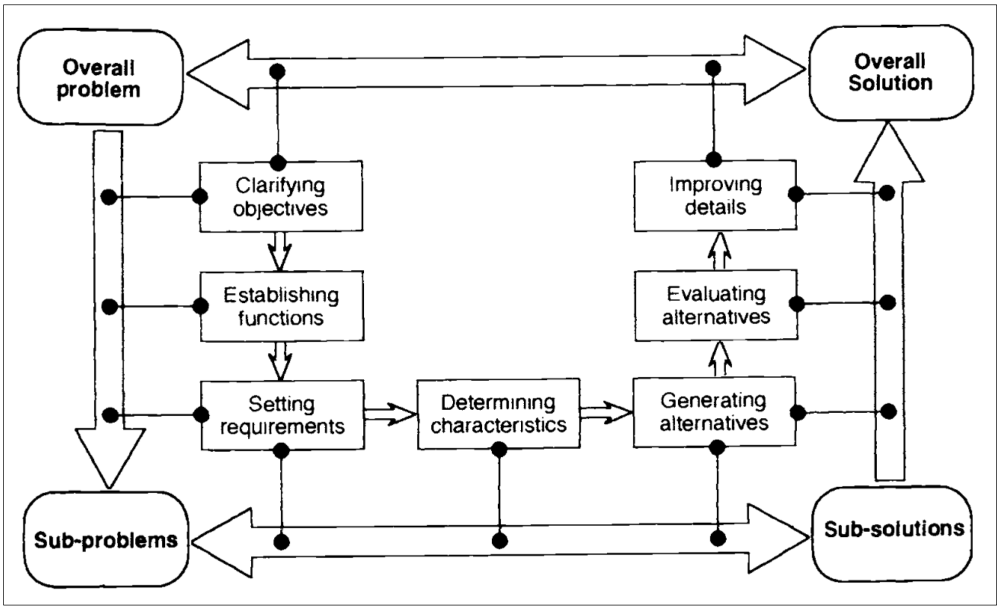

Figure 12-Rational Method Chart [15]

3.1 Clarifying Objectives

In the 'Clarifying Objectives' stage of our design process, we meticulously define the essential goals and functionalities that the product must fulfill. This step is crucial as it sets the foundational objectives that guide all subsequent design decisions. An 'Objectives Tree' is used to systematically break down and display these goals, illustrating a clear hierarchy of primary and secondary objectives. This visualization aids in ensuring that every aspect of the product design is aligned with achieving these defined outcomes.

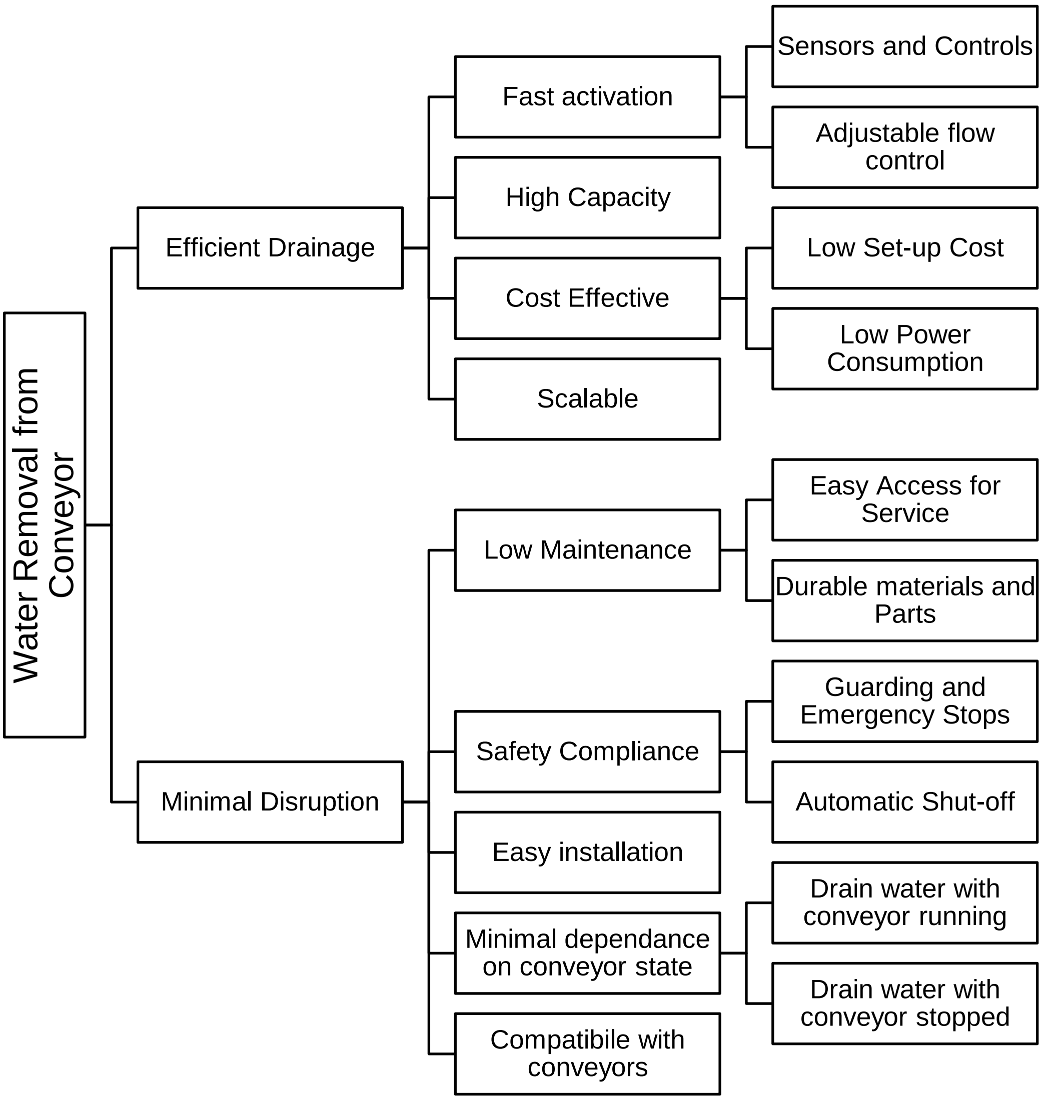

Figure 13-Objectives Tree

3.2 Establishing Functions

In the 'Establishing Functions' phase of our design process, we delineate the specific functions that the product must perform to fulfill the objectives previously set. This crucial step ensures that the design's functionality aligns directly with its goals. To visually represent and organize these functions and the methods of their execution, a 'Function and Means Tree' is employed. This chart not only lists the functions required but also maps out the various means through which each function will be achieved. It serves as a critical tool for tracing how each function contributes to meeting the overall objectives and for identifying the most effective methods for implementation.

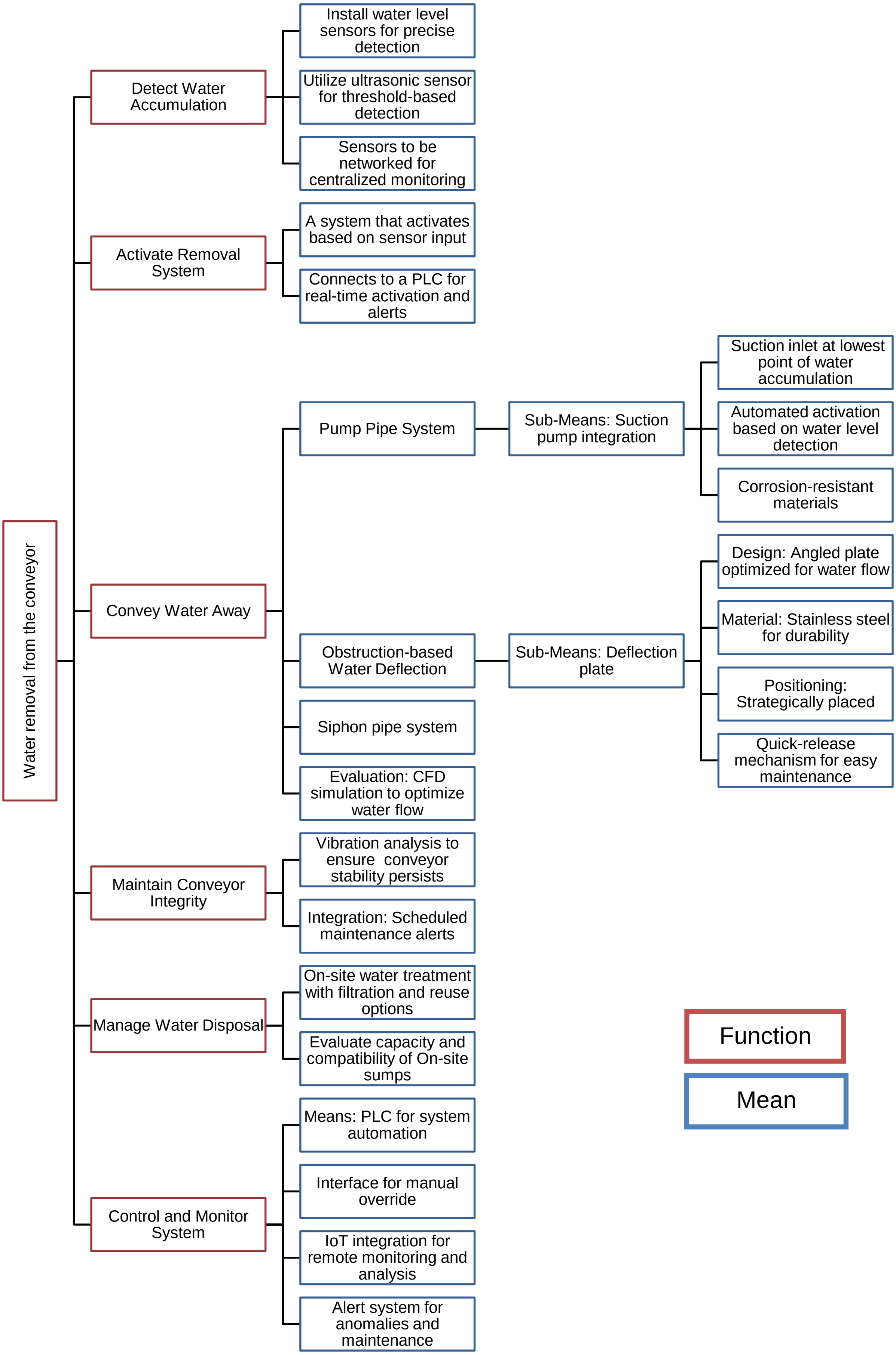

Figure 14-Functions and Means Tree

3.3 Setting Requirements

In the 'Setting Requirements' stage of our design methodology, we specify the performance criteria that the product must meet. This crucial phase involves outlining the precise targets and acceptable tolerances for various specifications, ensuring that the product performs reliably under expected conditions. A 'Performance Specification Table' is utilized to systematically list these requirements, providing a clear and organized reference for the desired characteristics of the product. This table not only serves as a guideline for design and testing but also as a benchmark for evaluating the product’s adherence to its functional and operational goals.

Table 1-Performance Specification Table

Specification	Requirement	Measurement Method	Target	Tolerance
Water Detection Sensitivity	Must accurately detect minimal water presence on the conveyor	Sensor output vs. actual water depth comparison	≤ 0.01 m (1 cm)	± 0.001 m (±1 mm)
Water Removal Rate	The system's capacity to remove water from the conveyor	Mass of water removed per second (m^3/s)	≥ 500 kg/s (0.5 m^3/s)	± 5.00 kg/s
System Activation Time	The delay between water detection and the start of the removal process	Time from detection signal to system activation	≤ 5 seconds	± 1 second
Energy Consumption	Energy usage by the water removal system during its operation	Measurement in kilowatt-hours (kWh)	≤ 100 kWh per day	± 0.5 kWh
Noise Level	Noise emitted by the system should not exceed a comfortable level	Measured in decibels (dB) at 1 meter from source	≤ 80 dB	± 5 dB
Maintenance Frequency	Specifies the intervals for routine checks and maintenance to maintain optimal performance	Based on operational hours or calendar time	Every 6 months	N/A
System Durability	The expected operational lifespan without major repairs or performance degradation	Ageing tests, historical data of similar systems	≥ 5 years	± 1 year
Environmental Compliance	Compliance with environmental standards and regulations	Review of environmental certifications and audits	100% compliance	N/A
Installation Compatibility	The system's adaptability to different conveyor configurations without significant modifications	Compatibility tests with various conveyor models	High flexibility	Custom modifications if necessary
Water Disposal Efficiency	Effectiveness in conveying the removed water to the designated disposal or treatment system	Efficiency rate measured by water volume successfully conveyed to disposal	≥ 85% efficiency	± 2%
Pump System Efficiency	The efficiency of the pump in terms of energy use versus water volume pumped	Energy used per cubic meter of water pumped (kWh/m^3)	≤ 0.02 kWh/m^3	± 0.005 kWh/m^3
Operational Safety	The system must operate safely without posing risks to conveyor operations or personnel	Safety audits, incident reports	Zero safety incidents	N/A
Water Detection System Redundancy	The presence of backup systems to ensure water detection continuity in case of primary sensor failure	Number of redundant systems and failover tests	At least 1 redundant system	N/A
Control System User Interface	The ease of use and accessibility of the system's control interface for operators	User feedback, usability testing	Intuitive UX design	Customizable interface as needed

3.4 Determining Characteristics

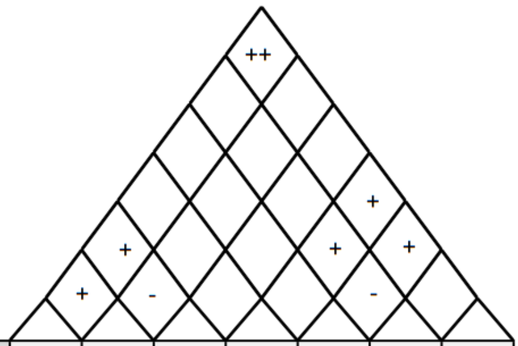

House Of Quality

	Minimize or Maximize			↑	↓	↓	↑	↓	↑	↑			
				Technical Specifications (How)							**Competitive Assessment**		
				Water removal Rate (m^3/min)	Noise Level (dB)	Energy consumption (kWh)	Maintenance access (measured qualitatively)	Installation time (hours)	Compatibility with existing system (qualitative assessment)	Modularity (qualitative assessment)			
	Customer Requirements (What)	**% Imp.**	**Imp.**	A	B	C	D	E	F	G	Our Sol.	JP	KR
1	Efficient Water Removal	17%	**4**	9	0	3	1	0	3	1	2	4	3
2	Low Operational Noise	4%	**1**	0	9	0	1	0	0	0	1	3	3
3	High Energy Efficiency	13%	**3**	3	0	9	0	0	0	2	2	3	4
4	Easy maintenance	13%	**3**	1	1	0	9	0	3	2	3	2	2
5	Easy to Install	13%	**3**	0	0	0	0	9	9	3	4	1	1
6	Minimal modification	21%	**5**	3	0	0	3	3	9	9	4	1	1
7	Scalable	21%	**5**	2	0	1	2	2	3	9	4	1	1
	Importance			**73**	**12**	**44**	**57**	**52**	**108**	**115**	**76**	**47**	**46**
	% Imp.			16%	3%	10%	12%	11%	23%	25%	Comparative Score		

Figure 15-House of Quality Chart

In the 'Determining Characteristics' phase of the design process, we utilize the House of Quality chart to methodically assess and prioritize the product specifications. This tool is integral in identifying which features are critical to meeting the customer and market requirements. It facilitates a structured comparison of our product against competitors, highlighting areas where our product excels or needs improvement. By mapping out relationships between customer desires and product features, the House of Quality chart enables us to focus our design efforts on enhancing key characteristics that are most valuable to users and essential for competitive differentiation.

3.5 Generating Alternatives

In the 'Generating Alternatives' stage of our design process, we systematically explore a range of potential solutions to fulfill the defined requirements and objectives. This exploration is crucial for fostering innovative designs and ensuring the final product is both effective and competitive. To facilitate this process, we employ a detailed table that lists various alternative designs. This table allows us to visualize and compare different approaches based on specific criteria such as feasibility, cost, and performance. By presenting these alternatives side-by-side, we can rigorously evaluate each option's potential before selecting the most promising one for further development. A total of three alternatives were generated as detailed in the following table. Each cell includes a letter (A, B or C) each of which denote which option has been chosen for a particular function to generate a particular alternate.

Table 2-Generating Alternatives Table

FUNCTION	OPTION 1	OPTION 2	OPTION 3	OPTION 4
Detect Water Accumulation	Ultrasonic sensors A	Float switches	Water level indicators B C	Capacitive sensors
Deployment Mechanism	Motor powered pulley C	Hydraulic or pneumatic System A B	Screw Jack System	Counterweight System
Activate Removal System	Sensor-triggered A B	Manual valve system	Hydrostatic pressure activation C	Hydrodynamic pressure activation
Convey Water Away	Obstruction-based design A	Suction pumps B	Self-starting siphon pipe C	Gravity-fed channels

Handle High Water Volume	Variable speed pumps B	Oversized channels/pipes C	Capable of handling surges A	High-capacity pumps
Energy Efficiency	Manual systems A	Low-energy consumption motors B	Zero-energy operation C	Efficient electric pumps
Maintenance Access	Self-cleaning systems	Easy-access panels A	Minimal moving parts C	Modular design B
Compatibility With Conveyors	Custom-fit designs A	Universal fit kits C	Easy retrofit to existing systems	Adjustable mounting system B
Scalability	Plug-and-play additional units	Adjustable output levels B	Extensible design for system expansion A C	Modular expansion slots
Safety Mechanism	Emergency Stop Button with Auto shutdown ABC	Manual Override	Alarm system	Automatic shutdown
Conveyor State for Operation	System operates when conveyor is stationary B C	System operates when conveyor is operating A		
Alternate: A	Plate-based Design			
Alternate: B	Pump-based Design			
Alternate: C	Siphon system			

3.6 Evaluating Alternatives

In the 'Evaluating Alternatives' stage of our design process, we employ a more analytical approach to assess the various design alternatives generated previously. This assessment is facilitated by transforming the objectives tree into a weighted objectives tree. Each objective within the tree is assigned a specific weight based on its relative importance to the overall project goals. This weighted system provides a structured framework for quantitatively evaluating how well each alternative design meets the defined objectives. By applying this method, we can systematically compare the alternatives, ensuring that the selected design maximizes alignment with our strategic goals and customer needs.

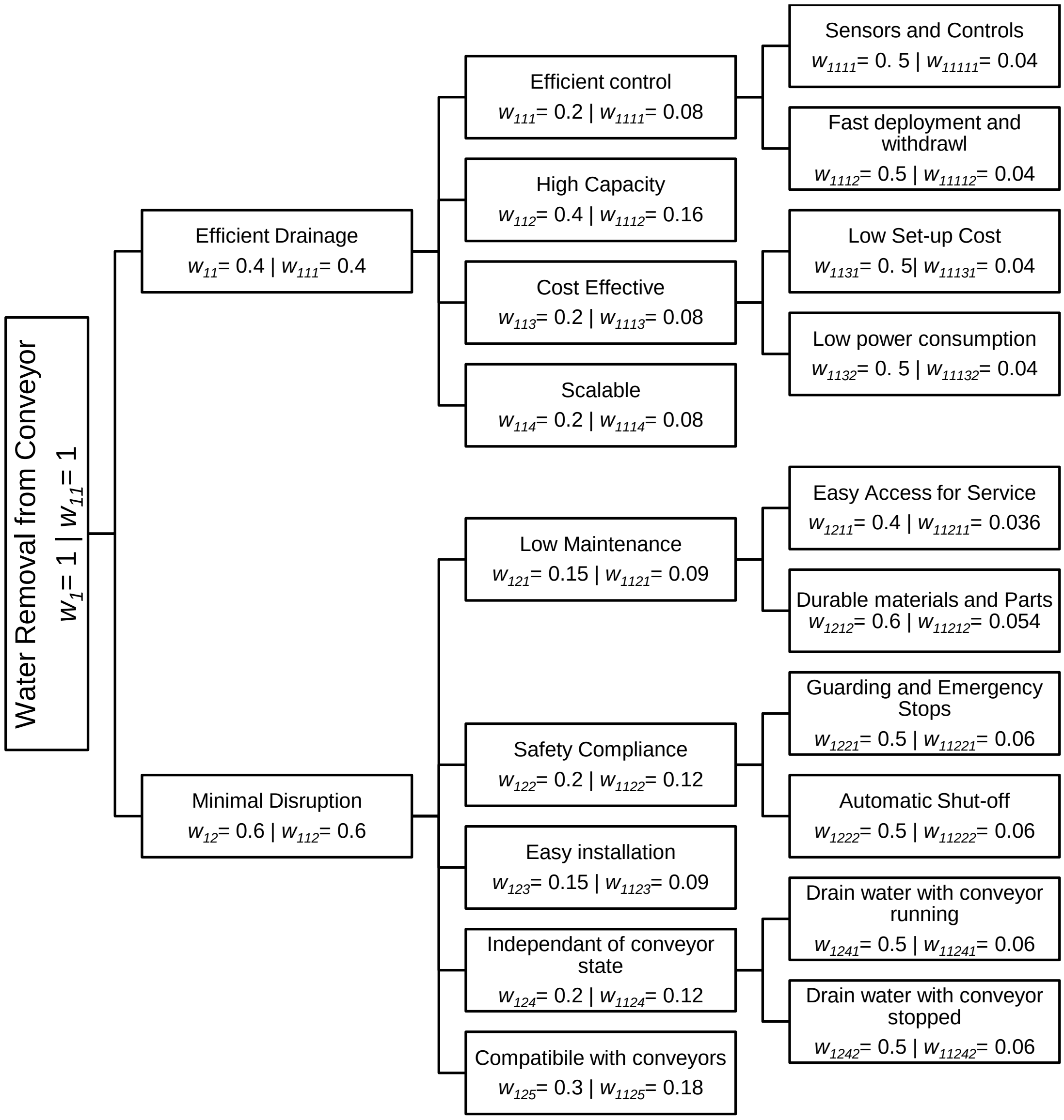

Figure 16-Weighted Objectives Tree

Later in the 'Evaluating Alternatives' stage, an evaluation chart plays a crucial role in assessing the various design alternatives. This chart allows us to systematically score each alternative against predefined criteria derived from our weighted objectives. Each criterion is assigned a score based on how well the alternative meets the specific requirement, and these scores are aggregated to produce an overall rating for each option. This quantitative analysis facilitates a transparent and objective comparison of the alternatives, enabling us to identify the most viable and effective design solution based on empirical data. This rigorous evaluation ensures that the chosen alternative not only meets but potentially exceeds our project’s requirements.

Table 3-Evaluation Chart

Sr #	Evaluation criteria	Wt.	Alternate: A (Plate)			Alternate: B (Pump)			Alternate: C (Siphon)			Remarks
			Est. Perf.	Val.	Total	Est. Perf.	Val.	Total	Est. Perf.	Val.	Total	
1	Sensors and controls	0.04	Acceptable	6	0.24	Acceptable	6	0.24	Acceptable	6	0.24	Similar sensors for all alternates
2	Fast deployment and withdrawal	0.04	Acceptable	6	0.24	Acceptable	6	0.24	Acceptable	6	0.24	Similar deployment mechanism
3	High Capacity	0.16	Good	8	1.28	Good	7	1.12	Poor	1	0.16	Siphon has lower flow rate
4	Low Set-up Cost	0.04	Good	7	0.28	Low	4	0.16	Good	8	0.32	Pumps have higher up front cost
5	Low Power Consumption	0.04	Good	7	0.28	Low	4	0.16	Good	8	0.32	Siphon and plate design are efficient.
6	Scalable	0.08	Good	8	0.64	Good	8	0.64	Good	8	0.64	Equal scalablity
7	Easy Access for Service	0.04	Average	5	0.18	Average	5	0.18	Average	5	0.18	Equal level of maintenance access.
8	Durable materials and parts	0.05	Good	7	0.38	Low	4	0.22	Good	7	0.38	Pumps may be less durable.
9	Guarding and emergency stops	0.06	Average	5	0.3	Average	5	0.3	Average	5	0.3	Similar safety mechanism
10	Automatic shut-off	0.06	Average	5	0.3	Average	5	0.3	Average	5	0.3	Similar safety mechanism
11	Easy Installation	0.09	Acceptable	6	0.54	Acceptable	6	0.54	Acceptable	6	0.54	Similar installation
12	Drain water with conveyor running	0.06	Good	8	0.48	Poor	1	0.06	Poor	1	0.06	Excess load on pipes.
13	Drain water with conveyor stopped	0.06	N/A	0	0	Sufficient	6	0.36	Poor	2	0.12	Plate inoperable with conveyor stopped.
14	Compatible with conveyor	0.18	Average	5	0.9	Average	5	0.9	Average	5	0.9	Equal compatibility
Final Score				83	**6.04**		72	**5.42**		73	**4.70**	

3.7 Product Design Results:

This section examines the outcomes of the Product Design Process, focusing on three engineered alternatives, each evaluated against a series of criteria to determine their suitability and performance.

Alternative A (Plate-based design):

Alternative A emerges as the optimal choice, scoring the highest in the evaluation process, particularly excelling in dealing with "High Capacity" where it outperformed the other alternatives. This design's simplicity and robust nature make it a favorable option. It requires minimal maintenance, leveraging the conveyor's kinetic energy to efficiently divert water. Not only is it cost-effective, but its scalability also makes it adaptable to varied site conditions. Due to its significant advantages and potential for widespread application, this design is prioritized in the ongoing discussion.

Alternative B (Pump-based design):

Although this option involves a higher initial setup cost, reflected in its lower scores for cost-effectiveness, it provides substantial operational benefits. It is particularly advantageous when the conveyor is stopped, offering a higher flow rate compared to the siphon-based design. This design is noted for its ability to manage water drainage continuously, an essential feature for settings with frequent conveyor stoppages.

Alternative C (Siphon-based design):

Ranked lowest in the evaluation, this design is noted for its energy efficiency but criticized for its inadequate flow rate, as highlighted in its performance under the "High Capacity" criterion where it scored poorly. While energy efficiency is a commendable attribute, the low flow rate limits its practicality for effective water management.

Conclusion:

Distinguished from previous patents and designs, the evaluated alternatives do not necessitate modifications to the existing conveyor infrastructure and act as external additions. This approach is crucial as it ensures no operational downtime. Considering the strengths of the top-scoring alternatives, a combined approach utilizing both plate and pump-based designs could greatly enhance system efficacy. This hybrid solution would ensure effective water management regardless of conveyor activity, thereby optimizing operational flexibility and efficiency.

4 Plate-Based Design

This design is engineered to function by deploying a plate onto the conveyor belt whenever water accumulates and needs to be removed. The plate is attached to a deployment mechanism that activates automatically through various automation devices, including sensors, instruments, and PLCs (Programmable Logic Controllers). The subsequent sections elaborate on the design, material selection, performance evaluation, and operation mechanism of this apparatus.

4.1 Design Philosophy

The plate is specifically intended for use when the conveyor contains water and trace amounts of raw material. It should not be engaged if only raw material is present or if the water is mixed with raw material. In such cases, vibrating screens are typically employed to separate and process the material.

When the conveyor is filled with water, it can be started so that the water moves in the conveyor's direction. The plate acts as an obstruction, providing a path that channels the water off the conveyor. With its kinetic energy, the water climbs to a higher level at an approximate angle of 23° and is then diverted to either left or right outlet and onto a sloped floor. This floor guides the water to sumps, where it is pumped to the plant's water management system.

At this stage, the design and testing phases have focused primarily on the plate to ensure its effectiveness in draining water from the conveyor. Details regarding the operational/deployment mechanism of the plate are elaborated upon in subsequent sections of this report.

4.2 3D Model

The final design was achieved after 3 iterations detailed below.

4.2.1 Design Iteration 1:

The design introduces a diverter plate that acts as an effective obstruction to redirect water (from rain and other sources) off the conveyor as it operates. To ensure smooth interaction with the conveyor belt and to prevent abrasion, the model incorporates rolling contact points. These contact points enable the diverter plate to maintain gentle contact with the moving conveyor belt, enhancing durability and efficiency. The following figures provide a detailed illustration of the design features and their operational integration.

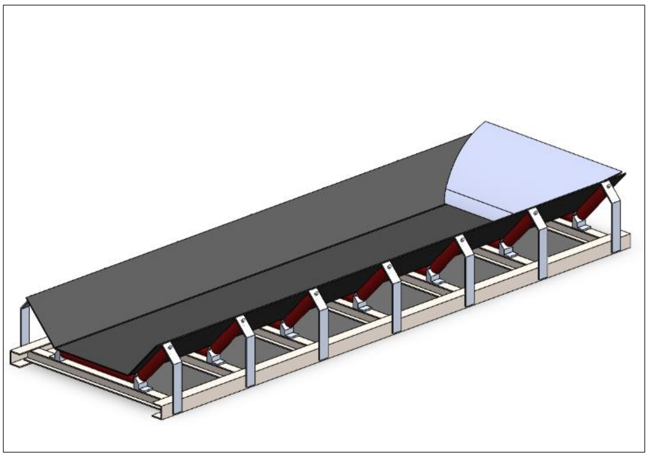

Figure 17-Plate Model (1st Iteration)

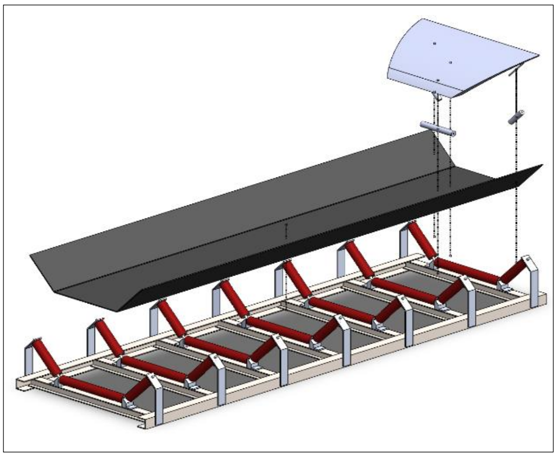

Figure 18-Plate Model (1st Iteration-Exploded View)

4.2.2 Design Iteration 2:

The design has been further refined to optimize water flow and ensure a smooth ejection from the conveyor system.

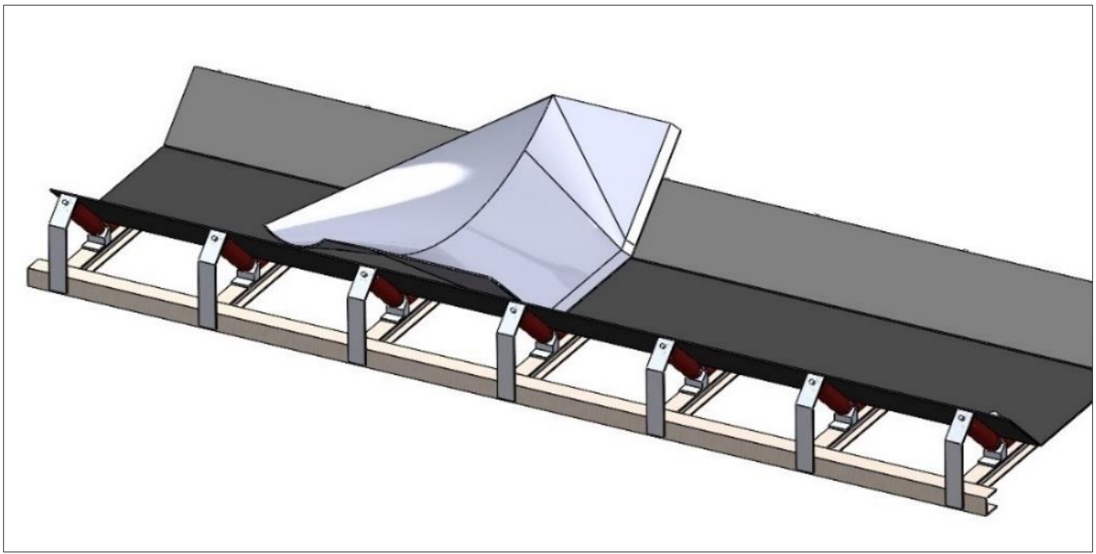

Figure 19-Plate Model (2nd Iteration)

Concerns arose regarding the potential for an asymmetrical load to induce instability. To address these concerns and mitigate any resulting issues, an additional iteration of the design was implemented, focusing on enhancing balance and operational stability.

4.2.3 Design Iteration 3:

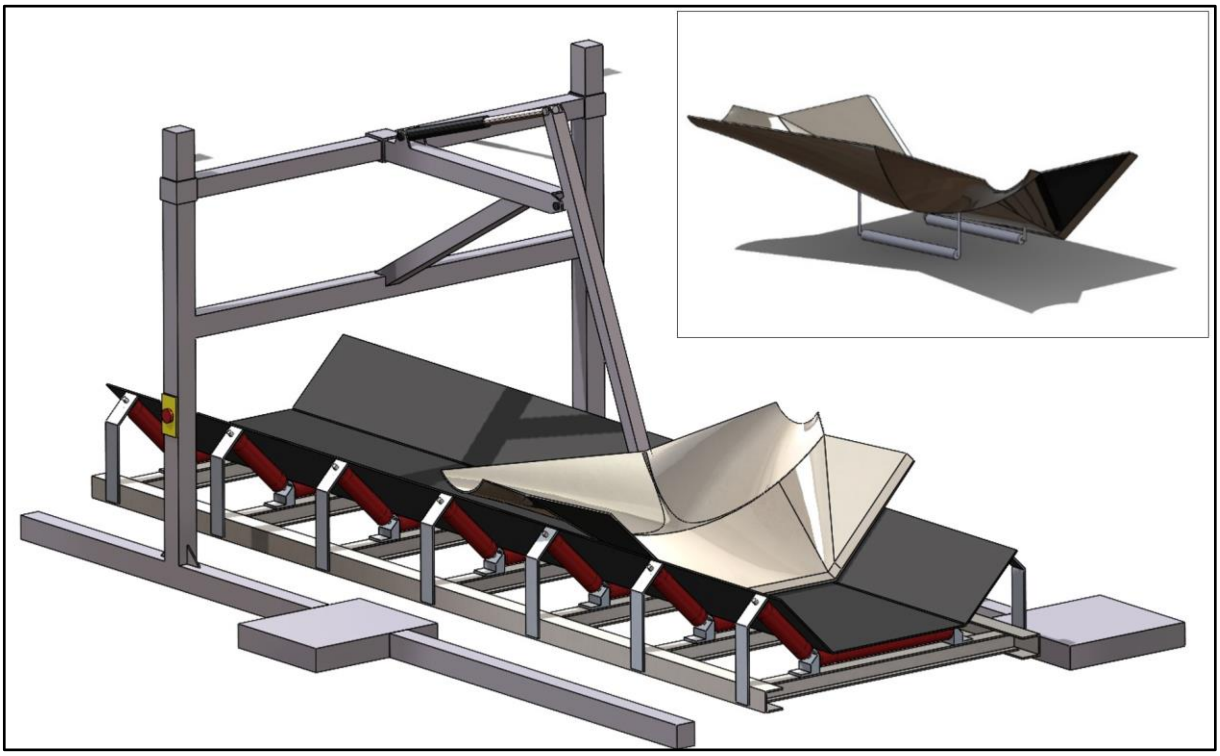

Figure 20-Plate Model (3rd Iteration)

In this iteration, the design has been modified to be symmetrical, enhancing overall stability during operation. The adaptations in this version were primarily guided by intuitive design principles and observations from previous iterations. The performance and effectiveness of this revised model are comprehensively tested and discussed in the upcoming section. Similarly, the operation of the deployment mechanism is also explained in detail in later section.

This design efficiently channels water off the conveyor, ensuring that there are no splashes onto the idlers, which could compromise their function. The removed water is directed onto a strategically sloped floor, guiding it towards a sump. From the sump, the water is then pumped out for further treatment or processing.

4.3 Material selection:

The material selection process was carried out as per the Ashby's Method [16]. In this method we find the material indices by starting with the design requirements as mentioned below.

Design Requirements

Function: Diversion Plate

Constraint: Bending stiffness S* specified (functional constraint)

Length L and width b specified (geometric constraints)

Objective: Minimize the mass, m

Free Variable: Choice of Material

Panel thickness h

Derivation of Material Indices

The objective is to minimize the mass of the plate. We get the following objective function.

$$m = AL\rho = bhL\rho$$

Since, the bending stiffness should be at least.

$$S = \frac{C_1 EI}{L^3} \geq S^* \qquad (a)$$

To simplify the problem, we will assume the plate to be rectangular in shape. So,

$$I = \frac{bh^3}{12} \qquad (b)$$

Using (a) and (b) we can eliminate h from the objective function, which gives us.

$$m = \left(\frac{12S^*}{C_1 b}\right)^{\frac{1}{3}} (bL^2) \left(\frac{\rho}{E^{\frac{1}{3}}}\right)$$

Here we see that the last term $\left(\frac{\rho}{E^{\frac{1}{3}}}\right)$, is the only term that we can manipulate to minimize the mass. If we invert this term and maximize it, we get the most suitable material that is light and stiff enough for our use.

$$M = \frac{E^{1/3}}{\rho}$$

However, if we repeat the calculations with different constraint, i.e. strength instead of stiffness, the index becomes,

$$M = \frac{\sigma^{1/2}}{\rho}$$

Now we use these materials indices in Ansys Granta to find the right materials.

4.3.1 Ansys Granta

Using Ansys Granta, we apply various filters to narrow down our choice of material. By selecting level 2 in Granta, we start off with a total of 100 materials. Which are then subjected to various stages. These stages/filters allow us to find the right material for the task. In this case a total of six stages were used to refine our search for the most suitable materials. The stages are shown in the image below.

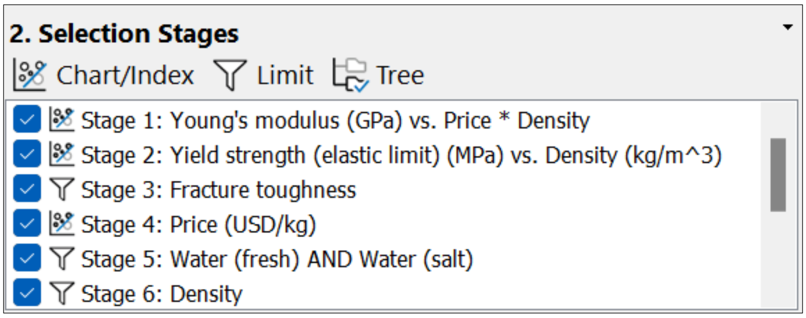

Figure 21-Ansys Granta Stages

Each of these stages included a certain “Pass” criteria. The materials that do not meet the pass criteria are eliminated from the pool of the available material. The table below details the criteria and the description of the stages. All of these stages refined our search for the right materials, except for the “Price” stage. The Price stage was included so that the materials can be sorted by their cost.

Table 4-Stage Criteria Table

Stage	Description	Pass Criteria	Pass Material-out of 100
1	Young's modulus (GPa) vs. Price * Density	Slope index=3	81
2	Yield strength (MPa) vs. Density (kg/m^3)	Slope index=2	35
3	Fracture toughness	Min: 1.7 MPa.m$^{0.5}$	19
4	Price (USD/kg)	N/A	19
5	Water (fresh), Water (salt)	Good compatibility	8
6	Density	Max: 1750 kg/m^3	7

The seven materials that passed the stages are shown below.

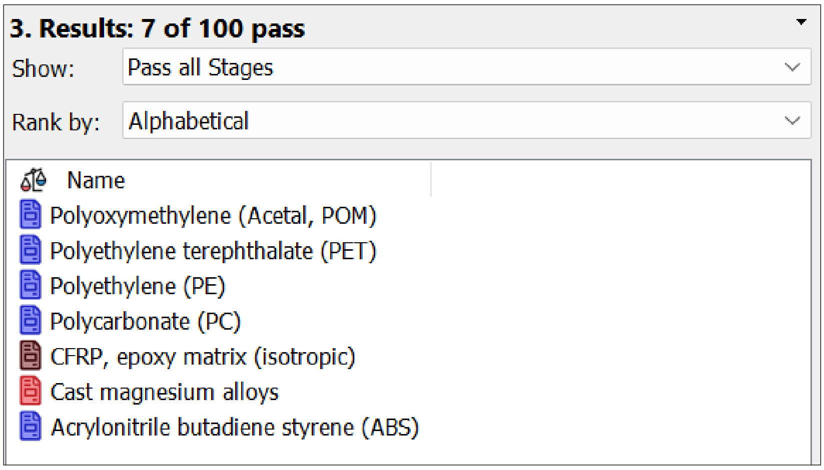

Figure 22-Pass Materials

Although all of the 7 materials provide acceptable performance, 4 were selected for further analysis. The selected materials were as following:

Table 5-Material Selected for Finite Element Analysis

Material	**Remarks**
Carbon Fiber (CFRP)	Offers highest yield strength
Cast Magnesium Alloys (CMA)	Second highest yield strength
Polyethylene Terephthalate (PET)	Offers sufficient performance at lowest price.
Polycarbonate (PC)	Offers most strength among the polymers

These materials will be used in our upcoming strength analysis.

4.4 Drag Coefficient and Pressure Analysis:

To evaluate the performance of the diverter plate, it is crucial to calculate key parameters such as the drag coefficient and the pressure exerted on the plate by fluid flow. A comprehensive CFD simulation was performed using StarCCM+ to model these dynamics accurately. The simulation set-up included the following boundary conditions:

- The diverter plate was enclosed as depicted in the accompanying Figure 25.
- An inlet velocity of 2.9 m/s was specified.
- Water was selected as the working fluid to simulate real conditions.
- The outlet of the enclosure was configured as a pressure outlet to model the fluid exit strategy.
- A symmetry plane was utilized to minimize computational demands by reducing the model's complexity.

These conditions were meticulously chosen to ensure that the simulation results would be both accurate and computationally efficient.

4.4.1 Fluid Properties:

First, to find out the type of flow, Reynold's number of flow is to be calculated, as shown below.

$$R_e = \frac{\rho v L}{\mu} \qquad (i)$$

ρ = density of water =1000 kg/m^3, v = Velocity of the fluid=2.9 m/s^2, μ = Dynamic Viscosity= 0.001 kg/(m.s), and,

$$L = \text{Characteristic Length} = \frac{4A}{P}$$

Since the cross section of the conveyor makes a trapezoid, with a=950mm, b=1692mm, c=525mm and h=371mm. These were found from LKAB conveyor TR010 as shown in Appendix A - LKAB Drawing

$$A = \frac{1}{2}(a+b) \times h = 490091\ mm^2$$

And the perimeter is given by.

$$P = a + b + 2c = 3692mm$$

So,

$$L = \frac{4 \times 490091}{3692} = 0.5309m$$

Putting in (i)

$$R_e = \frac{1000 \times 2.9\ \times 0.5309}{0.001} = 1539610 > 4000$$

Hence the flow is turbulent. Furthermore, the K-epsilon turbulent model was used. Water used in simulation is assumed to be incompressible throughout.

4.4.2 Simulation Set-up:

To optimize the mesh for the CFD simulation, specific settings were meticulously selected to ensure precision and efficiency in the computational results. The following mesh refinement parameters were employed:

- **Base Size:** 0.07 meters, providing a foundational scale for mesh elements.
- **Number of Prism Layers:** 10, enhancing the mesh's resolution near the diverter plate surface to capture boundary layer effects.
- **Prism Layer Total Thickness:** Set to 10% of the base size, this parameter adjusts the total thickness of the prism layers, influencing the gradient of the mesh near the surface.
- **Volume Growth Rate:** Classified as 'Slow', this setting controls how quickly the mesh cells increase in size away from the surface, affecting the gradation of the mesh density.
- **Maximum Cell Size:** Limited to 100% of the base size, ensuring uniformity in the largest mesh cells.
- **Mesher Execution Mode:** Set to 'Parallel' to leverage computational resources effectively and reduce simulation time.

These settings were strategically chosen to balance detailed flow resolution with computational efficiency.

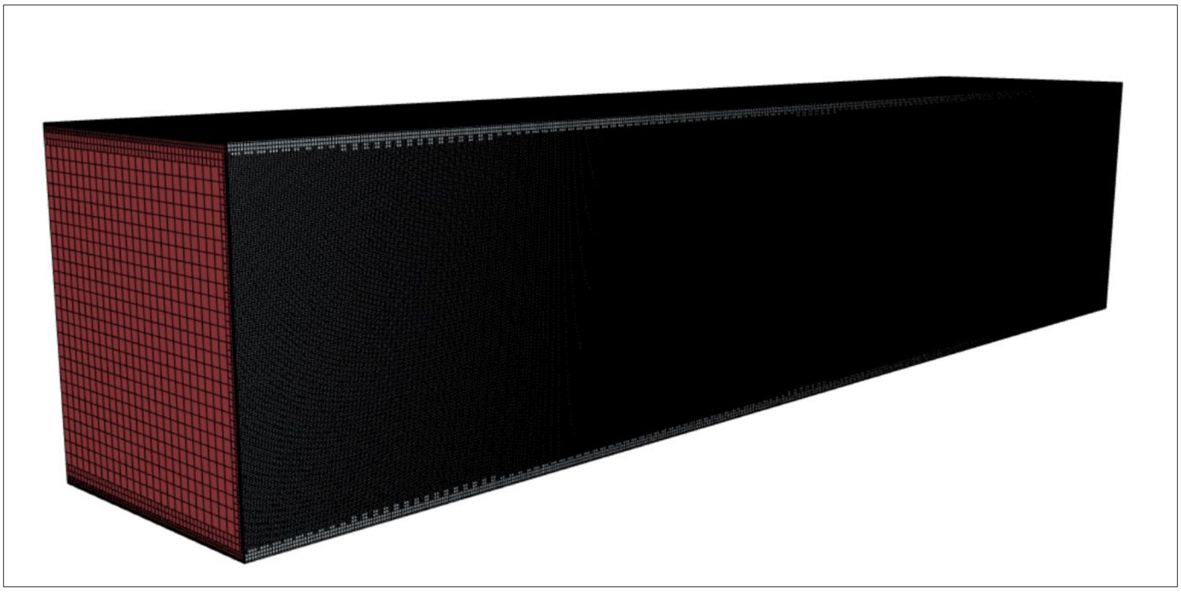

Figure 23-Meshing of Enclosure

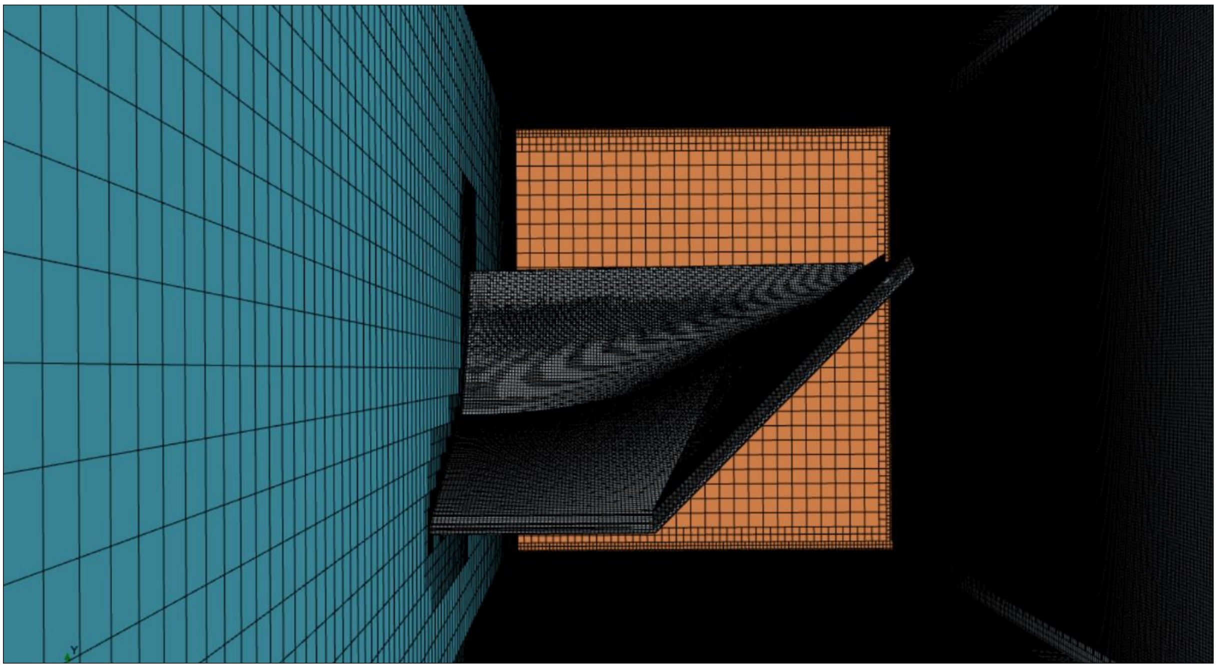

Figure 24-Meshing of half plate inside the meshed enclosure (domain)

The meshing details are visually depicted in Figure 24 and Figure 25.

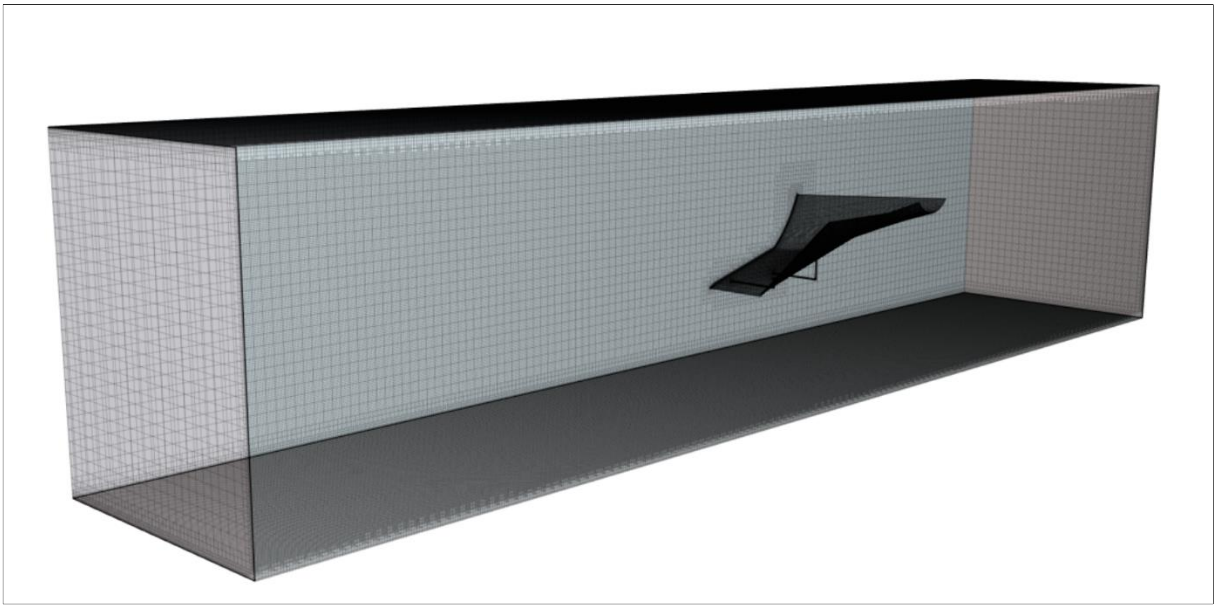

Figure 25-Meshing of Enclosure-transparent view

4.4.3 Results:

For both drag coefficient and Drag force we see that the results converge for each iteration, which signals that the results are correct, and the set-up was right.

Drag Force:

The graph shows that the results converge and give us the drag force as 4158.37 N.

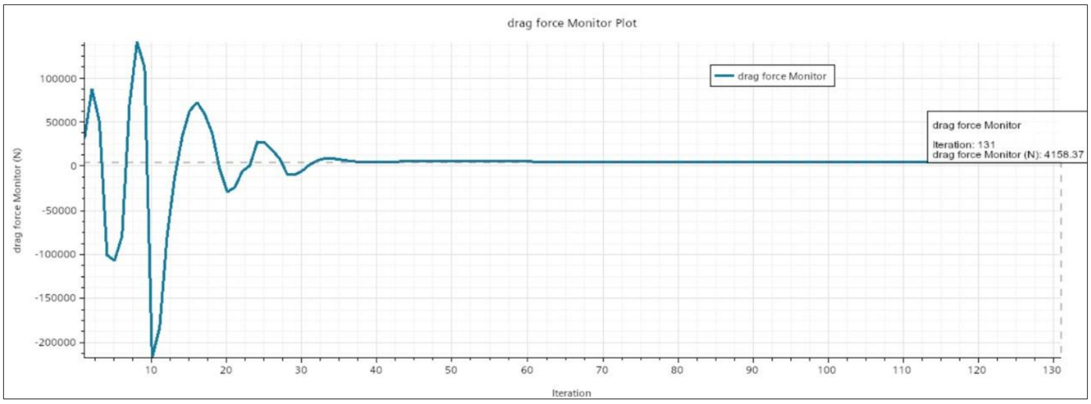

Figure 26-Drag Force Result

Drag Coefficient:

The results converge and give us the drag coefficient as 0.859285.

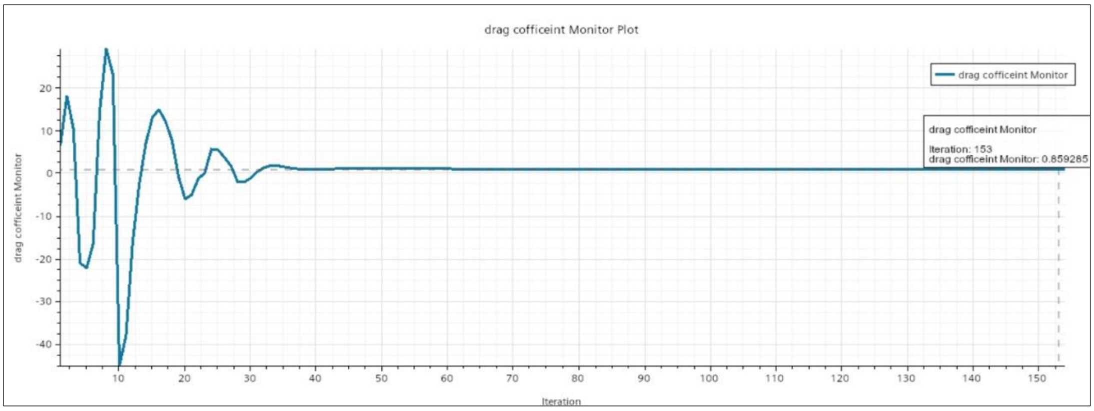

Figure 27-Drag Coefficient Result

Total (Absolute) Pressure:

The graph shows that the average pressure is below 1.08×10^5 Pa.

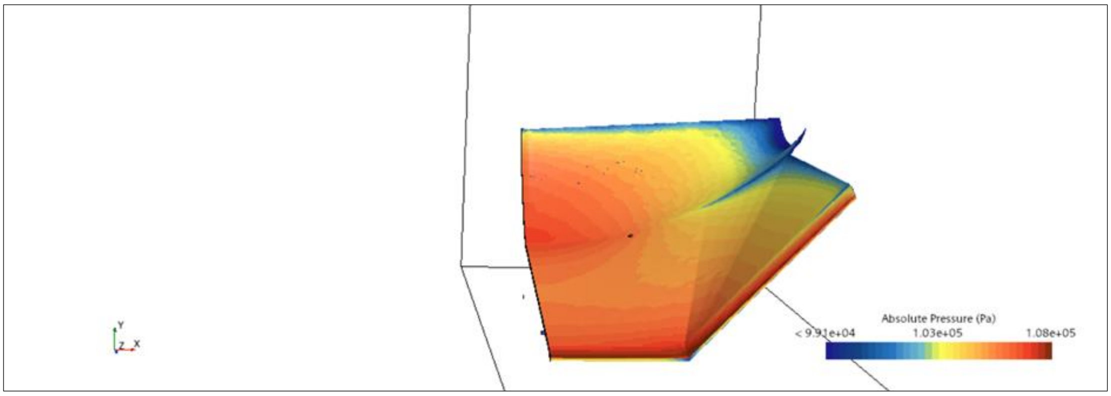

Figure 28-Total Pressure Result

Residual plot:

The residual plot, shown below, exhibits the logarithmically scaled residuals of continuity, momentum components, and turbulence quantities against the iteration number.

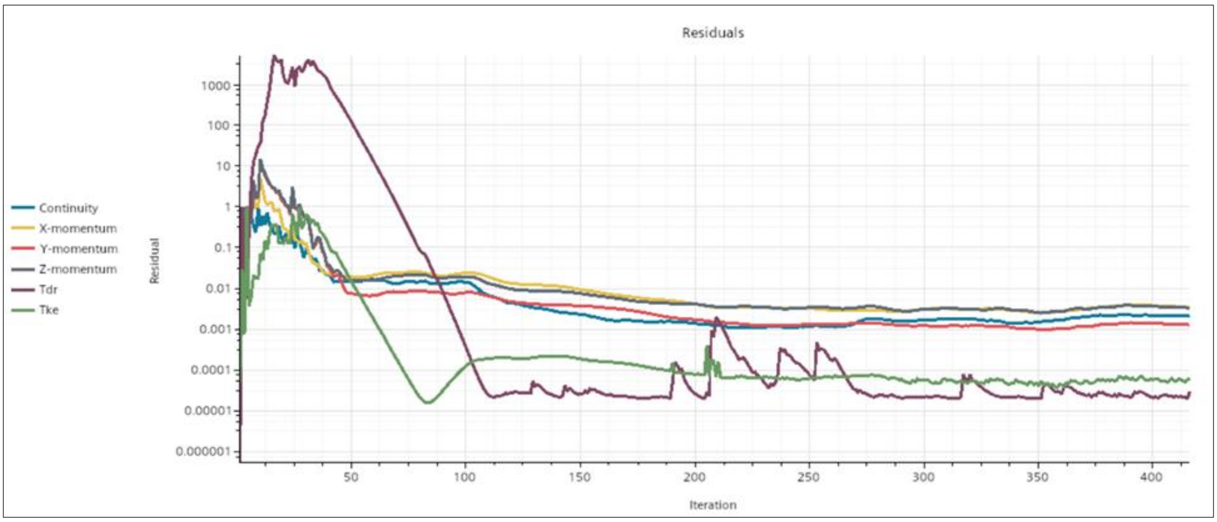

Figure 29-Residual Plot

Initial exponential decline in residuals is evident, indicating rapid movement towards conservation law satisfaction. Subsequent leveling off of residuals suggests approaching convergence, although transient spikes in the turbulent dissipation rate (Tdr) indicate iterative solver adjustments or transient physical phenomena. Conclusively, the stabilization of residuals at low magnitudes would be indicative of a converged solution. Hence, we can say that in this case the simulation converged to a satisfactory level.

4.4.4 Verification and Validation:

The drag force obtained from CFD can be plugged into the following equation to verify our results.

Drag Coefficient Validation:

To find the coefficient of drag, the frontal area of the plate is needed. This was found by using SolidWorks. And it was found to be 1.147379 m^2. The Figure 30 below shows us the frontal area.

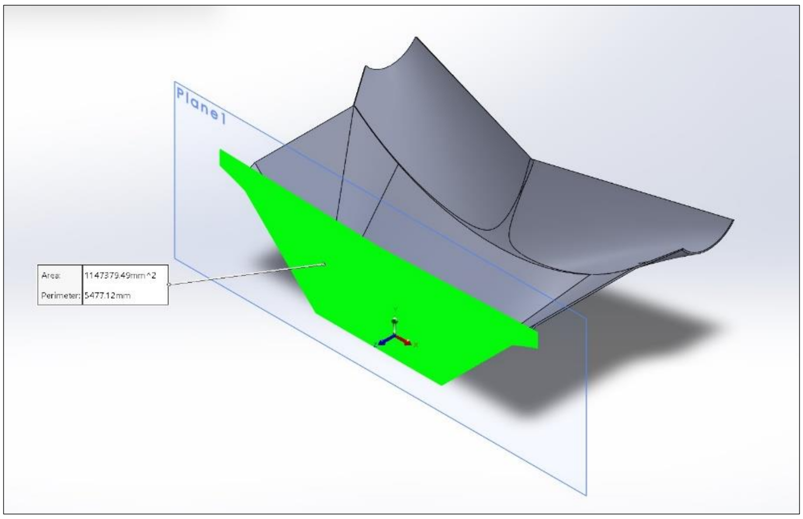

Figure 30-Frontal Area

We know that the drag coefficient is given by the following formula,

$$C_D = 2 \times \frac{F_D}{\rho v^2 A}$$

ρ = density of water =1000 kg/m^3, v = Velocity of the fluid=2.9 m/s^2, C_D=Drag Coefficient= 0.28, A= Projected Area= 1.147379 m^2 (Calculated from the above figure)

$$C_D = 0.86188$$

$$\text{Error} = \frac{|0.86188 - 0.85928|}{0.86188} = 0.30\ \%$$

The error is well within acceptable range.

Absolute Pressure:

The pressure exerted on the plate is given by the following formula:

$$P_{total} = \rho g h + \frac{1}{2}\rho v^2 + P_{atm}$$

ρ = density of water =1000 kg/m^3, v = Velocity of the fluid=2.9 m/s^2, h = height of water= 0.3 m, P_{atm}= 101325 Pa

$$P_{total} = 1.08470\ \times 10^5\ Pa$$

$$\text{Error} = \frac{|1.08470\ \times 10^5 - 1.08\ \times 10^5|}{1.08470\ \times 10^5} = 0.43\ \%$$

The error is well within acceptable range.

4.5 FEA Analysis:

Using the calculated pressure and selected materials, we can assess the plate's performance through simulation in Ansys Workbench.

4.5.1 Simulation Set-up.

An adaptive sizing meshing scheme was applied with a resolution of 7 to ensure a finely detailed mesh, particularly around the corners, for accurate results. The meshed plate is displayed below.

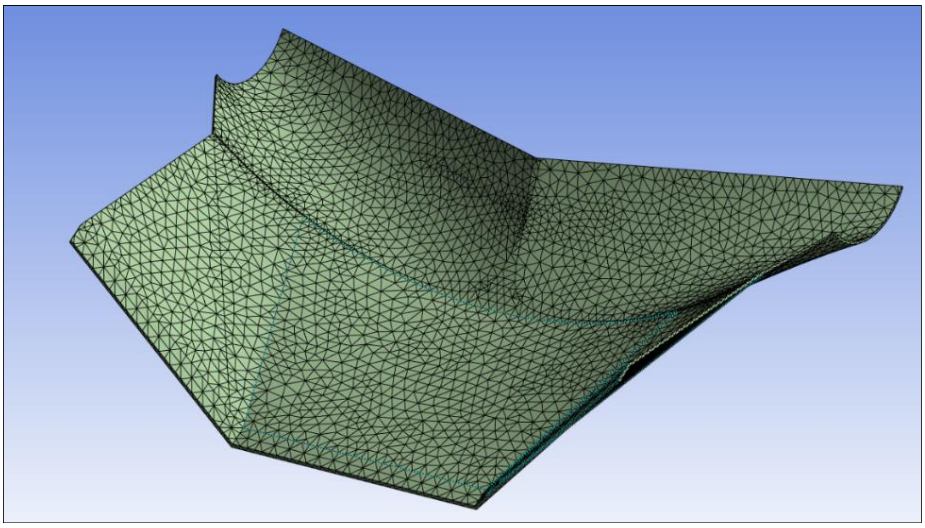

Figure 31-Plate Meshing

The boundary conditions, illustrated in the Figure 32, indicate the fixed supports and the surface where the calculated hydrodynamic pressure of 0.102 MPa is applied.

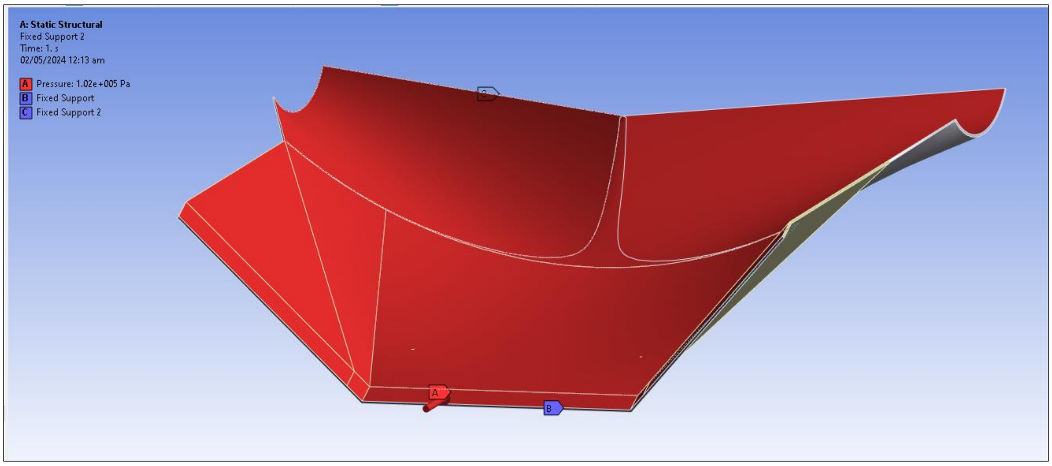

Figure 32-Plate Boundary Conditions

4.5.2 Results

The following image shows the results (deformation) of 5mm CFRP plate.

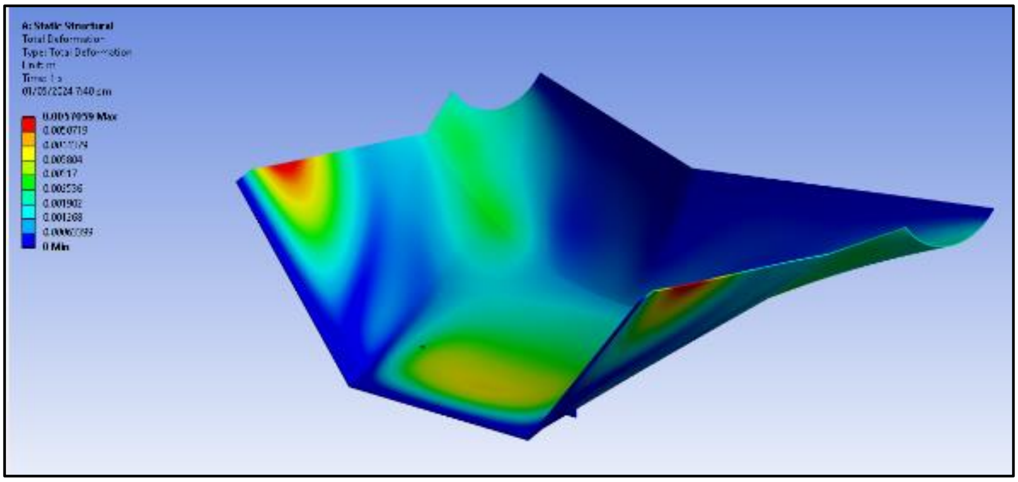

Figure 33-Deformation in 5mm CFRP Plate

The analysis was repeated for 5,8,12 and 15mm for Carbon Fiber Reinforced Composites (CFRP), Cast magnesium alloys (CMA), Polycarbonate (PC), and Polyethylene terephthalate (PET). The results are listed in the table below.

Table 6-Plate FEA Results

Thickness (mm)	Materials Used	Max Deformation (mm)	Mass (kg)	Equivalent Stress (MPa)	Average Price (USD/kg)
5	CFRP	5.70	29.414	40.6	40.2
8	CFRP	1.4623	45.357	31	40.2
12	CFRP	0.65	66.611	8.7	40.2
15	CFRP	0.43	82.456	6.4	40.2
5	CMA	19.182	32.089	38	2.495
8	CMA	4.7	49.48	14.3	2.495
12	CMA	2.1	72.666	8.3	2.495
15	CMA	1.4	89.952	6.1	2.495
5	PC	300	20.679	37.4	2.815
8	PC	80	31.887	13.9	2.815
12	PC	37	46.829	8.2	2.815
15	PC	25.0	57.969	6	2.815
5	PET	260	23.87	37.7	0.995
8	PET	66	36.808	14.07	0.995
12	PET	30.4	58.056	8.2	0.995
15	PET	20.09	66.915	6.1	0.995

Note: The screenshots for all the results are attached in the Appendix B-Plate FEA Results

4.5.3 Verification and Validation:

Since the Plate design is too complex to be analytically calculated, a flat test plate was used for validation purposes. By comparing the analytical and numerical results of a simple shape it can be verified that the simulation is set up correctly. This allows for verification of the results of the original plate.

The plate properties are listed below:

Material Name: Carbon Fiber (CFRP)
Young's Modulus: 1.5 x 10^5 MPa
Dimensions:450 x 230 x 5 mm
Load: 1.02 x 10^5 N/m^2

The Analytical

Analytical Calculation:

The deflection of a beam with two fixed ends and a uniformly distributed load is given by the following formula.

$$\Delta_{max} = \frac{wL^4}{384EI}$$

Where,

$$I = \frac{bh^3}{12} = 2.39583 \times 10^{-9}\ m^4$$

$$\Delta_{max} = \frac{wL^4}{384EI}$$

$$\Delta_{max} = 6.9710\ mm$$

To find the max stress, we use the following formula.

$$\sigma_{max} = \frac{M}{S}$$

Where $M = \frac{wL^2}{12}$ and $S = \frac{bh^2}{6}$, this gives us,

$$\sigma_{max} = 413.1\ MPa$$

Now we get the numerical results.

Numerical Calculation:

The following image depicts the loading conditions.

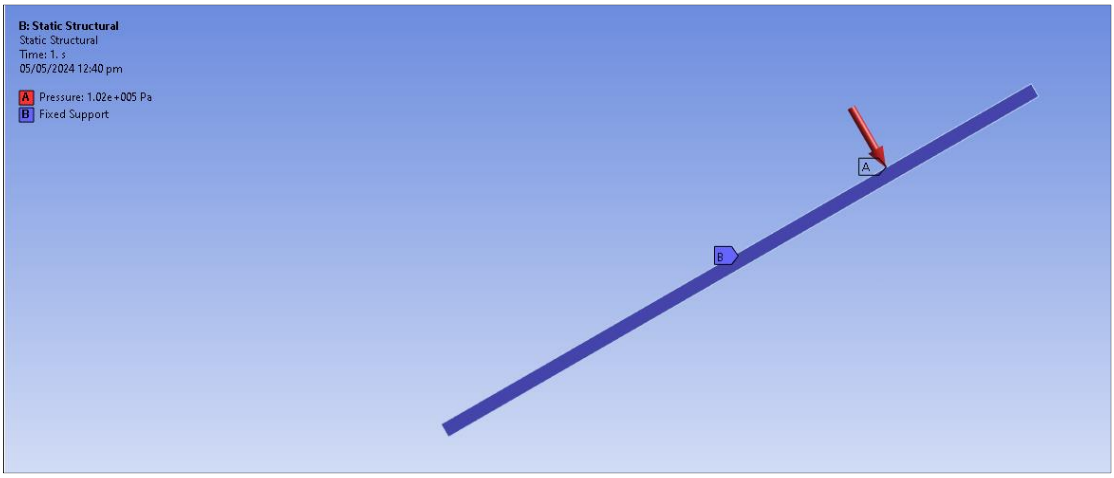

Figure 34-Test Plate Boundary Conditions

And the figures below show deformation and stress respectively.

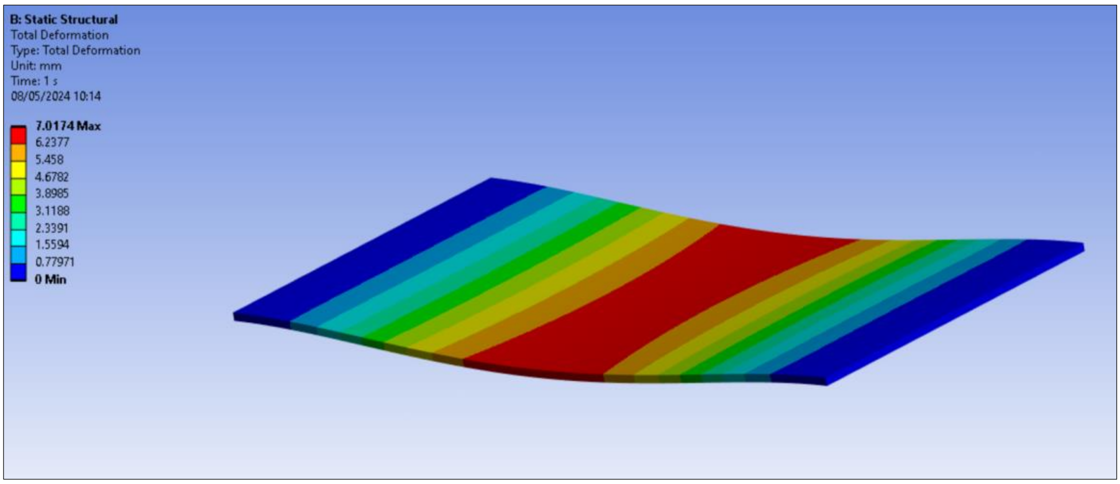

Figure 35-Test Plate Deformation Results

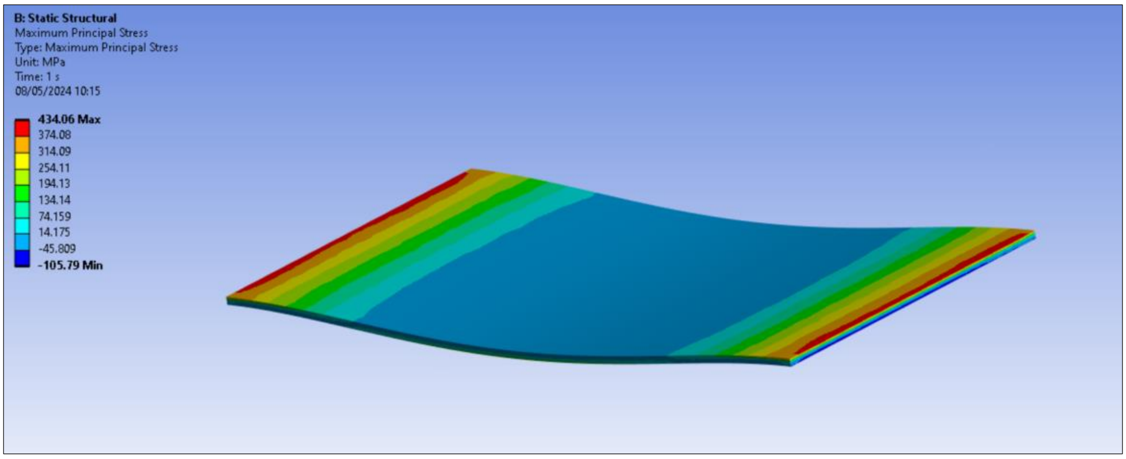

Figure 36-Test Plate Max Stress Results

Calculating the error for deformation.

$$\% \text{ error} = \frac{|7.0174 - 6.9710|}{6.9710} = 0.66\%$$

Hence our results are validated. Now for stress,

$$\% \text{ error} = \frac{|434.06 - 413.1|}{413.1} = 5.07\%$$

4.5.4 Discussion

The Table 6-Plate FEA Results was used to generate the following graph. Using the graph, we can do an in-depth analysis of how these materials perform at various thicknesses. The discussion is continued after the graph.

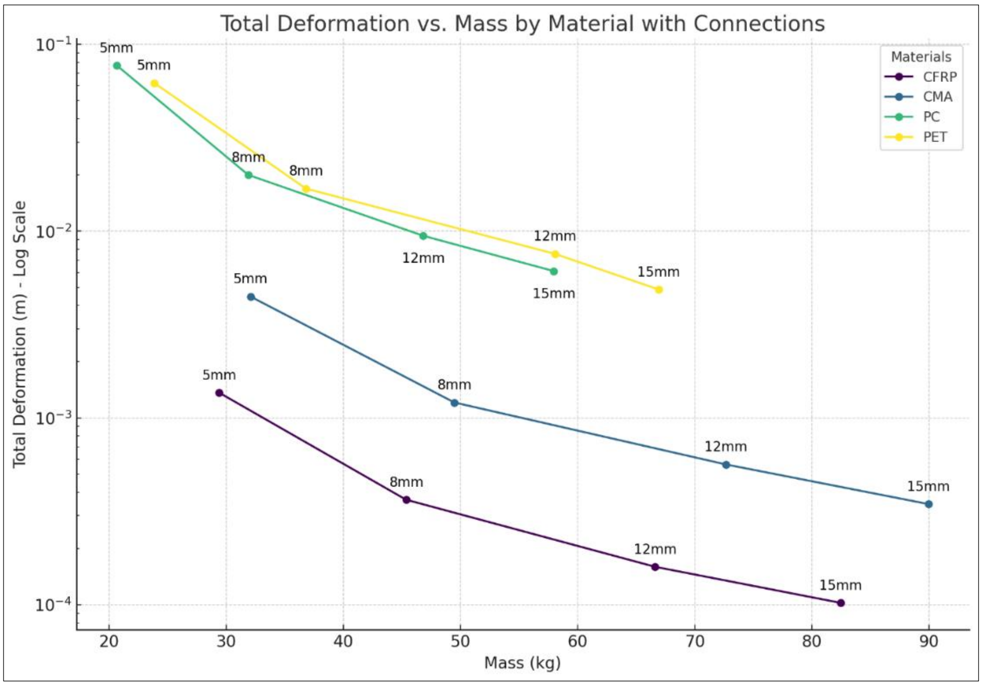

Figure 37-Plate FEA Results Graph

- **CFRP** shows the highest deformation resistance and a good strength-to-weight ratio, but it's significantly more expensive than the other materials.
- **PC** has the highest strength-to-weight ratio among all materials but has poor deformation resistance.
- **PET** provides moderate strength-to-weight ratio and the lowest price, though its deformation resistance is low.
- **CMA** offers a balance between moderate strength-to-weight ratio and deformation resistance at a reasonable cost.

CMA emerges as a highly appealing material choice when considering a balance between cost and performance. While it exhibits moderate deformation compared to

CFRP, it is significantly less expensive, with an average price of approximately $2.50 per kg, which is almost sixteen times cheaper than CFRP. This price advantage, combined with its reasonable rigidity, makes CMA an excellent option for applications where some flexibility is permissible, but cost constraints are tight. Furthermore, its performance in terms of deformation, with a minimum of 0.35 mm and a maximum of 4.46 mm, suggests that it can withstand considerable stress without excessive bending or breaking. Therefore, for the plate-based design, since it is intended to optimize material costs without severely compromising on quality and durability, CMA offers an outstanding compromise. Its cost-effectiveness paired with decent mechanical properties positions it as an ideal candidate for this case.

Among the various thicknesses, 8mm appears to be a reasonable middle ground. Where we see that the deformation is significantly reduced compared to 5mm and it is a lot lighter than the bulkier 12 and 15mm plates.

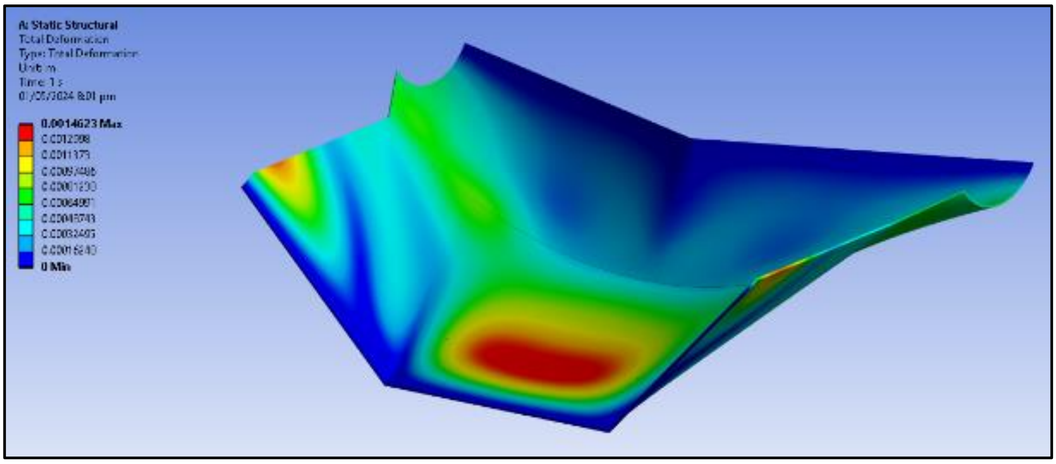

Figure 38-Deformation in 8mm CMA Plate

It shall be noted that Polycarbonate also offers a decent alternative in case multiple plates are to be used.

4.6 Mass Flow Rate Analysis:

The Mass Flow Rate Analysis of the plate will provide information about its capacity to divert water off the conveyor. The experiment was run with two different configurations. Once with default configuration (23˚) and then with the plate with increased inclination (30˚). The following section outlines the set-up and results obtained using Ansys Fluent.

4.6.1 Simulation Set-up

The set-up details for the experiment are as follows:

Fluid domain:

A standard domain was created before and after the plate with height equal to the water level in the conveyor.The domain was elevated till the height of diverter plate as can be seen in the image attached below.

Boundaries marked as inlet and outlets:

The inlet and outlet boundaries were clearly marked. One inlet was specified for mass flow based on constraints. Three outlets were considered: one at the conveyor's end to account for water passing through the plate, and two to the left and right of the plate to measure the mass flow diverted by the plate.

In the Figure 39, blue arrows indicate the inlet, while red arrows represent the outlets.

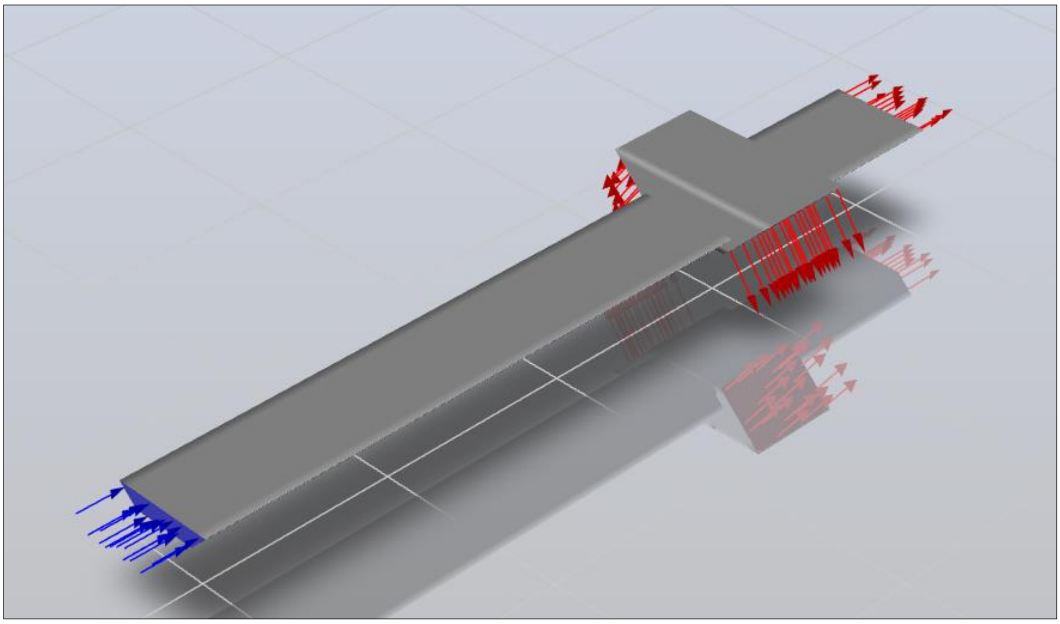

Figure 39-Inlet and Outlets for Mass Flow Rate CFD

Mass Flow Rate Calculation

The mass flow rate is calculated by using the equation**:**

$$\dot{m} = \rho \times A \times v$$

Where $A = 0.4900\ m^2$= Cross sectional Area, $v = 2.9\ ms^{-1}$= Conveyor speed

$$\dot{m} = 1421\ kgs^{-1}$$

This mass flow rate was set as the inlet condition. The figure below shows a transparent view of the plate placed within the domain.

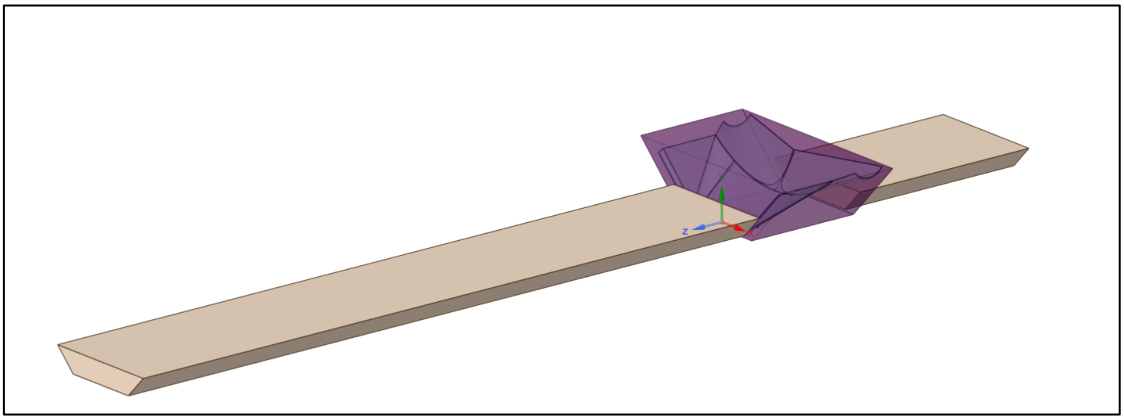

Figure 40-Mass Flow Rate CFD Transparent View

4.6.2 Results:

The results for the first case are shown for reference in the figure below.

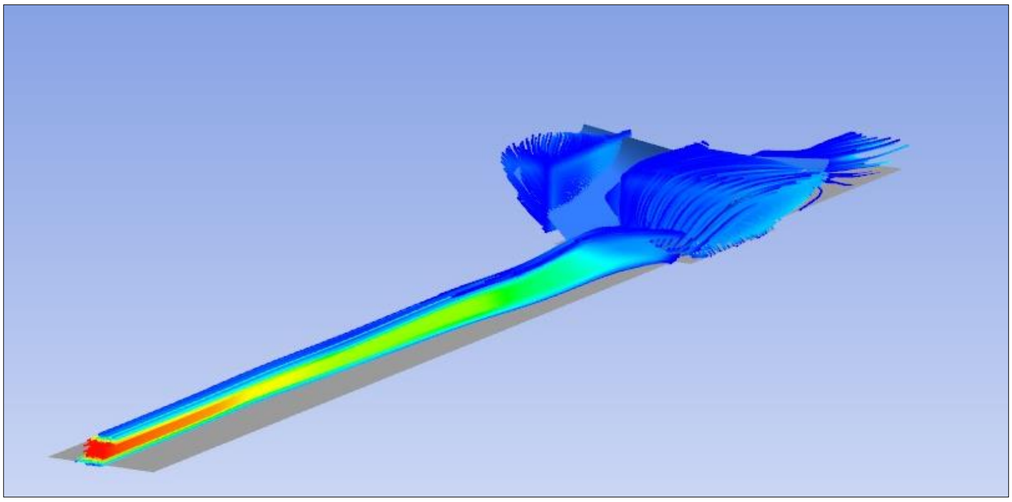

Figure 41-Mass Flow Rate CFD Velocity Contours

However, the mass flow rate is the key parameter that is required. The table below shows the values obtained for both configurations (23° and 30°)

Table 7-Mass Flow Rate CFD Results

Variables	Plate 23°	Plate 30°
Computed Mass Flow Left (kg/s)	719.495	550.987
Computed Mass Flow Right(kg/s)	712.037	553.400
Computed Mass Flow End (kg/s)	20.052	321
Total	1451.584	1425.387

The screenshots for the results are attached in the Appendix C-Plate Mass Flow CFD Results.

4.6.3 Verification:

To verify the accuracy of the results, the system's mass conservation can be assessed by comparing the mass flow rates in and out. The total mass flow rate entering the system (1421 kg/s) is nearly equivalent to the total mass flow rate exiting (1451 kg/s and 1425 kg/s). With this close alignment and the convergence achieved, as illustrated in Appendix C-Plate Mass Flow CFD Results, the results can be considered sufficiently accurate.

4.6.4 Discussion:

The plate demonstrates exceptional performance at a 23° angle, displacing a greater volume of water compared to a 30° angle, achieving drainage rates of 98% and 77%, respectively. It is noteworthy that the plate may have underperformed at the 30° angle due to increased spacing on the sides, which could be minimized with a redesign. However, given the 98% drainage rate achieved at 23°, a redesign may not be necessary.

4.7 Deployment Mechanism of Plate:

To ensure smooth, efficient movement of the diverter plate, a deployment mechanism incorporating a hydraulic actuator assembly is employed. The entire mechanism is supported by a horizontal beam mounted between two vertical pillars. The deployment system primarily consists of two arms: one fixed and one movable, connected via a rotating joint. A hydraulic actuator is mounted on the fixed arm, with its opposite end attached to the movable arm.

The diverter plate is firmly connected to one end of the movable arm. The actuator's internal pressure differences cause the movable arm to move up or down, which, in turn, drives the diverter plate towards or away from the conveyor belt. This ensures precise and controlled positioning of the diverter plate during operation.

The image below shows the plate in a disengaged position.

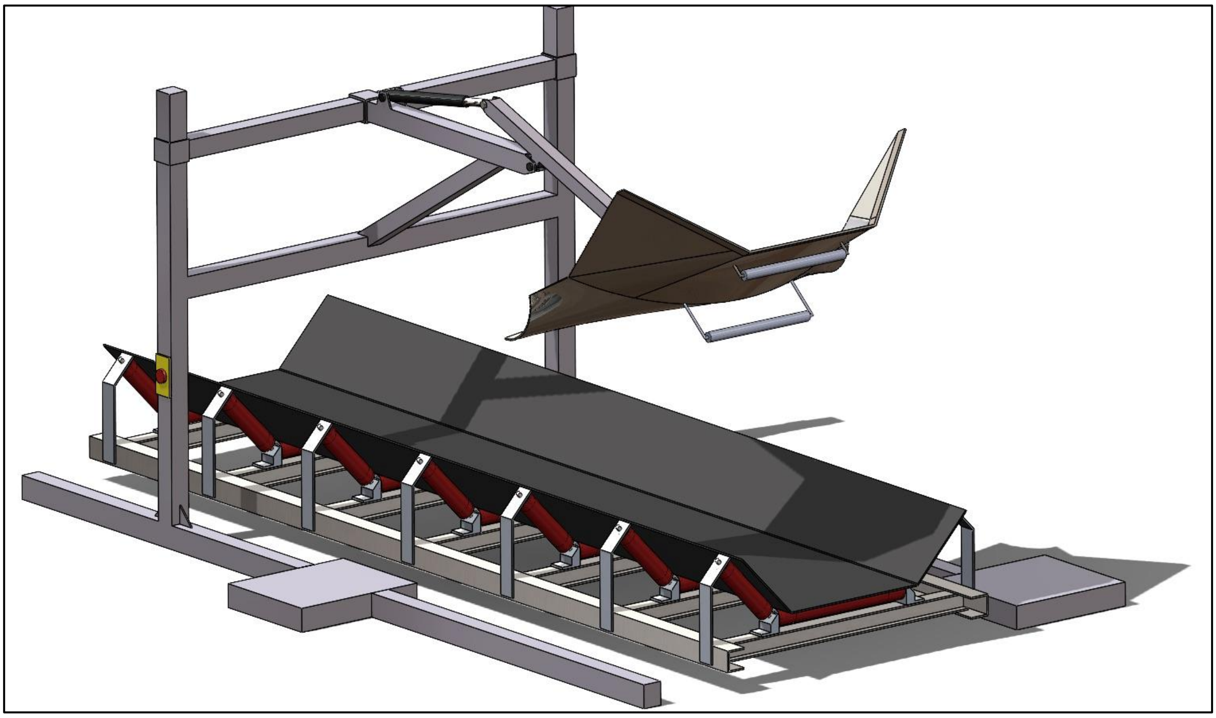

Figure 42-Plate in Disengaged Position.

And the Figure 43 shows the actuator in an extended position i.e. the plate is engaged. It shall be noted that the emergency button on the structure immediate disengages the plate.

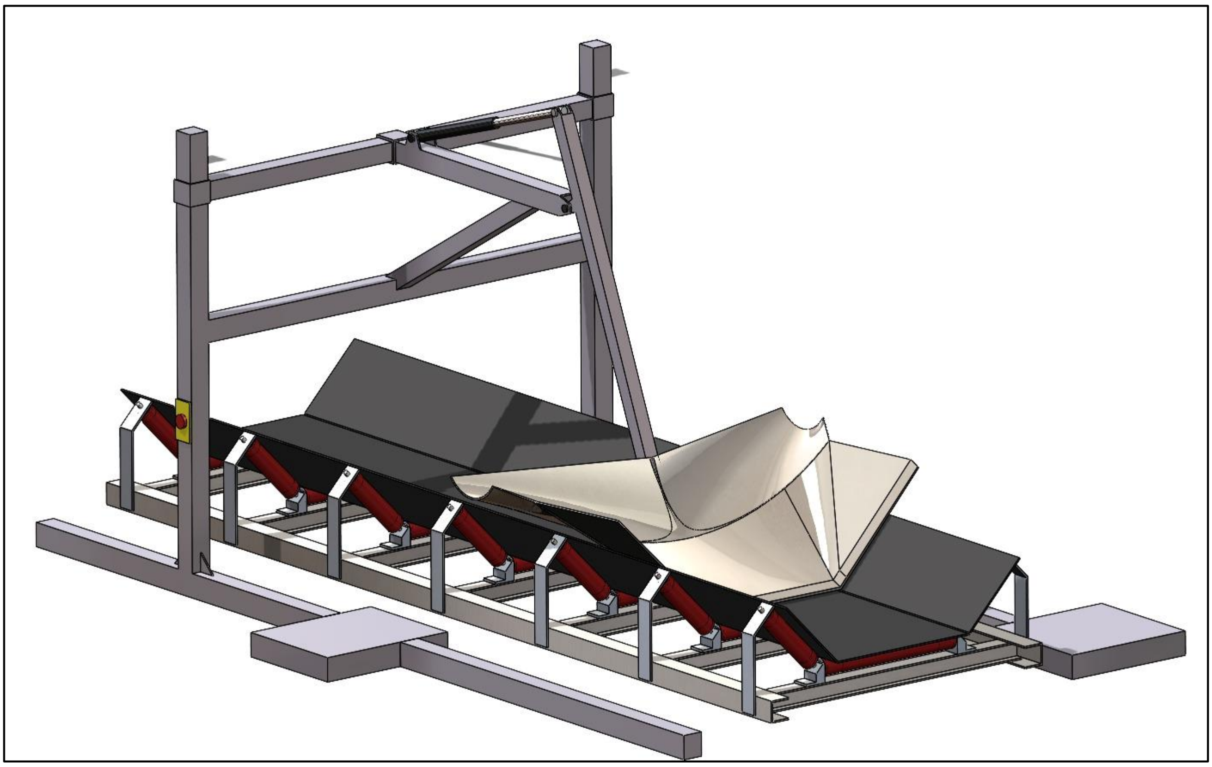

Figure 43-Plate in Engaged Position

4.7.1 Hydraulic System Overview

The deployment mechanism for the diverter plate leverages a hydraulic actuator that operates based on Pascal's law. This principle posits that a pressure change in an incompressible fluid is transmitted uniformly throughout the system. Here's how the hydraulic system works in this application:

Actuator Functionality:

The hydraulic actuator used in this mechanism relies on pressure changes within the fluid to move a piston inside the main cylinder. The piston's motion directly drives the load attached to it (the diverter plate). The fluid flow, primarily consisting of hydraulic oil, is controlled through a spool valve, ensuring the system operates efficiently. The Figure 44 presents a schematic representation of a hydraulic system, illustrating the key components and flow of hydraulic fluid.

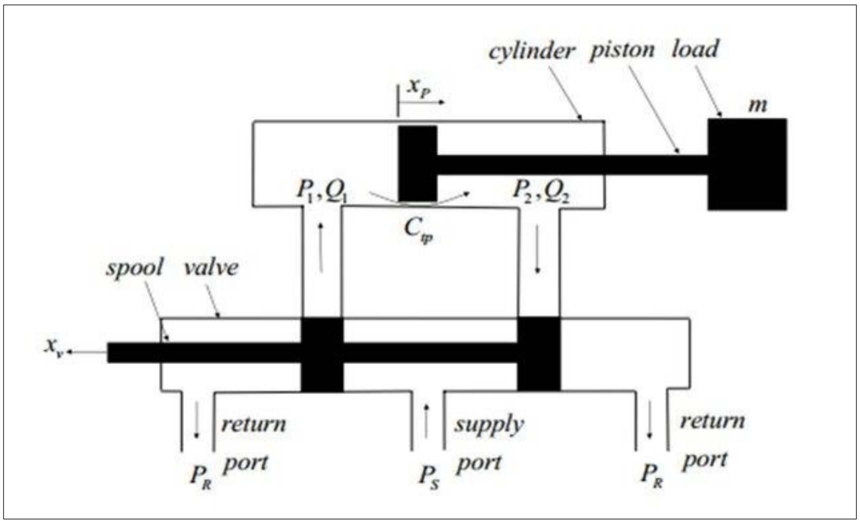

Figure 44-Actuator Schematic [17]

1. **Parker's Tie Rod Cylinder 3L Series Actuator:**

The actuator employed here is a Parker Tie Rod Cylinder 3L series [18], chosen due to its moderate pressure capacity (up to 70 bars) and customizable stroke lengths and bore sizes. For this application, it was selected to prevent overkill while still lifting the diverter plate effectively. The hydraulic oil used ensures a smooth movement of the piston.

2. **Key Specifications:**

The following specs are used based on the plate mass and the distance needed for the plate to be lifted.

- **Bore Diameter:**

The actuator operates under a tension force on the rod, pulling the 50 kg (CMA, 8mm) diverter plate. To handle the required load of 0.49 kN, an actuator with a rod diameter of 1.75 inches was chosen (shown in the table below), operating at a pressure of 5 bars and producing a push force of 0.8 kN.

Table 8-Datasheet for Actuator [18]

Piston Rod Ø	Piston Rod Area		Piston Rod Forces in kN						Piston Rod Forces in Pounds Force						Displacement per 10mm Stroke	
	mm^2	sq.in.	5 bar	10 bar	25 bar	70 bar	100 bar	140 bar	80 psi	100 psi	250 psi	1000 psi	1500 psi	2000 psi	Litres	Imp. Galls
12.7 (1/2")	130	0.196	0.1	0.1	0.3	0.9	1.3	-	16	20	49	196	294	-	0.0013	0.0003
15.9 (5/8")	200	0.307	0.1	0.2	0.5	1.4	2.0	2.8	25	31	77	307	461	614	0.0020	0.0004
25.4 (1")	500	0.785	0.3	0.5	1.3	3.5	5.0	7.0	65	79	196	785	1177	1570	0.0050	0.0011
34.9 (1 3/8")	960	1.49	0.5	1.0	2.4	6.8	9.6	13.5	119	149	373	1490	2235	2980	0.0097	0.0021
44.5 (1 3/4")	1560	2.41	0.8	1.6	3.9	10.9	15.6	21.9	193	241	603	2410	3615	4820	0.0156	0.0034
50.8 (2")	2020	3.14	1.0	2.0	5.1	14.1	20.2	28.3	251	314	785	3140	4713	6280	0.0202	0.0044
63.5 (2 1/2")	3170	4.91	1.6	3.2	7.9	22.2	31.7	44.4	393	491	1228	4910	7364	9820	0.0317	0.0070
76.2 (3")	4560	7.07	2.3	4.6	11.4	32.0	45.6	63.9	566	707	1767	7070	10604	14140	0.0456	0.0100
88.9 (3 1/2")	6210	9.62	3.1	6.2	15.5	43.4	62.0	86.7	770	962	2405	9620	14430	19240	0.0621	0.0137
101.6 (4")	8110	12.57	4.1	8.1	20.3	56.8	81.1	114.0	1006	1257	3143	12570	18856	25140	0.0811	0.0178
127.0 (5")	12670	19.64	6.4	12.7	31.6	88.7	126	177.3	1571	1964	4910	19640	29460	39280	0.1267	0.0279
139.7 (5 1/2")	15330	23.76	7.7	15.3	38.4	107	153	214.7	1901	2376	5940	23760	35640	47520	0.1523	0.0335

All dimensions are in millimetres unless otherwise stated.

- **Mounting Type:**

Pivot mountings are used because the diverter plate moves in a curved path during deployment. The rod is pivoted but not firmly attached, allowing it to move counterclockwise while deploying the plate.

- **Piston Rod Length:**

The length is selected based on the desired displacement of the plate. For this assembly, a maximum stroke length of 750 mm was determined via the SolidWorks design, which is sufficient for full deployment and retraction.

3. **Alternative Actuators:**

- Series CHGH Metric Compact Hydraulic Cylinders [19]: Offers a maximum operating pressure of 160 bars.
- Double Acting Hydraulic Cylinder 70H-8 [20]: Provides a maximum operating pressure of 70 bars.

5 Pump-Based Design

The pumps are intended to function as part of a larger water removal system. When the conveyor is stopped and not moving, the plate system cannot effectively remove water, thus necessitating the use of pumps. The pump-based design is designed and analyzed in the subsequent part of the report.

5.1 Design Philosophy

The pipes are designed with a movable end section positioned directly above the conveyor. This section will be oriented perpendicularly to the conveyor belt when engaged. The pump is activated once the pipe is submerged, initiating the drainage process. Although the outlet pipe for the pump is not shown in the model, its configuration will depend on site-specific conditions. The outlet pipe can channel the drained water into a sump or a channel. Once the sensors detect that the desired water level has been reached, the pump automatically shuts off, and a unidirectional valve prevents backflow, ensuring that no air enters through the inlet.

After the pump is turned off, the pipe rotates upwards to allow raw materials to pass without damaging it. This rotation is achieved through a swivel joint, enabling the pipe to disengage smoothly from the conveyor and avoid interference with the material flow. The system uses 3-inch PVC pipes, and the pump employed is a Pedrollo HF Centrifugal Pump [21], shown in the Figure 45 below. With a flow rate of 132 m^3/h and a suction lift of 7 meters, this pump efficiently handles the drainage demands.

Figure 45-Pedrollo HF Centrifugal Pump [21]

The thoughtful design of the pump system ensures effective water removal when the conveyor is idle while preventing damage to the raw material handling process.

5.2 3D Model

The 3D model depicts one single pump and its connected pipe. When implementing the system multiple pumps can be utilized depending on the site requirements. Notable features of the model are the PVC pipe, pipe support frame, swivel joint (allows rotation), and the pump along with its concrete base. The dimensions of the pipe and the structure are for demonstration purpose only. And that implies that the actual dimensions of the pipe, height, and the dimensions of the frame will be subject to change as per requirements.

Following image shows the pump and pipe along with its support frame.

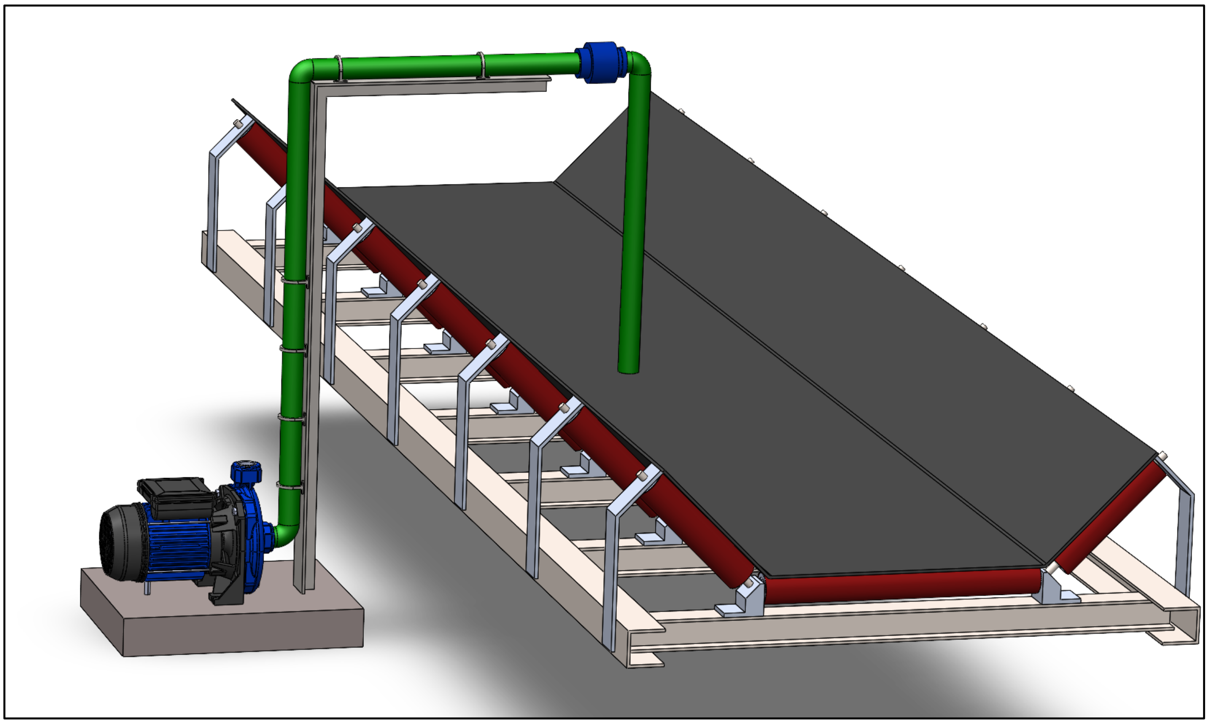

Figure 46-3D Model of Pump-Based Design

The pipe support frame is made from structural steel and has a T cross sectional shape. This provides extra stifness, and the amount of deformation produced in this support frame will be calculated in the upcoming section.As for the height of the pipe, it was selected as such so that it allows passing through of the raw material when the pipe is disengaged.

5.3 CFD of pipe:

A CFD simulation was conducted on two samples of pipes to determine whether the shape of the pipe will improve the flow. The two pipes are shown below (Figure 47 and Figure 48). below. The notable difference is the 90 degrees bend opposite to the direction of water flow in one of the pipes. A complete comparison is provided in this report. ANSYS Workbench 2023 R1 was used throughout both the simulations.

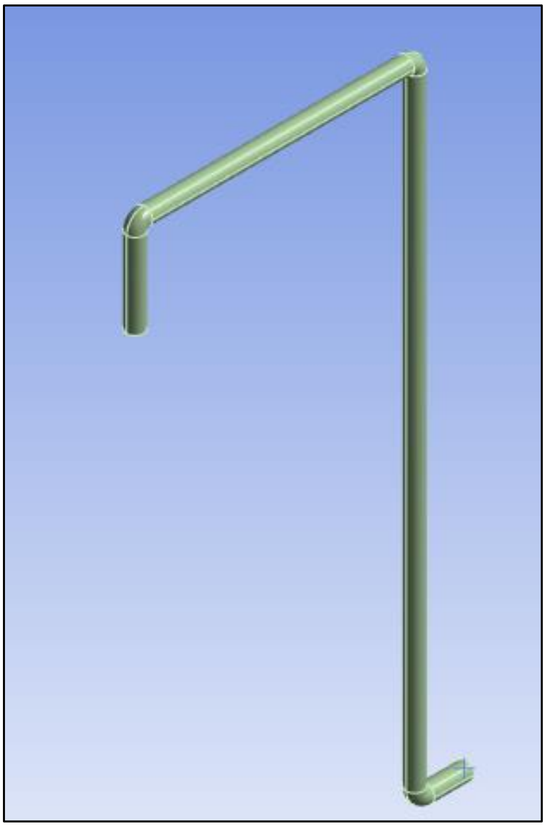

Figure 47-Pipe domain (Without Elbow)

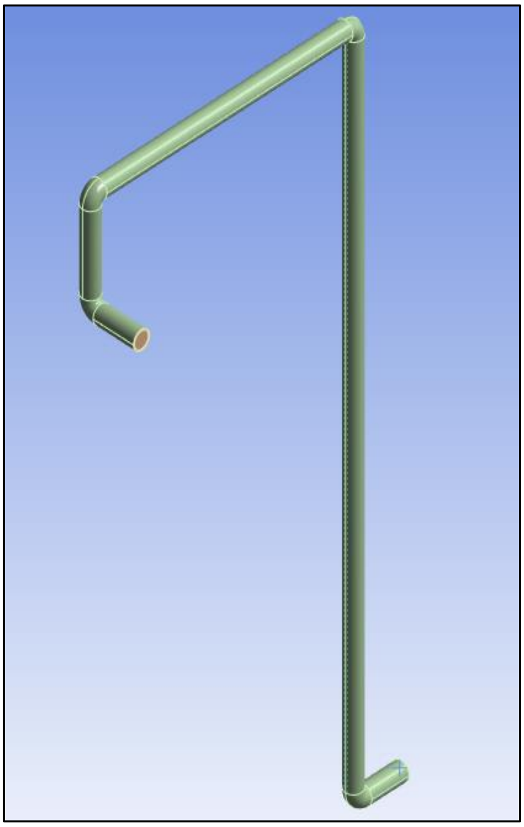

Figure 48-Pipe domain (With Elbow)

5.3.1 Simulation Set-up:

After extraction of volume from the pipe, the following set-up was used to carry the analysis. Pipe was considered as fixed wall in both the cases. The mass flow is calculated to determine the inlet condition.

Calculation: In our case the pump, Pedrollo HF Centrifugal Pump, has the capacity of Q=132 m^3/hr. (0.03m^3/s), and the diameter of the pipe used is 3 inch i.e 76.2mm (A=4.56x10^{-3} m^2).

To verify the velocity, we use the following.

$$v = \frac{Q}{A} = \frac{0.03}{4.56 \times 10^{-3}} = 6.57\ m/s$$

The mass flow rate would be.

$$\dot{m} = \rho\ Q = 1000\ \times 0.03 = 30\ kg/s$$

The mesh size is 0.14m (tetrahedral) adaptive sizing with 7 resolution size selected automatically by ANSYS algorithm. The flow setting is k-epsilon due to turbulent flow (Reynold's number calculation done in fluid properties section) and as for the boundary conditions, at Inlet the mass flow is set as 30kg/s. And the outlet was a pressure outlet.

5.3.2 Results:

Consider the following results based on the simulations carried out as complied in the table below. The complete set of screenshots of results is shown in Appendix E-Pipe CFD Results .

Table 9-Pipe CFD Results

Variable	Pipe without Elbow	Pipe with Elbow
Maximum Pressure	1.02e+05 Pa	4.05e+04 Pa
Average Pressure	1.64e+04	-1.13e+4 Pa
Maximum Velocity	13.7m/s	12.1m/s
Average Velocity	6.86 m/s	6.05 m/s
Average Velocity (Analytical)	6.57 m/s	6.57 m/s
% Error (Avg Vel.)	4.22 %	7.91%

5.3.3 Discussion:

This analysis validates our analytical calculation and additionally we see that both pipes show similar performance. The pipe without elbow does have higher average velocity and lower pressure indicating fewer losses. In addition to better slightly improved performance, the simpler design makes it the better choice.

5.4 FEA

The FEA was done for the support frame of the pipe. The boundary conditions and set-up is mentioned below.

5.4.1 Simulation Set-up

Meshing:

Firstly, the mesh size of around 0.05 m with the employment of adaptive sizing meshing scheme is used, and the options of refine, resolution (set to 7 factor max) are manipulated to get as refine mesh as could be.

Boundary Conditions:

The two boundary conditions have been used:

- Fixed Support at the end of T shaped support frame.
- Uniformly Distributed Load at the top surface of cantilever T beam where the pipe will be placed.

For the load calculations, we have considered both the load of pipe and the water, and then at the end for the total load, both were added to get the total load.

5.4.2 Results

The analysis output was the following results.

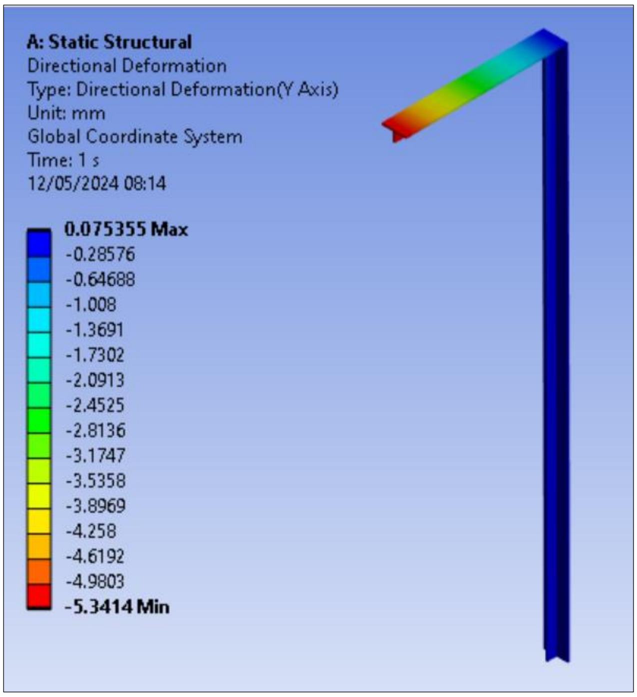

Figure 49-Pipe Support Frame FEA-Deformation

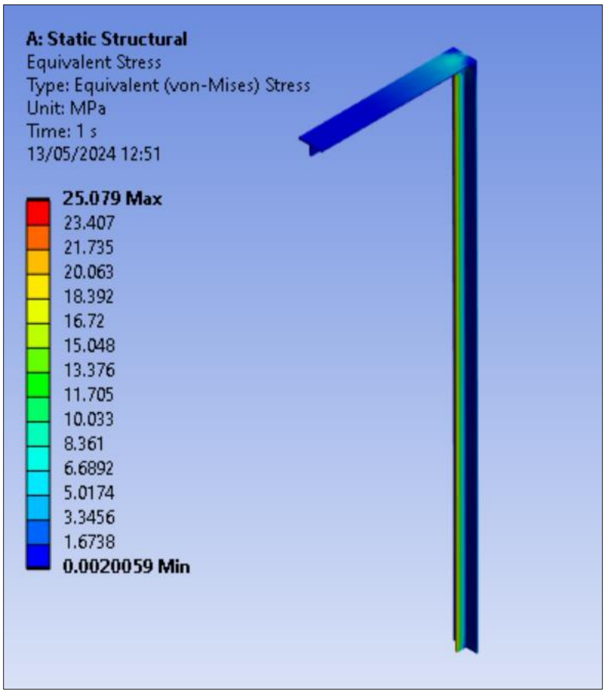

Figure 50-Pipe Support Frame FEA-Total Stress

Table 10-Pipe Support Frame-FEA Results

Variable	**Result**
Total Stress	25.079 MPa
Deformation (y-axis)	5.3414 mm

Analytical Calculation:

The support frame structure consists of T-bar of Steel, (E=$2\text{x}10^{11}$Pa), with a profile (in mm) of t=10, b=130, h=60 which gives us ($I_x=4.4\text{x}10^{-7}m^4$). And the dimensions (in mm) of the frame is h=2870 and L=862.57. The deflection at the top corner of the frame in y-axis is given by

$$\Delta c_y = \frac{wL^3}{8EI}(L + 4h)$$

$$\Delta c_y = 5.637 \times 10^{-3} m = 5.637 mm$$

5.4.3 Verification

Error calculations:

$$\%\ \text{error} = \frac{|5.3414 - 5.637|}{5.637} = 5.24\%$$

The error is within acceptable range.

5.4.4 Discussion

The deformation was small enough to be inconsequential and hence acceptable. However, it shall be noted that the stress results were not verified, and a suitable analytical verification should be done before the results are considered to be correct.

5.5 Deployment Mechanism of pipes:

The deployment structure shown is like plate deployment. This was done to have similar design across the system. And, as mentioned in the hydraulic section, similar actuators can be used to deploy the pipes. However, the selection of the exact specs will vary based of the lower weight and the stroke length required. The design requires more iterations to be optimized further for prototyping. The second iteration would have repositioned the actuator, redesigned the arm and lowered the overall dimensions. One main hydraulic system can be set up to operate both the plate and the pumps. However, with separate actuators and deployment structures. The figures show the pipes in engaged and disengaged configuration below.

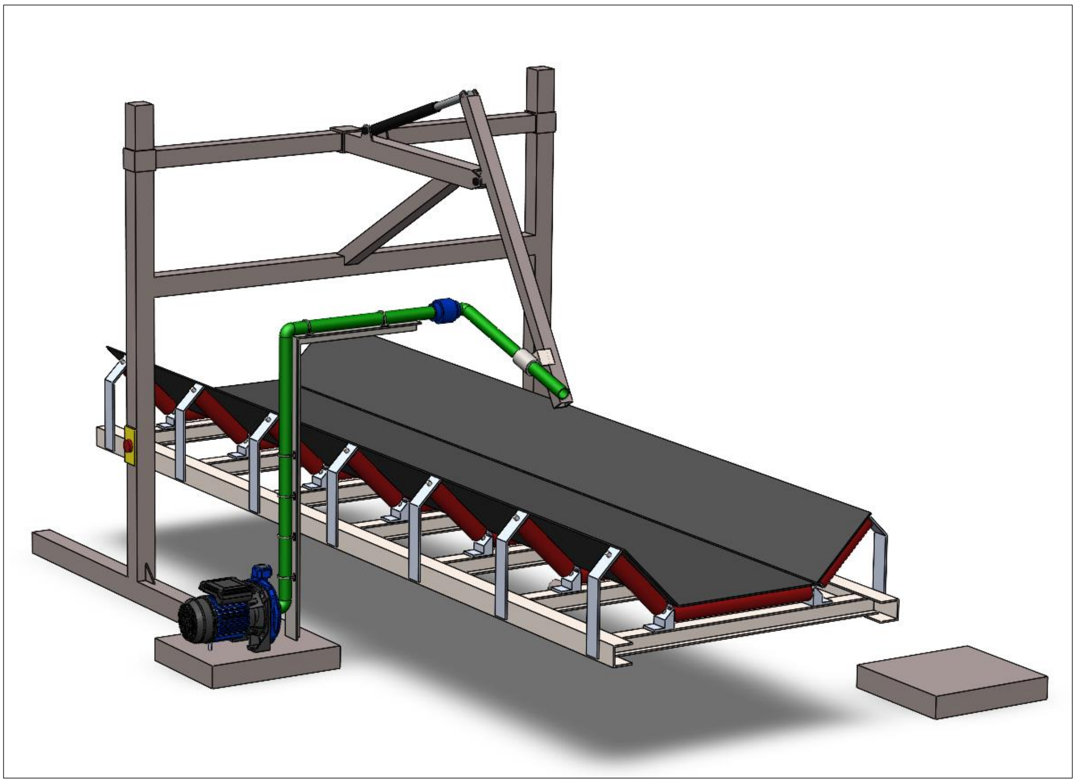

Figure 51-Pipe in Disengaged Position

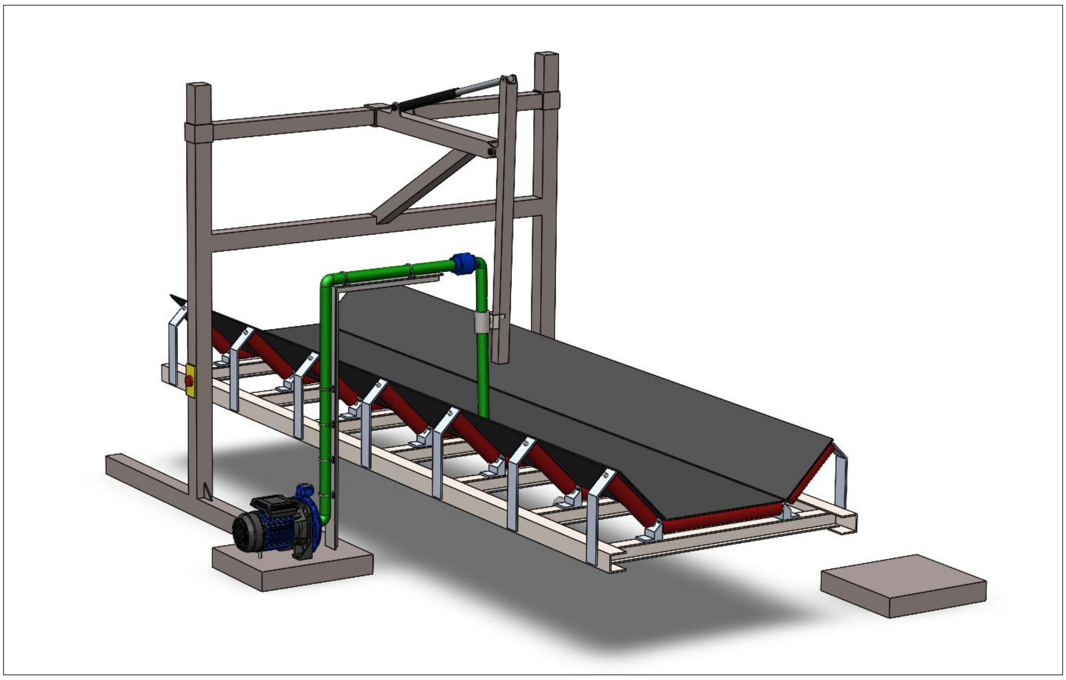

Figure 52-Pipe in Engaged Position

6 Results

The report has included in-depth analysis of the plate and the pump system. This section contains a summary of the results of such analyses.

6.1 Plate-Based Design

As mentioned earlier, the plate-based design was the primary focus of this solution, and it was for this reason that extensive study was done on this part of the solution. In the table below the results of all the analyses are compiled.

Table 11-Plate-Based Design Results Summary

Analysis	Description	Method	Result	% Error
Material Selection				
Material Selection	4 materials were selected best suited to our needs	Material selection Method by Ashby/ Ansys Granta	CFRP, CMA, PC, PET	N/A
CFD-Wind tunnel				
Drag Coefficient	The drag was calculated for the plate.	Star CCM+ was used for the analysis.	0.859285	0.30%
Total Pressure	The pressure was calculated for the plate.	Star CCM+ was used for the analysis.	1.08×10^5 Pa	0.43%
FEA				
Max Deformation	The deformation for CMA 8mm thk. is shown	Ansys Workbench was used for the analysis	4.7mm	0.66%
Total Stress	The total stress for CMA 8mm thk. is shown	Ansys Workbench was used for the analysis	14.3 MPa	5.07%
CFD-Mass flow				
Mass flow rate	The ability of the plate inclined at 23° to disperse water was tested.	Ansys Fluent was used for the analysis	1431	2.15%

The table above shows us that 4 types of analysis was done. These results were accurate as evident by the calculated errors and the convergence of results for all the analyses.

The material selection allowed us to narrow down the material selection to 4 materials. The first CFD was done to calculates the drag exerted on the plate. We found the drag and the pressure on the plate and used it in our FEA. All these materials with varying thickness were analyzed. Ultimately CMA at 8mm thickness was selected due to its high stiffness, high strength, low mass and low cost. The last stage in the performance analysis was to find the mass flow out of the water, which showed promising results with 98% water removal rate.

6.2 Pump-Based Design

The second system was designed as an auxiliary part of the system, and hence it was not studied as thoroughly as the first one. Although, some key analyses were done to establish its viability, further work will be required to optimize and better understand its shortcomings. The table below shows these results for the pump system.

Table 12-Pump-Based Design Results Summary

Analysis	Description	Method	Result	% Error
FEA				
Max Deformation	The deformation for support frame was analyzed.	Ansys Workbench was used for the analysis	5.637mm	5.24%
CFD				
Avg Velocity	Two pipes' routes were tested to optimize flow.	Ansys Fluent was used for the analysis	6.86 m/s	4.22%

The pipe support frame, designed to hold and support the pipe was tested for it's ability to resist deformation under load. While CFD was done on the pipe to verify the flow and compare other possible pipe design. We see that the a single pump can pump out 30kg/s of fluid, which can be scaled according to site requirements.

These results, though limited, provide sufficient groundwork to build on top of it. The discussion on the further work that can be done for both, the plate and the pump system is in the upcoming chapter.

7 Conclusion

This chapter includes discussion on the findings of this report and what future work may be done in order to develop the products into a working prototype.

7.1 Discussion

The proposed solution, consisting of a combination of plate-based and pump-based designs, offers an innovative approach to addressing water flooding in conveyor belt systems. This dual solution ensures that water can be effectively drained from the conveyor, regardless of whether it is moving or stationary. Such flexibility enhances the system's operational efficiency and reduces the risk of production interruptions.

In the plate-based design, an 8mm cast magnesium alloy plate inclined at approximately 23° and weighing about 50 kg effectively removes up to 98% of the water. Assuming that the total volume of water is 300 m^3 and a conservative assumption for the plate's mass flow rate of 700 kg/s, the conveyor can be drained within 7.14 minutes. In reality, the system demonstrated a significantly higher mass flow rate of 1431 kg/s in testing, surpassing initial estimates. This performance underscores the plate-based design's remarkable efficiency in water removal. Its straightforward structure, featuring minimal moving parts, ensures reliable operation and requires minimal maintenance. Additionally, the hydraulic deployment mechanism allows for rapid engagement and disengagement, which is crucial in high-demand mining environments.

However, the plate's performance depends on several factors, including its position on the conveyor and the deflection or sway of the deployment arm under hydrodynamic force. Incorrect positioning or excessive deflection can reduce efficiency and potentially lead to damage. Thus, careful consideration of these factors is essential.

Although the plate design showed promising results, further refinements and comprehensive testing are needed to optimize its performance, as highlighted in the "Further Work" chapter. The pump-based system serves as a secondary drainage solution, designed to address cases where the plate underperforms or when the conveyor is mainly operational. However, the pump system is inherently less efficient in removing water quickly. It introduces challenges such as higher noise levels, increased maintenance due to cavitation and mechanical failures, and greater energy consumption. With a maximum mass flow rate of 30 kg/s per pump, this system is best used as a secondary drainage measure, subject to a site-specific assessment.

Despite its limitations, the pump-based system can be advantageous in certain situations, particularly in preventing water buildup during conveyor downtimes. It offers scalability and flexibility by allowing multiple units to be strategically placed along the conveyor system.

Overall, the plate-pump combination forms a scalable, versatile, and efficient solution for water removal. The system can be installed at multiple positions along the conveyor without requiring significant structural or operational modifications. Its quick engagement and rapid drainage capabilities ensure minimal production interruptions and optimal operational efficiency.

7.2 Further Work

This section outlines potential areas for future research and development based on the findings and conclusions of this study. Building upon the proposed solutions for water flooding in conveyor belt systems, this chapter identifies opportunities for refining the existing designs, integrating advanced technologies, and conducting comprehensive field trials. It also discusses the potential for adapting these solutions to various industrial sectors and differing operational environments. The chapter emphasizes the importance of continued innovation in water management strategies to enhance the durability of mining infrastructure, reduce downtime, and maintain optimal production and safety standards.

7.2.1 Experimentation and Testing

Extensive experimentation and testing are essential before full-scale implementation of the proposed systems. Prioritizing the plate-based design due to its promising results, the following aspects should be thoroughly assessed:

Mass Flow Rate: The mass flow rate should be measured and validated using scaled models and real-life scenarios. This testing will confirm the simulation results and identify potential issues, such as unpredictable water flow patterns or splashing. By understanding the exact trajectory of the water exiting the plate, engineers can refine the design to reduce uncontrollable flow and mitigate potential hazards, ensuring safer working conditions.

Plate Strength and Deformation: Real-world testing will allow engineers to observe how the plate reacts under hydrodynamic forces, ensuring it maintains structural integrity without excessive deformation. Testing will also ensure that the plate remains clear of the conveyor belt, preventing catastrophic damage that could halt production or compromise safety.

Plate Rollers: Mockup testing of the plate rollers on a conveyor will verify their compatibility with the belt. Different materials and roller sizes should be experimented with to minimize any risk of belt damage, as even minor scratches can worsen under the heavy raw material load. This testing will help identify the optimal roller composition, reducing friction and wear.

Deployment Time and Strength: The hydraulic deployment mechanism needs to be tested for swift engagement and disengagement while maintaining structural integrity. The frame must be structurally sound and stiff to prevent excessive arm deflection, which could negatively impact both the plate and the conveyor belt.

Pump-Based Design: The pump system requires extensive testing to check for flow rate efficiency and potential issues like air entrapment and cavitation. The swivel joint and other potential weak points should be closely examined to ensure durability. Analyzing the pump-based system under different operational conditions will highlight any limitations and guide further optimization.

Energy Consumption: A detailed analysis of energy consumption is required for both systems. While the pump system is presumed to be more energy-intensive, the plate indirectly relies on conveyor operation. Identifying areas for improvement will lead to energy-efficient designs.

7.2.2 Design Optimization

Optimizing various system components through an iterative design process can significantly improve the system's performance and reliability.

Plate Design: Experimentation and testing will reveal how the plate can be optimized for improved flow and structural integrity. Streamlining water outflow will help control water flow paths and reduce splashing. Strengthening the plate design can prevent structural failures under hydrodynamic loads.

Plate Rollers: As the rollers can potentially damage the conveyor belt, redesigning them after thorough testing will ensure minimal impact. Focus areas should include reducing friction, optimizing positioning to prevent deflection, and selecting suitable materials.

Deployment Mechanism: The deployment mechanism should be redesigned for greater stiffness to maintain the plate's position. Utilizing the push stroke instead of the pull stroke of the actuator may offer a more efficient design. Incorporating a counterweight will ensure that the default disengaged position is maintained.

Suspended Plate Design: An alternative design without plate rollers can prevent belt damage. A suspended plate eliminates contact with the conveyor belt, relying solely on the hydraulic mechanism for controlled movement.

Pump-Based Design: Optimization of the pump-based design includes experimenting with various pump types, pipe sizes, and valve configurations. Pressure relief valves and other safety mechanisms can prevent pump damage and improve flow rates.

These efforts will lead to a robust, versatile, and efficient water removal system that addresses the industry's unique challenges while ensuring safety and operational continuity.

7.2.3 Automation and control

In the following section the expected working of the entire water removal system will be explained. The sensors are designed to work together and allow for a robust system that activates the diverter plate and pumps based on the conditions on the conveyor.

The system will operate in conjunction with the existing automation system of the plant/site. The plate will be deployed if the following conditions are met:

- The conveyor is running.
- There is presence of water and no iron ore.
- The level of water is above a set value that will be determined by the end user.

If any of these conditions are not met the plate will be disengaged and returned to its original spot.

Similarly, the pumps will be turned on when the following conditions are met.

- The conveyor is stopped.
- There is presence of water and no iron ore.
- The level of water is above a set value that will be determined by the end user.

As soon as any of the conditions are not met, the pumps will be turned off and the pipe will be lifted away from the conveyor.

In the next section some possible sensors are mentioned that may be used as part of the automation system.

Material detection sensors:

The iron ore being transported is a magnetic material, so a magnetic sensor can be used to detect the presence of raw material. Magnetic sensors detect the material due to change in magnetic field and provide the output (analog or digital) to the output station. It shall be noted that the sensitivity of the sensor will be adjusted based on the type of ore, amount of ore and the distance of the sensor from the raw material.

Examples:

One possible sensor that may be used is Magnetic field sensor MB80-12GM50-E0-PUR [22] as shown in the figure below.

Figure 53-Magnetic field sensor MB80-12GM50-E0-PUR [22]

It has a detection range of 80mm. It shall be noted that most manufacturers offer wide variety of choices depending on site/system specific needs.

Water Detection:

For proper working of autonomous deployment of mechanism, water must be detected on the conveyer. The detection of water is crucial before the deployment of plate or pipe. For this scenario a capacitive sensor will be attached over the conveyer belt. These sensors detect changes in capacitance caused by the presence of water.

Examples:

The figure below shows a potential sensor that maybe used. The Omron E2K-C Series [23] offers sensing of material up to a distance of 20mm [24].

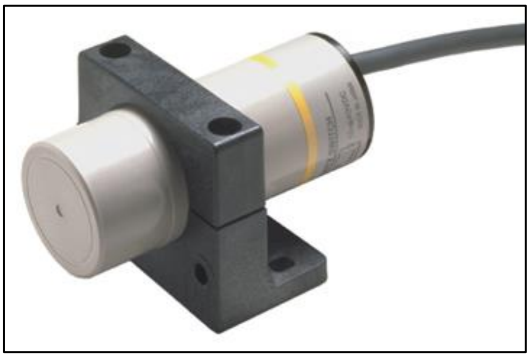

Figure 54-Omron E2K-C Series [23]

Water level detection:

Now the next step will be measurement of water level on the conveyer belt. For this there are a couple of option i.e., the pressure transducer and ultrasonic sensors. Both give the same output while working on completely different mechanisms. The former one is attached below the conveyer belt and will measure the height of water by the pressure difference created while the later one absorbs the already emitted ultrasonic radiations and give information regarding the depth of water body on conveyer. While keeping in view that the conveyer will be filled with ore after the removal of water the option of using an ultrasonic sensor looks more highlighted.

Examples:

To detect water level on the conveyor, Siemens SITRANS LUT400 Series [25], as shown in the figure below, can be used. It is a versatile device that can be connected directly to a PC or to a larger automation system. And it can detect changes in level up to 60m [26].

Figure 55-Siemens SITRANS LUT400 Series [25]

Integration/Installation of sensors:

The suite of sensors will be installed based on the manufacturer recommended distances and orientation. All sensors are non-contact sensors as the conveyor will be moving mostly. On any above surface from which the conveyer below is clearly at sight an ultrasonic sensor can be installed. Similarly magnetic sensors (for material detection) and capacitive sensor are also standalone sensors and are directly mounted near the conveyer belt system.

These sensors will be connected to a larger system such as a PLC or a SCADA (Supervisory Control and Data Acquisition) system.

Turn-Off Position of Actuator:

Once the water has been fully removed from the conveyor and the plate is in its original position above the conveyor, it must remain there without requiring continuous power usage. This is achieved through the installation of Directional Control Valves (DCVs) in the hydraulic system. The DCVs manage the hydraulic fluid flow to and from the actuator. When the actuator reaches its compressed state, the DCV centers or actuates to block fluid flow, effectively holding the actuator in place.

7.2.4 Emergency Stop and Safety Mechanism

A robust safety mechanism is essential to ensure that the plate and pump systems disengage promptly in the event of an error. Additionally, a manual stop button should be integrated to allow the operator to manually interrupt the system when necessary.

Automatic Safety System: To enhance safety, a spring can be integrated into the actuator body. During deployment, the hydraulic actuator's rod is under tension, causing the spring to compress due to the load exerted by the hydraulic fluid. In the event of a power outage, the compressed spring will move the actuator's rod back to its original position, leveraging the spring's restoring or compression force.

A check valve is installed to prevent hydraulic fluid from escaping the cylinder during this process. Once the spring returns the rod to its original position, the check valve blocks further fluid loss, locking the system in its default state.

Sensors and Alarms: Sensors should be installed to detect unusual vibrations in the plate or deployment mechanism, which can signal contact between the plate and the conveyor belt. Such vibrations can indicate potential damage or other mechanical issues, requiring immediate attention to prevent accidents. Further experimentation and testing can reveal other failure points, allowing engineers to integrate relevant sensors and safety mechanisms to mitigate damage to the conveyor and ensure worker safety.

Manual Override System: A manual stop button should be strategically located in both the control room and along the conveyor for quick and easy access. This button disengages the plate, lifting it to its safe position, and also disengages the pipe. To prevent confusion between emergency and conveyor stop buttons, the emergency stop should be distinctly labeled and color-coded.

Conveyor Stoppage Protocol: In the event of a conveyor stoppage, the plate will remain in its current position, whether engaged or disengaged. This prevents further damage to the conveyor belt. Similarly, the pipes will stay engaged to ensure stability, but the pump system will automatically shut off to conserve energy and prevent unnecessary operation.

This comprehensive safety system ensures that the water removal system operates securely, minimizing risks and preventing mechanical failures that could compromise the efficiency or safety of conveyor belt operations.

8 References

[1] L. M. Poukhonto, *Durability of Concrete Structures and Constructions: Silos, Bunkers, Reservoirs, Water Towers, Retaining Walls*. 2003. CRC Press.

[2] S. Jamle, "An Informative Review on Underground Storage Reservoir System," 2019, doi: 10.6084/m9.figshare.11663712.

[3] L. Brønnboring, "SILA Narvik," ed.

[4] L. dos Santos e Santos, W. Kleyson da Silva Soares, and P. Roberto Campos Flexa Ribeiro Filho, "A method for investigating the influence of rainwater on the useful life of idlers in pipe belt conveyors during seasonal operations," *Engineering failure analysis,* vol. 141, p. 106702, 2022, doi: doi/10.1016/j.engfailanal.2022.106702.

[5] M. Vasić, B. Stojanović, and M. Blagojević, "Failure analysis of idler roller bearings in belt conveyors," ed. Oxford ; New York :, 2020, p. 104898.

[6] P. Bortnowski, W. Kawalec, R. Król, and M. Ozdoba, "Types and causes of damage to the conveyor belt – Review, classification and mutual relations," ed. Oxford ; New York :, 2022, p. 106520.

[7] R. Król, "Studies of The Durability of Belt Conveyor Idlers with Working Loads Taken into Account," *IOP Conference Series: Earth and Environmental Science,* vol. 95, p. 042054, 2017, doi: 10.1088/1755-1315/95/4/042054.

[8] D. Friso, "Conveyor-Belt Dryers with Tangential Flow for Food Drying: Mathematical Modeling and Design Guidelines for Final Moisture Content Higher Than the Critical Value," *Inventions,* vol. 5, no. 2, p. 22, 2020, doi: 10.3390/inventions5020022.

[9] N. Schmidt, J. Denecke, J. Schmidt, M. Davies, and T. Heidermann, "Experimental investigation on condensation inside of storage tanks during rapid cooling in a heavy rain event," ed. [Rugby, Warwickshire] :, 2022, pp. 464-474.

[10] G. McPhail, R. Ugaz Palomino, and F. Garcia Araujo, "Practical tailings slurry dewatering and tailings management strategies for small and medium mines," 2019: Australian Centre for Geomechanics, Perth, doi: 10.36487/acg_rep/1910_15_mcphail. [Online]. Available: https://dx.doi.org/10.36487/acg_rep/1910_15_mcphail

[11] S. L. Yellin and K. Goldstein, "Clean air knife drying of clean parts," *Precision Cleaning '95. Chicago, IL,* 1995.

[12] D. Wojtkowiak, K. Talaśka, I. Malujda, and G. Domek, "Vacuum conveyor belts perforation–methods, materials and problems," *Mechanik,* vol. 12, no. 2017, pp. 1138-1142, 2017.

[13] M. T. SATO HIDEAKI, "BELT CONVEYOR DRAINING METHOD AND DEVICE," Japan Patent JP2000318827A, 1999. [Online]. Available: https://worldwide.espacenet.com/patent/search/family/015059935/publication/JP2000318827A?q=pn%3DJP2000318827A

[14] POSCO, "BELT CONVEYER HAVING WATER SEPARATOR," Patent KR101500125B1, 2015. [Online]. Available: https://worldwide.espacenet.com/patent/search/family/052578770/publication/KR101500125B1?q=pn%3DKR101500125B1

[15] N. Cross, *Engineering design methods: strategies for product design*. John Wiley & Sons, 2021.

[16] M. F. Ashby, *Materials Selection in Mechanical Design*. Elsevier Science, 2016.

[17] L. Gebrehiwet, "Servovalve design and simulation加伯瑞姆," ed, 2015.
[18] *3L inch series tie rod hydraulics cylinders catalogue*. [Online]. Available: https://www.parker.com/content/dam/Parker-com/Literature/Accumulator---Cooler-Division---Europe/catalogues/cylinder/HY07-1130UK_3L_Inch_Series_Tie_Rod_70_Bar_Hydraulic_Cylinders.pdf.
[19] P. Hannifin. "Series CHGH Metric Compact Hydraulic Cylinders." https://ph.parker.com/ca/en/product-list/compact-hydraulic-cylinders-metric-steel-body-construction-series-chgh (accessed.
[20] P. Hannifin. "Double Acting Hydraulic Cylinder 70H-8." https://ph.parker.com/us/en/product-list/7mpa-double-acting-hydraulic-cylindermodel-70h-8?facet:4099276460822254894623255534832116111324953484847954711 2115105&productBeginIndex:0&facetLimit:&orderBy:&pageView:list&minPrice:&maxPrice:&pageSize:&loadProductsList:true& (accessed.
[21] "Pedrollo HF Centrifugal Pump." https://pumpwarehouse.co.uk/shop/hf-centrifugal-pump-high-flow/ (accessed.
[22] "Magnetic field sensor MB80-12GM50-E0-PUR." https://www.pepperl-fuchs.com/great_britain/en/doci-showproductdocbypartno.htm?view=productdetails&amx_view=productdetails&prodid=93351 (accessed.
[23] "Omron E2K-C Series." https://automation.omron.com/en/us/products/family/E2K-C/e2k-c25mf1 (accessed.
[24] *Omron E2K-C Series Specs*, p. 4. [Online]. Available: https://assets.omron.com/m/047221f55b441320/original/E2K-C_Data_Sheet-pdf.pdf.
[25] "Siemens SITRANS LUT400 Series." https://www.siemens.com/us/en/products/automation/process-instrumentation/level-measurement/continuous/controllers/sitrans-lut400.html (accessed.
[26] *Siemens SITRANS LUT400 Series Datasheet*. [Online]. Available: https://cache.industry.siemens.com/dl/files/040/109765040/att_1159294/v1/sitransl_lut400_fi01_en.pdf.

Appendix A - LKAB Drawing

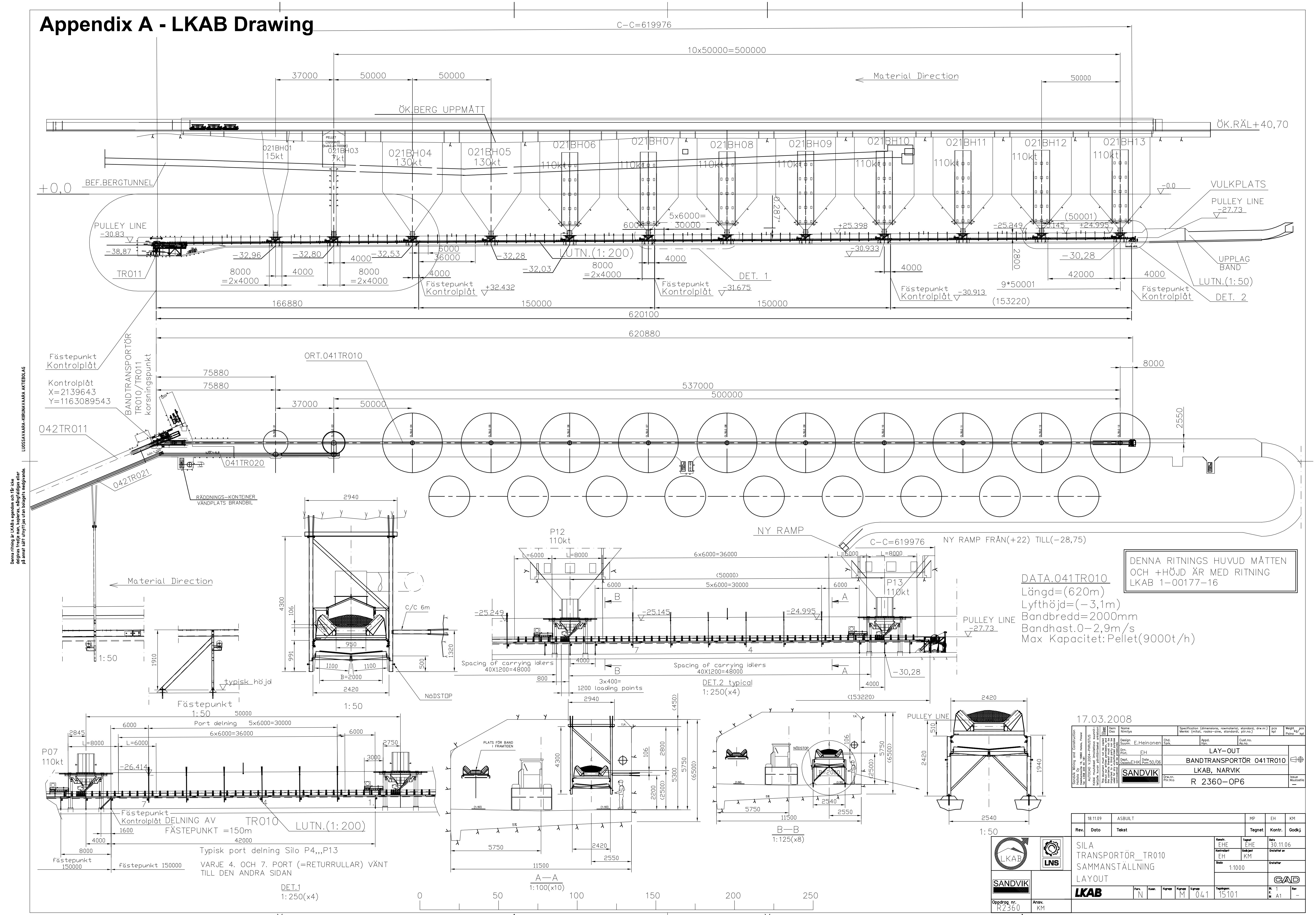

Appendix B-Plate FEA Results

Material: Carbon Fiber Reinforced Composites (CFRP)

Thickness: 5mm

Deformation

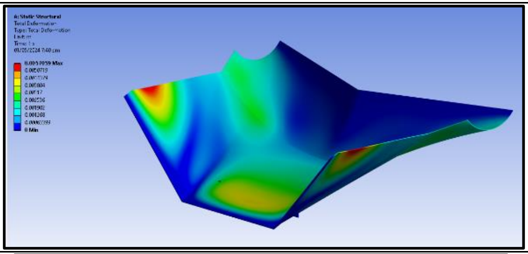

Results	
Minimum	0. m
Maximum	5.7059e-003 m
Average	1.364e-003 m

Stress

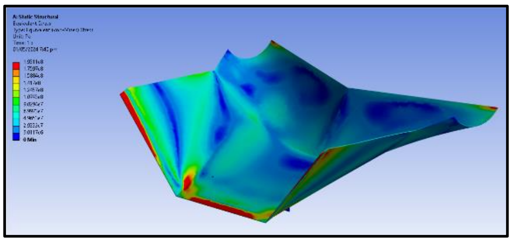

Results	
Minimum	0. Pa
Maximum	7.8312e+008 Pa
Average	4.0615e+007 Pa

Thickness: 8mm

Deformation

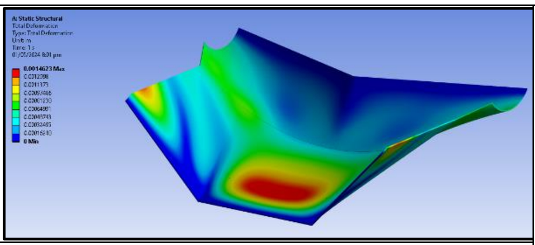

Results	
Minimum	0. m
Maximum	1.4623e-003 m
Average	3.6552e-004 m

Stress

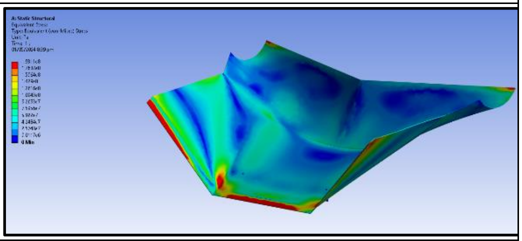

Results	
Minimum	0. Pa
Maximum	7.8312e+008 Pa
Average	4.0615e+007 Pa

Thickness: 12mm

Deformation

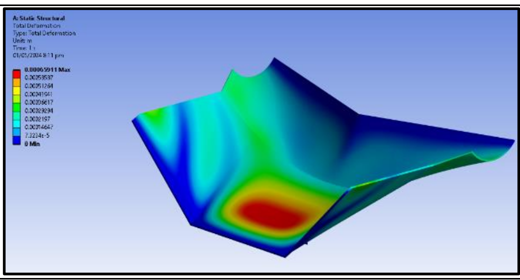

Results	
Minimum	0. m
Maximum	6.5911e-004 m
Average	1.5961e-004 m

Stress

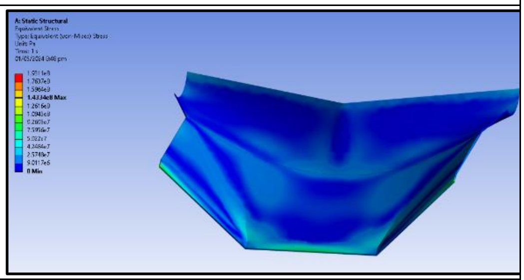

Results	
Minimum	0. Pa
Maximum	1.4334e+008 Pa
Average	8.7207e+006 Pa

Thickness: 15mm

Deformation

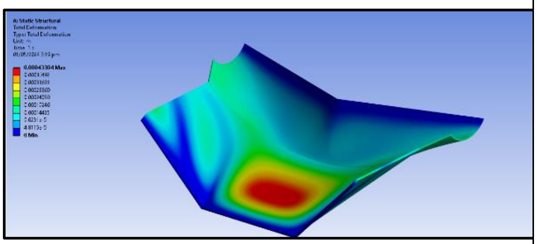

Results	
Minimum	0. m
Maximum	4.3304e-004 m
Average	1.0234e-004 m

Stress

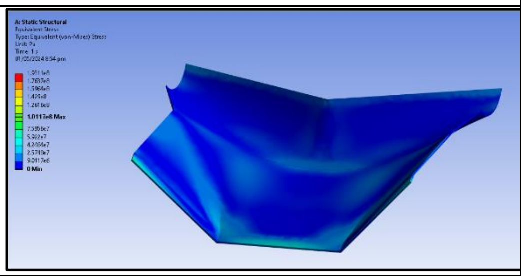

Results	
Minimum	0. Pa
Maximum	1.0117e+008 Pa
Average	6.4415e+006 Pa

Material: Cast magnesium alloys (CMA)

Thickness: 5mm

Deformation

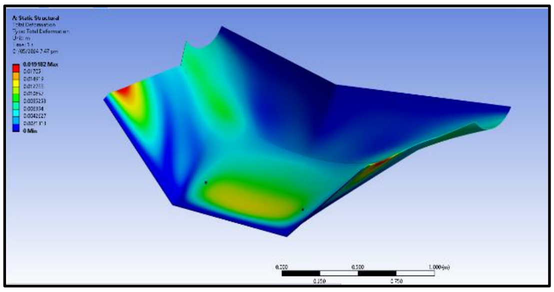

Results	
Minimum	0. m
Maximum	1.9182e-002 m
Average	4.4662e-003 m

Stress

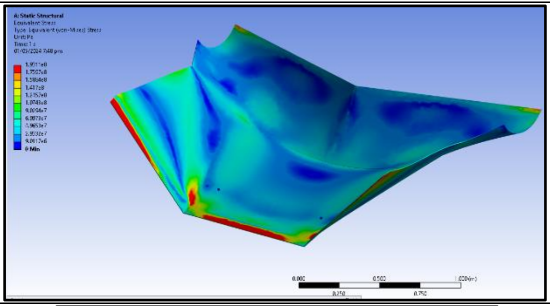

Results	
Minimum	0. Pa
Maximum	6.5738e+008 Pa
Average	3.8465e+007 Pa

Thickness: 8mm

Deformation

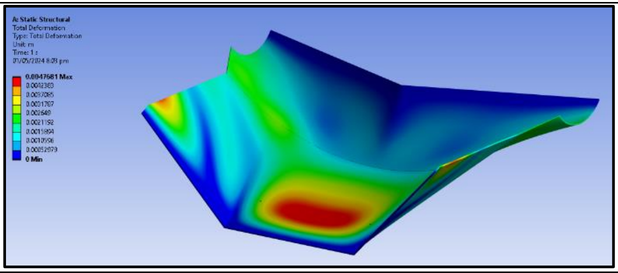

Results	
Minimum	0. m
Maximum	4.7681e-003 m
Average	1.2095e-003 m

Stress

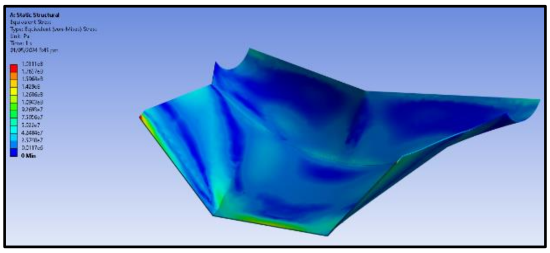

Results	
Minimum	0. Pa
Maximum	2.6995e+008 Pa
Average	1.4326e+007 Pa

Thickness: 12mm

Deformation

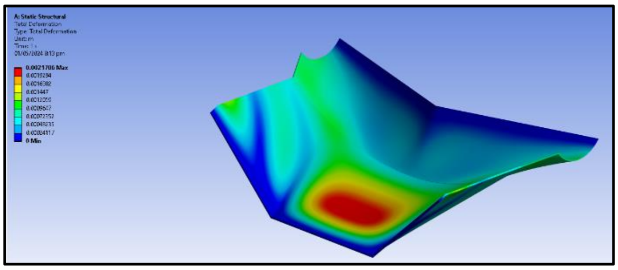

Results	
Minimum	0. m
Maximum	2.1706e-003 m
Average	5.364e-004 m

Stress

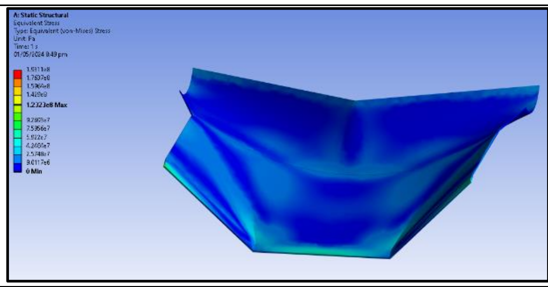

Results	
Minimum	0. Pa
Maximum	1.2323e+008 Pa
Average	8.3535e+006 Pa

Thickness: 15mm

Deformation

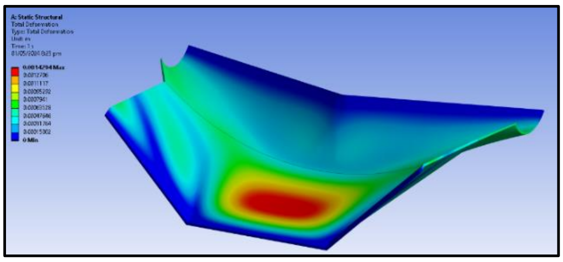

Results	
Minimum	0. m
Maximum	1.4294e-003 m
Average	3.4574e-004 m

Stress

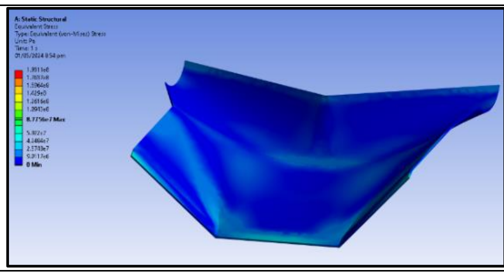

Results	
Minimum	0. Pa
Maximum	8.7756e+007 Pa
Average	6.1827e+006 Pa

Material: Polyethylene Terephthalate (PET)

Thickness: 5mm

Deformation

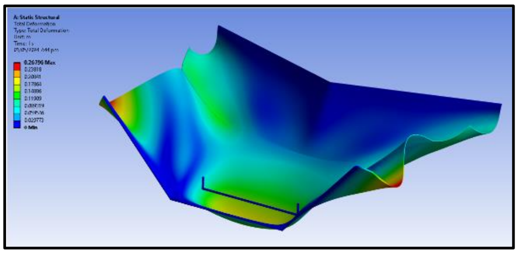

Results	
Minimum	0. m
Maximum	0.26796 m
Average	6.2175e-002 m

Stress

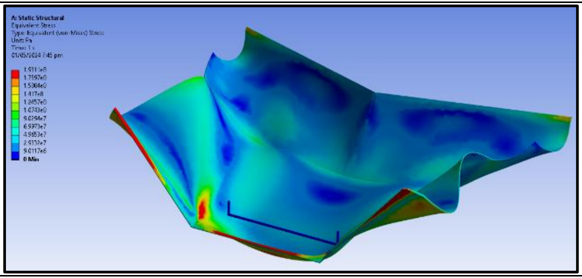

Results	
Minimum	0. Pa
Maximum	6.0145e+008 Pa
Average	3.7737e+007 Pa

Thickness: 8mm

Deformation

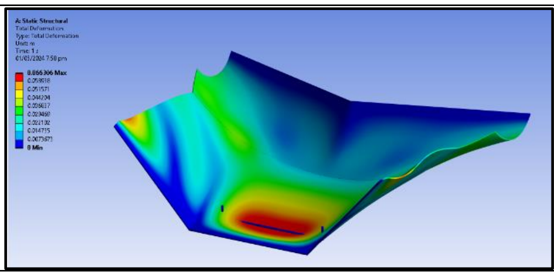

Results	
Minimum	0. m
Maximum	6.6306e-002 m
Average	1.6895e-002 m

Stress

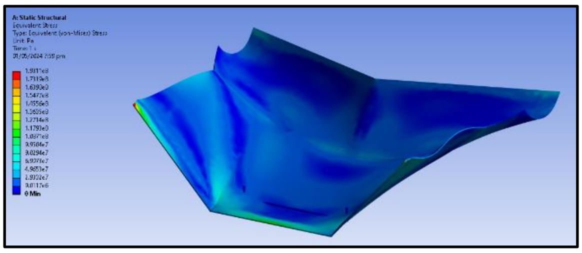

Results	
Minimum	0. Pa
Maximum	2.453e+008 Pa
Average	1.4058e+007 Pa

Thickness: 12mm

Deformation

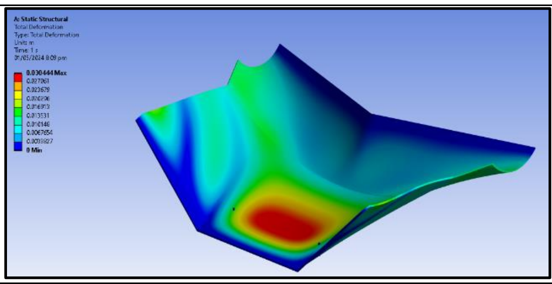

Results	
Minimum	0. m
Maximum	3.0444e-002 m
Average	7.5724e-003 m

Stress

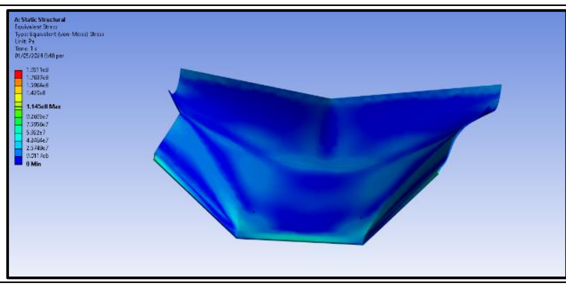

Minimum	0. Pa
Maximum	1.145e+008 Pa
Average	8.2397e+006 Pa

Thickness: 15mm

Deformation

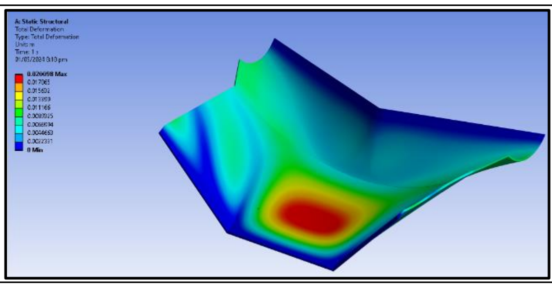

Results	
Minimum	0. m
Maximum	2.0098e-002 m
Average	4.8969e-003 m

Stress

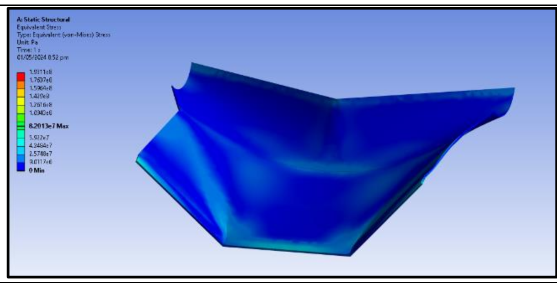

Results	
Minimum	0. Pa
Maximum	8.2013e+007 Pa
Average	6.1069e+006 Pa

Material: Polycarbonate

Thickness: 5mm			
Deformation	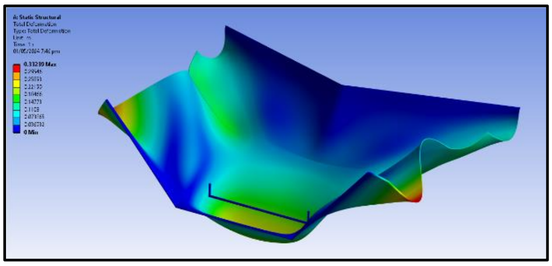 **Results** Minimum: 0. m Maximum: 0.33239 m Average: 7.7103e-002 m	Stress	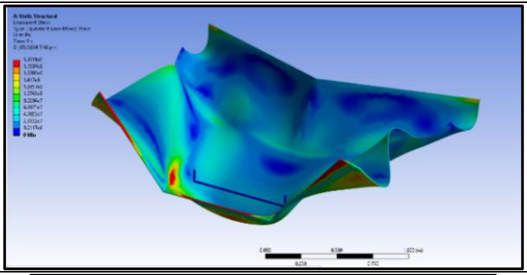 **Results** Minimum: 0. Pa Maximum: 5.8079e+008 Pa Average: 3.748e+007 Pa
Thickness: 8mm			
Deformation	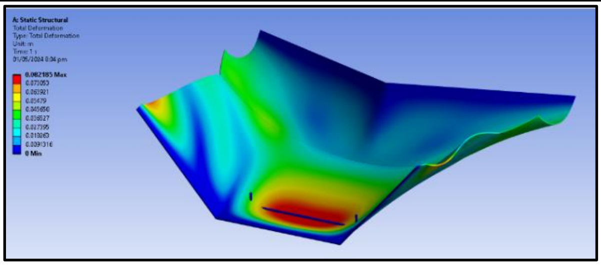 **Results** Minimum: 0. m Maximum: 8.2185e-002 m Average: 2.0973e-002 m	Stress	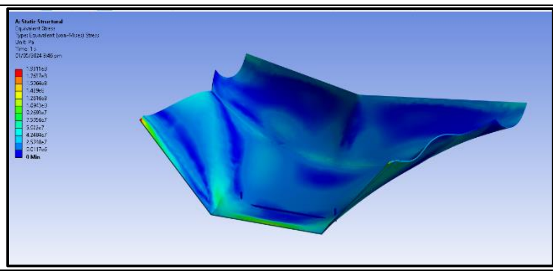 Minimum: 0. Pa Maximum: 2.3665e+008 Pa Average: 1.3963e+007 Pa
Thickness: 12mm			
Deformation	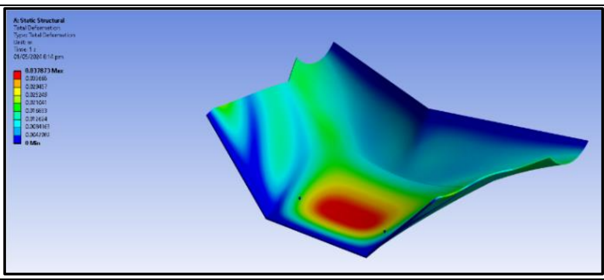 **Results** Minimum: 0. m Maximum: 3.7873e-002 m Average: 9.4415e-003 m	Stress	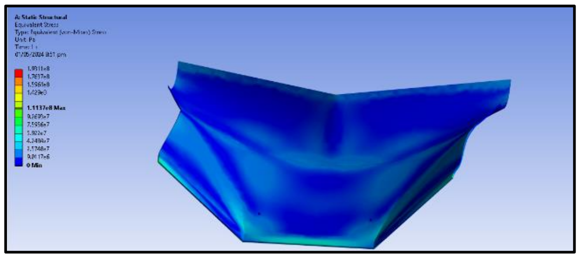 **Results** Minimum: 0. Pa Maximum: 1.1137e+008 Pa Average: 8.2009e+006 Pa
Thickness: 15mm			
Deformation	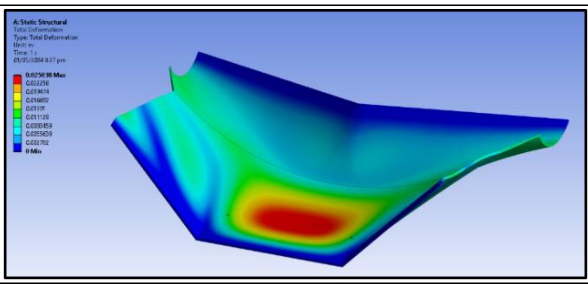 **Results** Minimum: 0. m Maximum: 2.5038e-002 m Average: 6.1135e-003 m	Stress	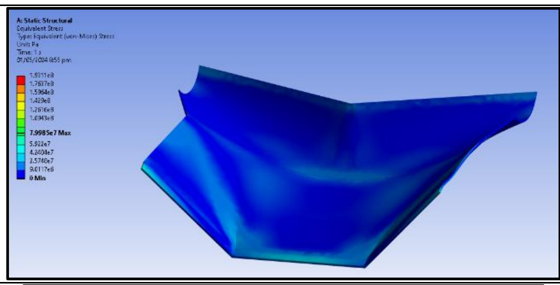 **Results** Minimum: 0. Pa Maximum: 7.9985e+007 Pa Average: 6.0816e+006 Pa

Appendix C-Plate Mass Flow CFD Results

<table>
<tr><th colspan="4">Plate 23°</th></tr>
<tr><td>Convergence Left Output</td><td>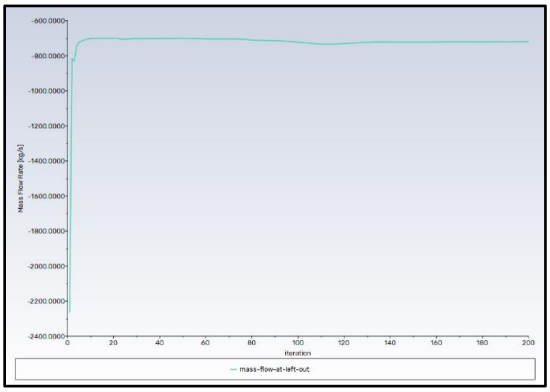
</td><td>Convergence Right Output</td><td>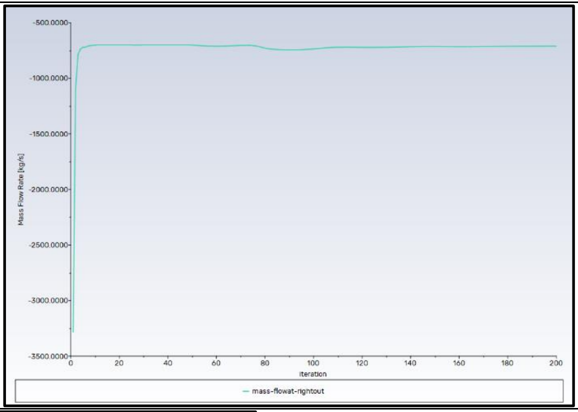
</td></tr>
<tr><td>Mass flow Results</td><td colspan="3">mass-flow-at-endout
Mass Flow Rate [kg/s]
outlet_end -20.052

mass-flow-at-left-out
Mass Flow Rate [kg/s]
outlet_l -719.49507

mass-flowat-rightout
Mass Flow Rate [kg/s]
outlet_r -712.03709</td></tr>
<tr><th colspan="4">Plate 30°</th></tr>
<tr><td>Convergence Left Output</td><td>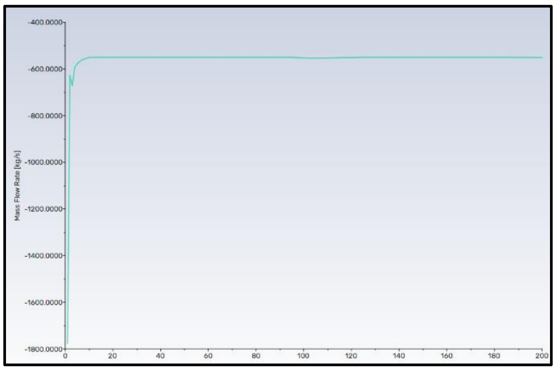
</td><td>Convergence Right Output</td><td>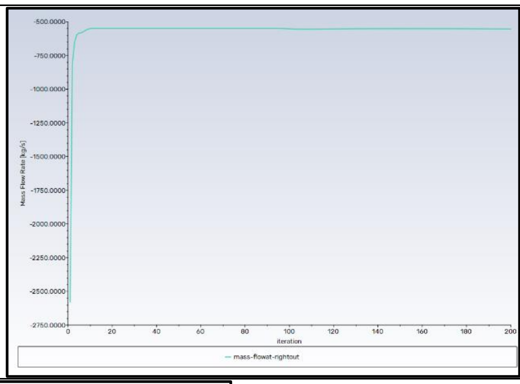
</td></tr>
<tr><td>Mass flow Results</td><td colspan="3">mass-flowat-rightout
Mass Flow Rate [kg/s]
outlet_r -553.40002

mass-flow-at-left-out
Mass Flow Rate [kg/s]
outlet_l -550.98742

mass-flow-at-endout
Mass Flow Rate [kg/s]
outlet_end -321</td></tr>
</table>

Appendix D-Plate 2D Drawing

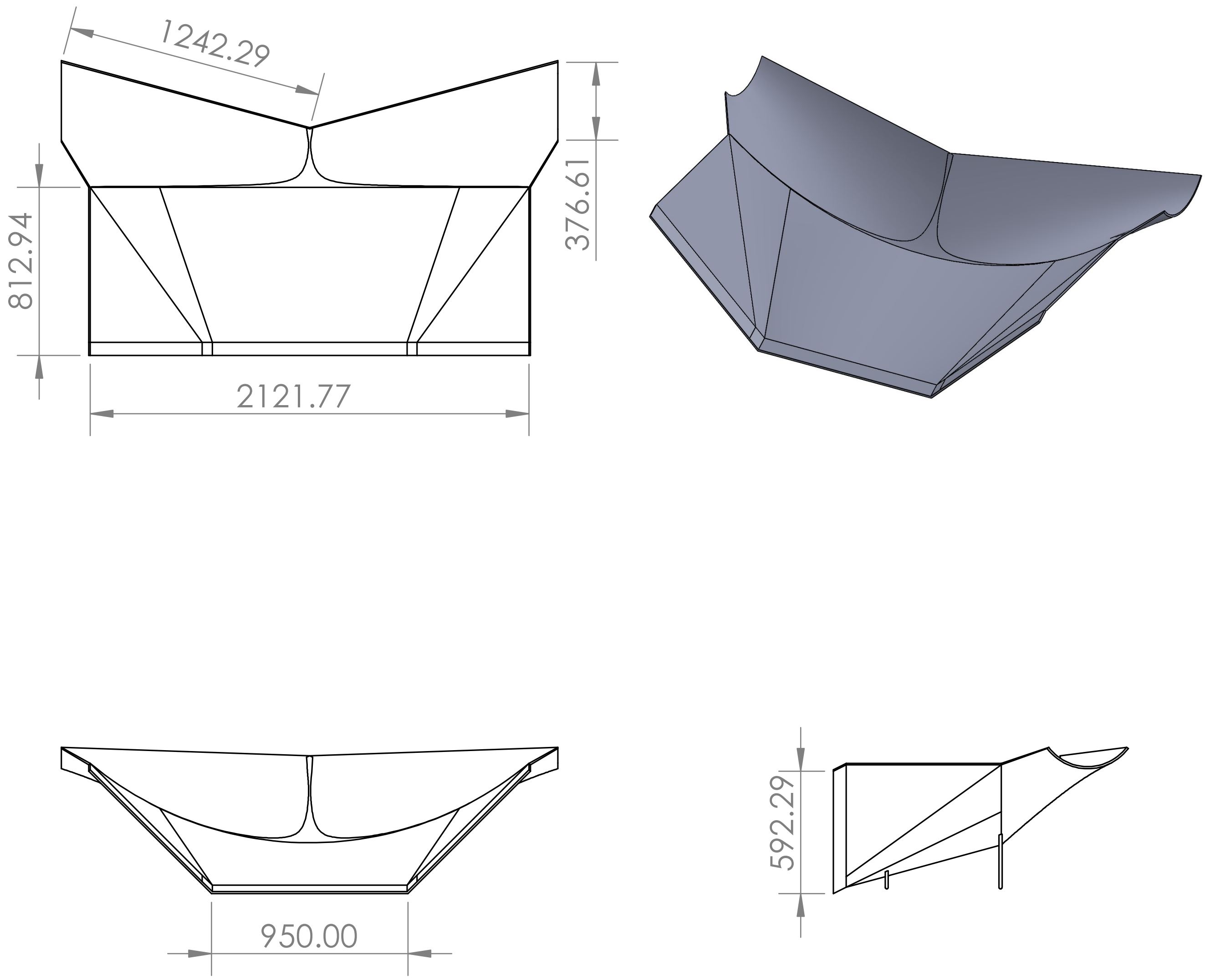

UNLESS OTHERWISE SPECIFIED:
DIMENSIONS ARE IN MILLIMETERS
SURFACE FINISH:
TOLERANCES:
LINEAR:
ANGULAR:

FINISH:

DEBURR AND BREAK SHARP EDGES

DO NOT SCALE DRAWING

REVISION

	NAME	SIGNATURE	DATE
DRAWN	Uzair Zulfiqar		12-05-24
CHK'D			
APPV'D			
MFG			
Q.A			

TITLE:

Plate General Dimensions

MATERIAL:

Cast Magnesium Alloy

DWG NO.

DWG-001

A4

WEIGHT:

SCALE:1:33.3

SHEET 1 OF 1

Appendix E-Pipe CFD Results

Pipe with elbow			
Velocity Contour	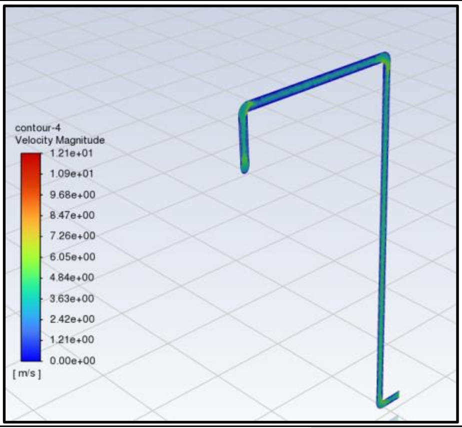	Pressure Contour	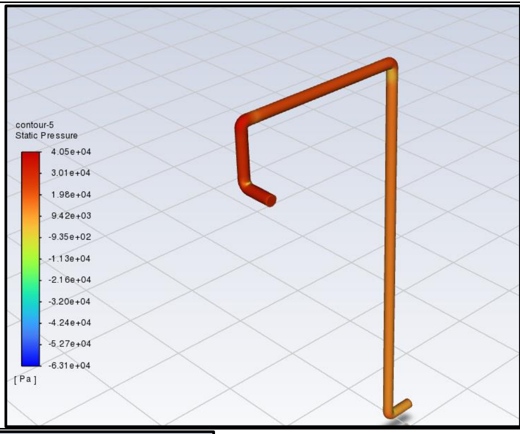
Convergence	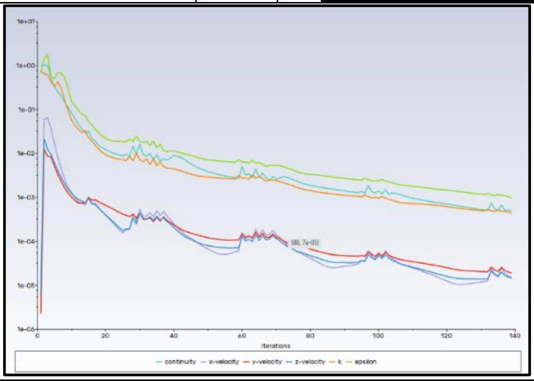		
Pipe without Elbow			
Velocity Contour	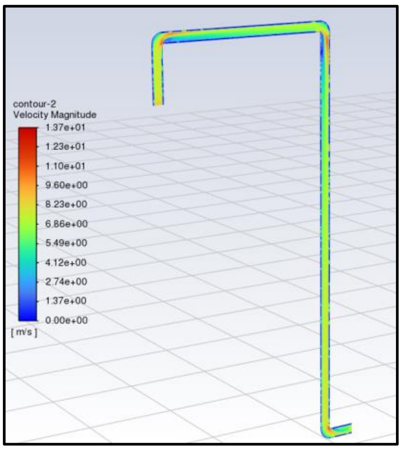	Pressure Contour	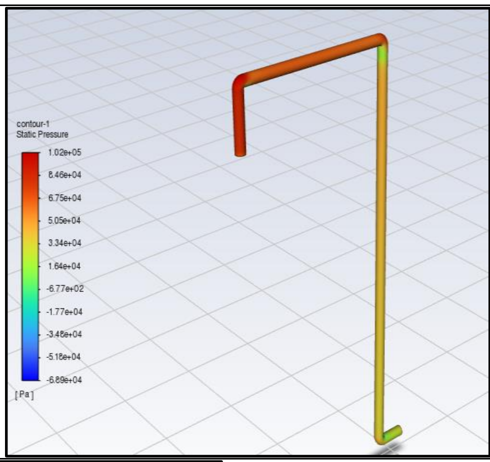
Convergence	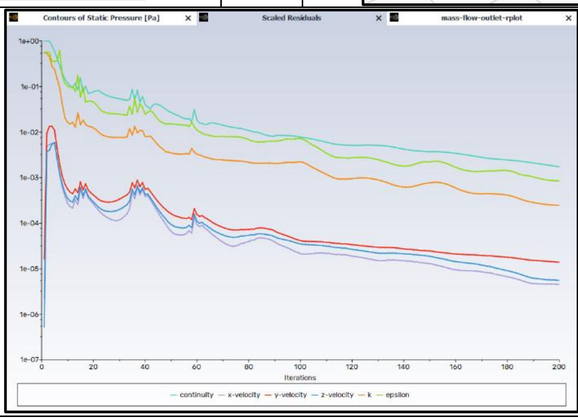		

Appendix F-Pipe 2D Drawing

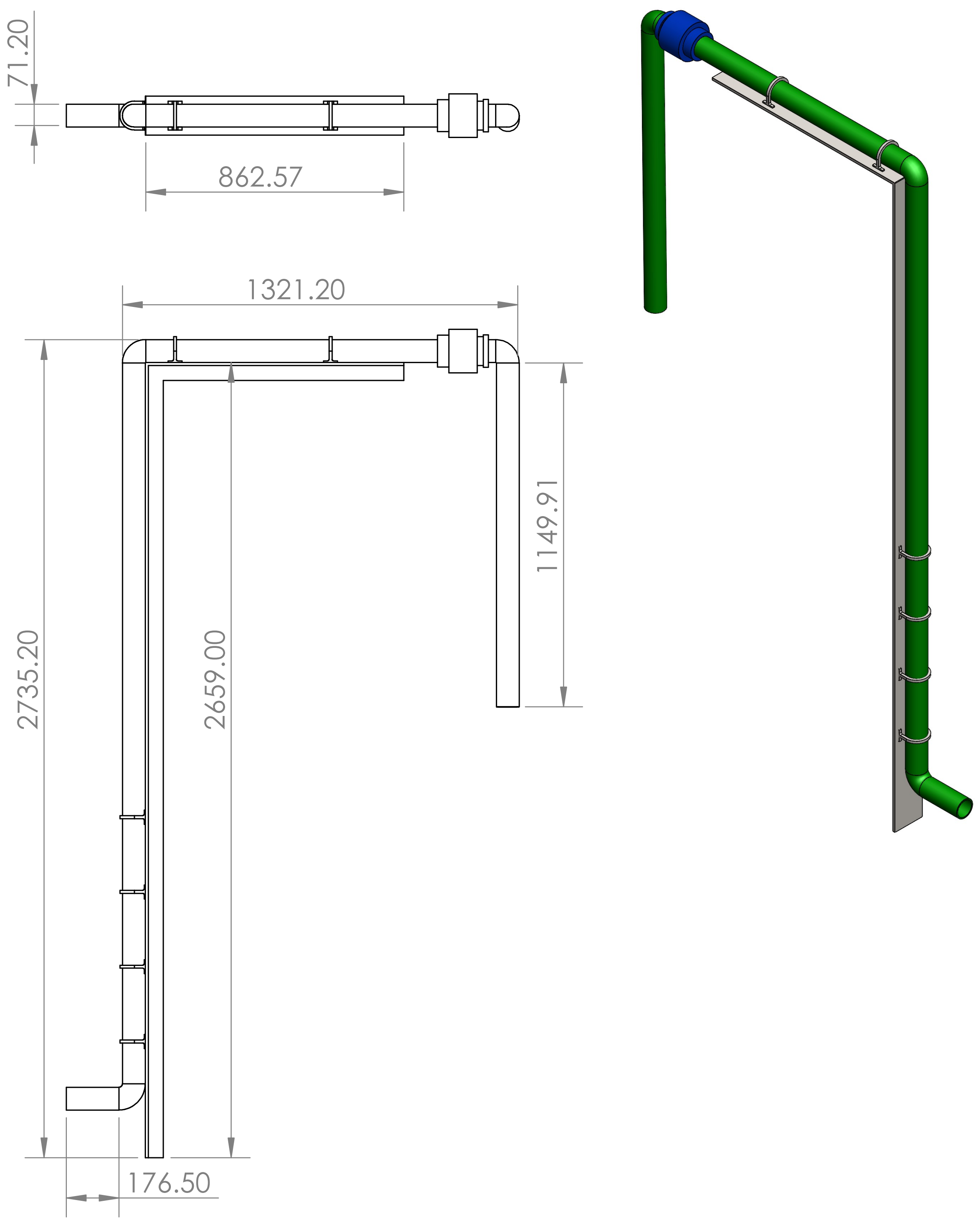

UNLESS OTHERWISE SPECIFIED: DIMENSIONS ARE IN MILLIMETERS SURFACE FINISH: TOLERANCES: LINEAR: ANGULAR:			FINISH:		DEBURR AND BREAK SHARP EDGES	DO NOT SCALE DRAWING	REVISION
	NAME	SIGNATURE	DATE			TITLE: Pipe General Dimensions	
DRAWN	Uzair Zulfiqar		13-05-24				
CHK'D							
APPV'D							
MFG							
Q.A				MATERIAL: PVC Pipe and Steel Support		DWG NO. DWG-002	A4
				WEIGHT:		SCALE:1:20	SHEET 1 OF 1

Appendix G-Plate-Based Design Rendered Images

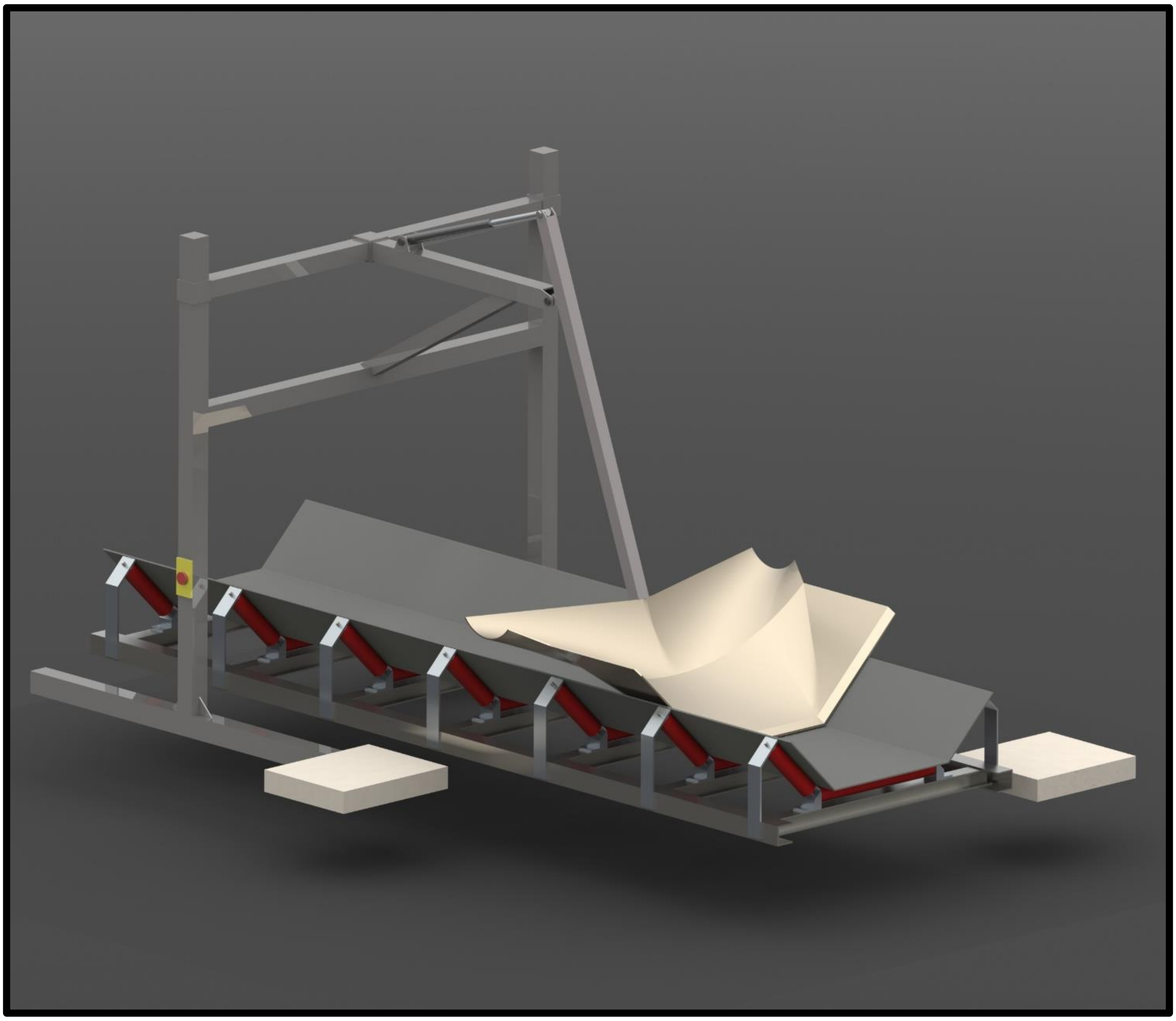

Plate-Based Design Rendered in SolidWorks

Appendix H-Pump-Based Design Rendered Images

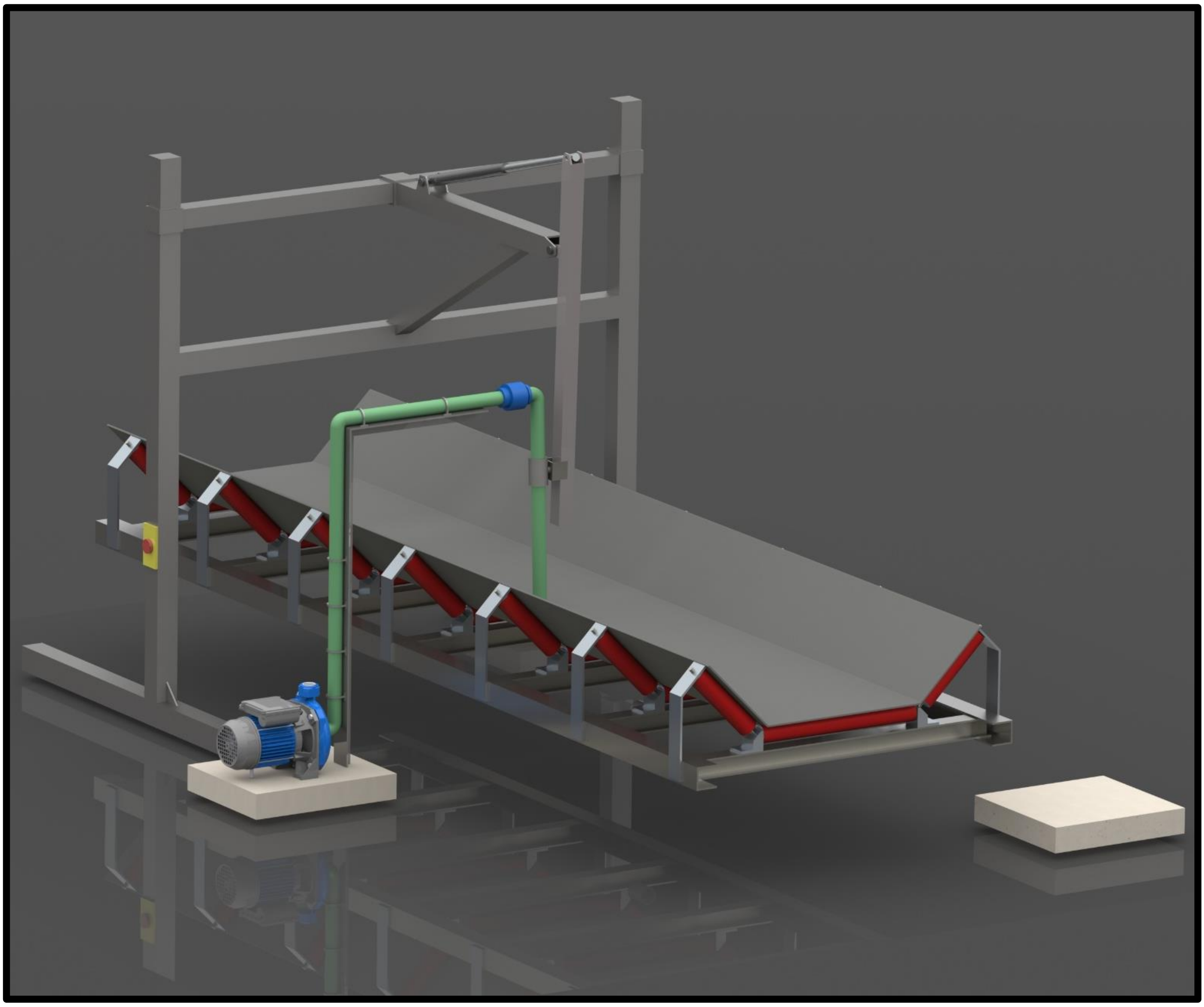

Pump-Based Design Rendered in SolidWorks